NAVAL
POSTGRADUATE
SCHOOL

MONTEREY, CALIFORNIA

THESIS

WAVE MAKING RESISTANCE CHARACTERISTICS OF TRIMARAN HULLS

by

Zafer Elcin

December 2003

Thesis Advisor: Fotis Papoulias

Approved for public release; distribution is unlimited.

THIS PAGE INTENTIONALLY LEFT BLANK

REPORT DOCUMENTATION PAGE			Form Approved OMB No. 0704-0188
Public reporting burden for this collection of information is estimated to average 1 hour per response, including the time for reviewing instruction, searching existing data sources, gathering and maintaining the data needed, and completing and reviewing the collection of information. Send comments regarding this burden estimate or any other aspect of this collection of information, including suggestions for reducing this burden, to Washington headquarters Services, Directorate for Information Operations and Reports, 1215 Jefferson Davis Highway, Suite 1204, Arlington, VA 22202-4302, and to the Office of Management and Budget, Paperwork Reduction Project (0704-0188) Washington DC 20503.			
1. AGENCY USE ONLY ***(Leave blank)***	**2. REPORT DATE** December 2003	**3. REPORT TYPE AND DATES COVERED** Master's Thesis	
4. TITLE AND SUBTITLE: Wave Making Resistance Characteristics of Trimaran Hulls			**5. FUNDING NUMBERS**
6. AUTHOR(S)			
7. PERFORMING ORGANIZATION NAME(S) AND ADDRESS(ES) Naval Postgraduate School Monterey, CA 93943-5000			**8. PERFORMING ORGANIZATION REPORT NUMBER**
9. SPONSORING /MONITORING AGENCY NAME(S) AND ADDRESS(ES) N/A			**10. SPONSORING/MONITORING AGENCY REPORT NUMBER**
11. SUPPLEMENTARY NOTES The views expressed in this thesis are those of the author and do not reflect the official policy or position of the Department of Defense or the U.S. Government.			
12a. DISTRIBUTION / AVAILABILITY STATEMENT Distribution Statement (mix case letters)			**12b. DISTRIBUTION CODE**

13. ABSTRACT

Recently, there has been an increased demand for high speed vessels both for military and commercial applications. Many navies are exploring the potential of novel hull forms as part of efforts to achieve transformation in both combat and logistics missions in littoral seas. This demand for high speed vessels has resulted in a need for unconventional hull forms in order to balance speed with payload requirements. One such hull form is the trimaran. The purpose of this thesis is to investigate the effects of side hull position on the wave making resistance characteristics of powered trimarans. Resistance calculations were performed by a three dimensional, Rankine panel code. A systematic series of runs was conducted in order to classify ship resistance in terms of major trimaran hull geometric configurations. The results of this thesis can be directly utilized in design, in order to minimize ship resistance, and maximize available payload.

14. SUBJECT TERMS High Speed Vessels, Littoral Seas, Unconventional Hull Forms, Trimaran, Wave Making Resistance.			**15. NUMBER OF PAGES** 91
			16. PRICE CODE
17. SECURITY CLASSIFICATION OF REPORT Unclassified	**18. SECURITY CLASSIFICATION OF THIS PAGE** Unclassified	**19. SECURITY CLASSIFICATION OF ABSTRACT** Unclassified	**20. LIMITATION OF ABSTRACT** UL

NSN 7540-01-280-5500 Standard Form 298 (Rev. 2-89)
Prescribed by ANSI Std. 239-18

THIS PAGE INTENTIONALLY LEFT BLANK

Approved for public release; distribution is unlimited.

WAVE MAKING RESISTANCE CHARACTERISTICS OF TRIMARAN HULLS

Zafer Elcin
Lieutenant Junior Grade, Turkish Navy
B.S., Turkish Naval Academy, 1997

Submitted in partial fulfillment of the
requirements for the degree of

MASTER OF SCIENCE IN MECHANICAL ENGINEERING

from the

NAVAL POSTGRADUATE SCHOOL
December 2003

Author: Zafer Elcin

Approved by: Fotis Papoulias
Thesis Advisor

Anthony J. Healey
Chairman, Department of Mechanical and Astronautical Engineering

THIS PAGE INTENTIONALLY LEFT BLANK

ABSTRACT

Recently, there has been an increased demand for high speed vessels both for military and commercial applications. Many navies are exploring the potential of novel hull forms as part of efforts to achieve transformation in both combat and logistics missions in littoral seas. This demand for high speed vessels has resulted in a need for unconventional hull forms in order to balance speed with payload requirements. One such hull form is the trimaran. The purpose of this thesis is to investigate the effects of side hull position on the wave making resistance characteristics of powered trimarans. Resistance calculations were performed by a three dimensional, Rankine panel code. A systematic series of runs was conducted in order to classify ship resistance in terms of major trimaran hull geometric configurations. The results of this thesis can be directly utilized in design, in order to minimize ship resistance, and maximize available payload.

THIS PAGE INTENTIONALLY LEFT BLANK

TABLE OF CONTENTS

LIST OF FIGURES

LIST OF TABLES

THIS PAGE INTENTIONALLY LEFT BLANK

ACKNOWLEDGMENTS

I would especially like to express my gratitude to all of the people who live in my country, Turkey. Thanks to them I was able to come to the United States for this great opportunity. I would like to thank all the people who helped support me throughout my graduate studies. I am especially grateful to my wife, Selin, for the support and love she offered me the whole period of my studies. I wish to dedicate my thesis to my wife and to my parents, Mustafa and Melek. They have given me all their love and support throughout my education.

I would like to thank my thesis advisor, Professor Fotis Papoulias, for his guidance and support throughout the last year.

THIS PAGE INTENTIONALLY LEFT BLANK

I. INTRODUCTION

Increasing demand for high-speed vessels for military and commercial applications has boosted the interest in unconventional ship types, which would possibly reduce high fuel consumption unavoidably linked to the higher speeds of conventional ships. There has been a long-standing military desire to move large amount of combat equipment across the seas as quickly as possible to counter threats anywhere in the world. Maritime countries have long recognized the easy access provided by the sea to a large percentage of the world's population. In the modern, faster moving world, there is a time gap between when airlift brings in the first forces and when traditional sealift delivers the heavier supporting equipment. Also, the United States Navy is undergoing dramatic changes as a result of the shift from an open ocean focus to operation in littoral environments. The need for unimpeded access to hostile shores is leading to increased emphasis on warships that can neutralize anti-access measures such as minefields, quiet diesel-electric submarines and swarms of small platforms. This mission requires high speed, in order to provide coverage of long coastlines and to respond rapidly to threats; low draft, permitting operations in shallow water; minimal signature, to prevent or delay detection by an enemy; a high degree of survivability; and the ability to perform multiple roles, either simultaneously or sequentially. High-speed vessels traveling at a sustained speed equal to or greater than 35 knots with bursts of speeds of 40-60 knots are often viewed as a means to fill the gaps in both logistics and combat missions.

However, higher speeds require a significant reduction of wave making resistance that is the most important component of the ship resistance when the speed increases. Generally, to reduce the wave making resistance, high values of $L/\nabla^{1/3}$ or the increase of the dynamic lift of the hull are required. The last way seems to be unfavorable since, for a given speed, lift/displacement ratio is reduced as the ship dimensions grow. Therefore, in order to design a high-speed ship with reasonable power requirements a very slender hull must be selected. The slenderness ratio about 9 seems to be the maximum value over that the hull stability becomes critical, then the hull configuration must be changed and multihull ships have to be used.

The trimaran configuration, consisting of a slender center hull and two side hulls, can be an interesting proposition to reduce the high fuel consumption inevitably linked to the higher speeds of conventional ships. Trimarans may possibly be able to combine the best of both worlds between monohulls and catamarans. By making the main hull very slender the increase in wave making resistance at higher speeds can be kept within reasonable limits. The required stability can be obtained from sidehulls, which can be relatively small and slender, therefore producing little resistance. A certain increase in total wetted surface is unavoidable and this causes less favorable fuel economy at lower speeds, but at sufficiently high speeds considerable gains are possible.

Consequently, in order to achieve 35-60 knots speed range and still maintain an acceptable level of payload, it is imperative that the wave making resistance is minimized. Although there is a large amount of work done with regards to wave making resistance of monohulls, the corresponding work for multihull ships is relatively small. By proper positioning the side hulls a considerable wave reduction may be possible, resulting in lower wave making resistance. The purpose of this thesis is to investigate the effects of side hull position on the wave making resistance characteristics of trimaran ships. Chapter II provides an overview of the various types of hull forms and presents some arguments in favor of trimarans. Chapter III presents the mathematical and modeling background, while Chapter IV discusses the results. Finally, the conclusions and recommendations of this study are summarized in Chapter V.

II. WHY TRIMARANS?

A. ADVANCED HULL FORMS

The most important ship performance features are both her payload/weight ratio and speed. Customers are always in demand for delivery of more cargo at higher speeds. These requirements are not an independent pair. Higher speeds usually require the demand for higher power, which results in high fuel consumption and less relative payload. The increasing demand for fast sea transportation has boosted the interest in advanced hull forms, which could possibly reduce the problem with the high fuel consumption inevitably linked to the higher speeds of conventional ships.

Monohulls have long dominated the maritime world from shipping to military combat. Most seagoing tonnage of the world consists of "displacement craft", of which monohulls have attributes that make them the most widely used hull forms:

- Transport;
- Small propulsion power requirements and long endurance at low speeds and moderate propulsion power at moderate speeds;
- Ruggedness, simplicity, and durability;
- Tolerance to growth in weight and displacement;
- Existing infrastructure of yards, docks, and support facilities is designed for monohulls; and
- Low cost

Together, these characteristics describe affordable ships that can carry large payloads of any composition over great distances at low to moderate speed, less than about 25 knots, and with good mission endurance when away for long periods of time from home ports. The ships have shortcomings that we have learned to live with. In high seas, most ships must sacrifice either speed or seakeeping ability, and neither can be achieved without size. To survive in high sea states and maintain speed, conventional displacement ships must be large.

There are multiple options available for high speed vessels for different purposes. The Navy is looking for beyond monohulls design ships to meet requirements of 21st century warfare- with faster, more stable, and shallower draft ships- to increasingly operate in the world's littoral regions. Classifying these based on hull form breaks down to include catamarans, small waterplane twin hull (SWATH), SLICE, ACV, surface effects ship (SES), hydrofoils, hybrids and trimarans. This chapter will look at these available designs and illustrate the advantages and disadvantages of the high-speed potential of the design.

1. Catamarans

The catamaran is a vessel with two hulls- normally arranged parallel and abreast- separated from each other but attached to a common deck. Catamarans perform better than monohulls in minimizing wave resistance because the distribution of displacement between the two hulls allows the individual hulls to operate with less wave making resistance at higher speed-length ratios, although this is offset somewhat by increased wetted surface area and increased frictional resistance. There is also the possibility for a high amount of wave interactions between the hulls. Catamarans become stable in the ship's roll response but are more susceptible to pitch and heave responses. Another advantage to catamarans is the draft. If a monohull and a catamaran of equal displacement were compared, the catamarans will have a lower draft. This is an advantage for littoral missions.

High-speed aluminum catamarans are widely used as vehicle and passenger ferries. Many designs are in service with displacement ranging from a few hundred tonnes to about 3,850 tonnes with speeds of 35-40 knots. Some small ferries have pushed the speed envelop above 50 knots, although generally only in sheltered water. The largest aluminum catamaran, Stena's HSS1500 displaces 3,850 tonnes and makes 40 knots fully loaded. Range of even the largest high-performance ferries is generally a few (200-400) hundred miles. Although catamarans are increasingly popular as commercial ferries in restricted or costal waters, their seakeeping quality is inferior to that of the SES and the small waterplane area twin hulls (SWATH), which limits for open-sea operations.

2. SWATH (Small Waterplane Area Twin Hulls)

The quest to improve seakeeping led to development of the SWATH hullform. SWATH type of vessels uses the concept of lifting bodies, generating lift from their hydrodynamic shape and from buoyancy. The SWATH usually has a pair of fully submerged hulls on which slender struts are mounted to support a cross structure. The struts present minimal waterplane area so that deeper immersion of the hulls causes a small increase in buoyancy. Designing the struts with appropriate water plane properties is the key to good seakeeping. In addition to having better seakeeping quality than comparable monohull vessels, a SWATH exhibits less falloff in speed with increasing sea state. One disadvantage is the high stress concentration on the hull versus more conventional designs where stress levels are more evenly distributed. The SWATH hull form can achieve speeds greater than 25 knots but require much more power than other hull forms at those speeds. This lack of speed limits the effectiveness of SWATH and to date, ship designers and operators are faced with the dilemma of choosing either speed or stability. Efforts to improve the seakeeping ability of the faster hullforms met with little success. Lockheed Martin, therefore, decided to attempt to increase the speed of the stable SWATH design. The result is the SLICE hull form.

3. SLICE

SLICE, a SWATH variation with four short hulls, or pods, instead of the SWATH's two long hulls was a recently developed under a joint Office of Naval Research (ONR). The four-pod design significantly reduces the wave making resistance. Data release by Lockheed Martin Marine Systems suggests that SLICE achieves power efficiencies 20-35% greater than those with conventional SWATH designs at speeds in excess of 18 knots. Lockheed Martin's SLICE prototype is 104 feet and a 55-foot beam that can maintain 30 knots in waves up to 12 feet in height. Claimed advantages over a conventional monohull are higher speed for the same power; lower installed power and fuel consumption for the same speed; more flexibility in strut/hulls arrangements; and lower wake signature at high speed. However, the SLICE concept is under evaluation and its various merits have not yet been proven.

4. ACV

The ACV rides on cushion of relatively low-pressure air, the escape of which is impeded by a flexible fabric skirt attached around the periphery of the underside of the craft's hard structure. Air must be supplied continuously to the using fans or blowers housed within the hard structure to maintain the supporting pressure over the broad base of the craft as air escapes beneath the flexible skirt. In this way, the hard structure can ride well above the surface of the sea or land while flexible skirt offers very little resistance to forward motion. Calm-water speeds in excess of 80 knots have been demonstrated since early 1960's. Its high speeds make the ACV useful for the fast-attack mission, and its amphibious nature gives it an over –the beach assault capability. Since its hull is not in contact with the water, it is less susceptible to damage by mine explosion. Consequently, the ACV has potential for mine hunting. The ACV performs as well as monohulls in moderate sea states.

5. Surface Effects Ship (SES)

The SES has approximately 40 years of development and operational experience in the U.S. and abroad. The SES, like the ACV, uses a pressured air cushion to reduce the drag significantly over that which conventional ships experience. But unlike the ACV, the SES has rigid catamaran-style sidehulls. When air cushion pressure raises the craft, its side hulls remains slightly immersed to contain the air cushion. Flexible skirts fore and aft allow waves to pass thorough the cushion area. The sidehulls enhance the underway stability and maneuverability of the SES. High speed and improved seakeeping make the SES also a candidate for the fast attack mission. Though not widely used in a military role, the SES, generally employed as car/passenger ferries overseas, has come into its own with the new emphasis on countering the terrorist threat and defending surface combatant forces from close-in attack. Most recently, a Raytheon-led team has proposed a SES vessel design based on the Norwegian Skjold, a 154-foot composite ship, as its preliminary bid for the LCS design contract. A disadvantage of SES's is that the air cushion causes a destabilizing effect on the roll restoring moment due to the water level inside the air cushion being lower than the waterline. SESs' use less power and maintain

higher speeds than a catamaran, but the speed loss in waves is more significant than catamarans.

6. Hydrofoils

Hydrofoils are monohulls with structural attachments that behave like aircraft wings to lift the main hull clear of the water. Two basic foil system types are used for hydrofoil crafts; the first one is surface- piercing V-shaped or U-shaped foils and the second one is fully submerged foil. The hull of the craft can be lifted out of the water completely at foil borne speeds. The higher speed, the greater lift, which can be controlled by changing the foils' angle of attack. As the hydrofoil slows below take-off speed, the foils no longer provide adequate lift, and craft sinks onto the sea surface. The size of the foils required to lift a hydrofoil vessel's hull completely out of the water for foil borne operation puts a practical limitation on the overall size of hydrofoil vessels. The scale size and weight of the foils grows disproportionately with increases in the hydrofoil vessel's displacement. As a consequence, in practice, hydrofoil vessels have been effectively limited to about 500 tonnes in displacement. In the commercial sector, hydrofoil vessels have been used extensively to transport passengers, as have ACV, SES, and catamaran vessels. High speed plus the ability to operate in rough water make the hydrofoil ideal for the fast-attack role in restricted waters.

7. Hybrid

The SES, which uses powered aerostatic lift to supplement hydrostatic lift from buoyancy, is a hybrid hull form. Another noteworthy hybrid is the hydrofoil small waterplane area ship (HYSWAS), which uses dynamic lift generated by hydrofoils to supplement buoyancy support. A HYSWAS design has a long central strut connecting the center of the upper small waterplane area ship hull to a lower hull on which hydrofoils are mounted. Tests of a 27 foot HYSWAS research vessel have revealed several advantages: (1) much less roll, pitch and heave compared with a monohull; (2) better hydrodynamic efficiency than for a monohull above 20 knots; (3) reduced drag and power hump compared with pure hydrofoil vessels; (4) very little wake; and (5) hydrodynamic and propulsive efficiencies that reduce fuel consumption and extend range

over comparable monohulls (Maritime Defense, 1997). The only limitation is the vessel's large draft. Success in an at-sea demonstration of the 27 foot version could lead to a Navy development of a much larger vessel as the next step in assessing the potential of HYSWAS.

8. Trimaran

An interesting possibility to reduce the problem with the high fuel consumption inevitably linked to the higher speeds of conventional ships is the trimaran. Trimarans may possibly be able to combine the best of both worlds between monohulls and catamarans. By making the main hull very slender the increase in wave resistance at higher speeds can be kept within reasonable limits. The required stability can be obtained from sidehulls, which can be relatively small and slender, thus producing little resistance. A certain increase in total wetted surface is unavoidable and this causes less favorable fuel economy at lower speeds, but at sufficiently high speeds considerable gains are possible.

Many research papers were found that investigated the benefits of trimaran hull design. The trimaran configuration may offer several advantages over the other hull forms. These advantages can be summarized in the following ship design considerations:

a. Resistance

At low speeds, where frictional resistance dominates, the trimaran is at a disadvantage because of its high wetted surface area. Residuary resistance, which is composed primarily of wave making resistance, dominates at higher speeds. It is commonly accepted that both wave making and form resistance decrease as a vessel becomes more slender, or fine. One point of interest is the interference effect between the main hull and the side hulls. By proper positioning of the side hulls a considerable wave reduction may be possible, resulting in lower wave resistance. Because of the stability gained from the side hulls, the trimaran can use slender hulls that reduce residuary resistance. Compared to a monohull, this reduction in residuary resistance can far outweigh the penalty for increased wetted surface at higher speeds. [1] Because of the

reduced resistance, the trimaran reduces fuel consumption compared to an equivalent monohull. However, fuel consumption depends on the speed profile and in particular the power weighted proportion of time spent above or below the crossover speed. It is therefore perfectly possible for installed power to be reduced, but for overall fuel consumption to be increased by trimaran selection if a lot of time is spent at low to medium speeds. Fuel consumption will be reduced if sufficient time is spent at high speeds.

b. Machinery Arrangement

The trimaran's three hulls have the flexibility to accommodate many propulsion plant arrangements. The center hull, with its greater continuous width in way of the machinery spaces, allows the use of larger, more efficient engines than a comparable catamaran. Other options might include the installation of waterjet thrusters or propulsors in the side hulls.

c. General Arrangement

An undoubted feature of the trimaran form is the additional upper deck and upper ship space that is created. For the same displacement or volume as a monohull, the trimaran form will generate a ship with a greater length and, in the useful central region, greater upper deck beam that is extreme breadth between the two side hulls. This additional topside space has a number of potential uses. For example the greater length could be used for better separation of upper deck sensors and antennae; thereby alleviating some of the EMC problems and improving survivability. [2] The side hulls provide greater stability offering growth potential for ship systems and the ability to mount sensors higher above the water line to improve early-warning missile defense capabilities. The transversely offset side hulls offer expanded deck area over comparable monohulls. Another benefit for surface combatant is equipment can be mounted higher on the vessel; this reduces the effect of the shock levels, which are one of the main causes of equipment failures in action.

d. Seakeeping and Motions

Both research and experience with existing trimarans have suggested that the trimaran may offer desirable motions performance. The long, slender waterline of the main hull provides excellent seakeeping performance, particularly in head and bow

quartering seas. Data release by Austal USA suggests that the overall seakeeping advantage can be significant. For example, an in-depth comparison between a 100 m catamaran and 130 m trimaran, both operating at 38 knots, showed an improvement in operability of 23%. In its conventional form, the trimaran form offers evolutionary, rather than revolutionary, improvements in symmetric seakeeping over a monohull, by reducing heave and pitch motion due to the increase in length to displacement ratio of the main hull. [2] The greater stability allows for heavy equipment, such as large aerial detection radars.

e. Survivability

All vessels can benefit from the added collision protection and damaged stability inherent in the trimaran layout. Warships may benefit from the use of the side hulls as armor for critical machinery and control spaces.

f. Signature Reduction

The trimaran hull form offers two major advantages in signature reduction to warship designers. First, the overhead thermal signature can be significantly reduced by venting exhaust gases down into the space between the main and side hulls. Second, the radar cross-section can be reduced by incorporating an inward sloping, or tumblehome shape to the deckhouse.

An additional benefit of the trimaran may be a reduced wake wash compared to other hull forms designed to equivalent mission requirements. The ability to vary hull form and side hull location to minimize wake amplitude and energy may lead to promising possibilities for trimaran. This advantage might allow the trimaran to operate in areas where shore and pier erosion restrict vessel speed and displacement.

B. ADVANCE HULLFORM COMPARISON CONCLUSIONS

Many of the designs discussed in the previous section can lend themselves to military applications while many are not useful. The trimaran offers the potential for relatively low powering requirements at high speeds, large deck areas, and more conventional machinery arrangements than twin-hull vessels. For the longer distance vessels transport efficiency is the most important criteria. In the higher speed displacement craft, waterline length is the key to minimizing the dominant component

wave making resistance. Very slender vessels offer reduced wave making. The higher the Froude number the more slender it pats for the vessel to be. Yet also still important is low weight and low wetted surface area. The monohull would be the minimum resistance hullform if it was not for the restrictions imposed by the requirements of stability. Monohulls have a powering advantage for some the large cargo slower speed missions; while trimarans have an advantage on the faster longer-range missions where the monohull hullform is stability constrained. These stability constraints cause a practical monohull to have a wider beam and reduced slenderness to provide the necessary stability. At slower speeds the monohull is competitive and in some cases have the advantage over trimarans, which have a wetted surface penalty. Thus for the higher speed long range missions, trimarans are able to employ the optimal main hull characteristics of a monohull with just enough stability added by low drag and weight side hulls.

THIS PAGE INTENTIONALLY LEFT BLANK

III. THEORETICAL BACKGROUND

A. THEORY

The following chapter investigates the calm water resistance of a trimaran. The research is using a time domain Rankine Panel Method CFD, SWAN-2 (ShipWaveANalysis).

1. The Exact Ideal-Flow Equations

Figure 1 illustrates a ship advancing with a time dependent forward speed $U(t)$ in ambient waves. The fluid flow equations of motion will be stated with respect to a Cartesian coordinate system $x=(x,y,z)$ translating with velocity $U(t)$ in the positive x-direction. The origin of the coordinate system is taken on the calm water surface, which coincides with the $z=0$ plane. With the assumption of potential flow, the disturbance fluid velocity $v=(x,t)$ is defined as the gradient of the velocity potential $\Phi(x,t)$, or $v=\nabla\Phi$. By virtue of continuity, Φ is subject to the Laplace equation in the fluid domain:

$$\nabla^2\Phi = \frac{\partial^2\Phi}{\partial x^2} + \frac{\partial^2\Phi}{\partial y^2} + \frac{\partial^2\Phi}{\partial z^2} = 0 \tag{3.1}$$

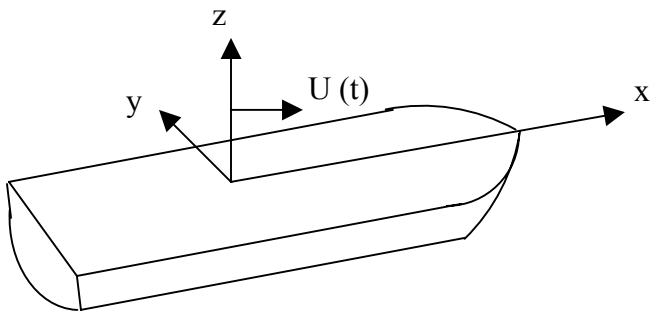

Figure 1. Coordinate System

The position of the free surface is defined by the wave elevations $\zeta(x,y,t)$, which along with the velocity potential $\Phi(x,t)$ are the pair of unknown quantities, or state

variables, to be determined by the Rankine Panel Method described in Section B. Two free surface conditions relate the state variables, the kinematic and dynamic free surface conditions. The kinematic condition corresponds to the velocity of the fluid on the boundaries and requires that a fluid particle on the air-water interface at t=0 will stay there for all times. The corresponding mathematical statement relative to the translating reference frame takes the form:

$$\left[\frac{\partial}{\partial t}-\left(\vec{U}-\nabla\Phi\right).\nabla\right]\zeta=\frac{\partial\Phi}{\partial z}, \qquad \text{on } z=\zeta(x,y,t). \tag{3.2}$$

The dynamic condition corresponds to the forces act on the boundaries and states that the fluid pressure on the free surface is equal to the atmospheric pressure, which is equal to zero. It follows from Bernoulli's equation that:

$$\left[\frac{\partial}{\partial t}-\vec{U}.\nabla\right]\Phi+\frac{1}{2}\nabla\Phi.\nabla\Phi+g\zeta=0, \quad \text{on } z=\zeta(x,y,t). \tag{3.3}$$

In other words, the pressure around a ship with forward speed U is defined as:

$$p-p_a=-\rho\left(\frac{\partial\Phi}{\partial t}+\frac{1}{2}\nabla\Phi.\nabla\Phi-\frac{1}{2}U^2+gz\right) \tag{3.4}$$

p_a is the atmospheric pressure and g is the gravity acceleration.

A more compact free surface condition which involves Φ explicitly and ζ implicitly can be found by eliminating the wave elevation ζ from (3.2) and (3.3).

The flow normal velocity equals the corresponding velocity of the rigid boundary on the ship hull. Denoting by n the unit vector normal to the instantaneous position of the ship hull, it follows that:

$$\frac{\partial\Phi}{\partial n}=\vec{U}.\vec{n}+\vec{v}.\vec{n} \tag{3.5}$$

where $\vec{v}=\frac{\partial\vec{\delta}}{\partial t}$, is the oscillatory velocity of the ship hull due to the wave-induced motions. Finally, at large distances from the ship the flow velocity must vanish.

The numerical solution of the exact set of equations (3.1)-(3.5) presents a very challenging task in steady or unsteady flow. Therefore, a number of linearization have been suggested and are discussed next.

2. Linearization of Free Surface Conditions

For the linearization of (3.2)-(3.5) to be justified the following two conditions must hold. The first one requires the ambient wave slope to be small. The second one requires the hull form to be sufficiently 'streamlined', i.e. thin, slender, or flat. At zero speed, the linearized equations follow trivially by dropping all quadratic terms in (3.2)-(3.3) and enforcing (3.2)-(3.5) over the mean positions of the free surface and the ship hull. In the case of finite speed the linearization is less evident. The principal consequence of the 'streamlined' ship assumption is that the fluid disturbance velocity caused by the ship forward translation and its oscillatory motion in waves is small compared to its forward speed U. The total velocity potential Φ may be therefore broken into two parts, the basis-flow potential φ_0 and the disturbance flow potential φ_D, defined as follows:

$$\Phi = \varphi_0 + \varphi_D \quad \text{where} \quad |\nabla\varphi_D| \ll |\nabla\varphi_0| \tag{3.6}$$

A similar decomposition is adopted for the wave elevation ζ.

$$\zeta = \zeta_0 + \zeta_D \quad \text{where} \quad \zeta_D \ll \zeta_0 \tag{3.7}$$

The Neumann-Kelvin linearization, the simplest one, assumes that the basis flow is the uniform stream. The corresponding basis wave elevation is zero and the resulting free surface condition for the two state variables take the form:

$$\left(\frac{\partial}{\partial t} - U\frac{\partial}{\partial x}\right)\zeta_D = \frac{\partial\varphi_D}{\partial z} \qquad z = 0 \tag{3.8}$$

$$\left(\frac{\partial}{\partial t} - U\frac{\partial}{\partial x}\right)\varphi_D = -g\zeta_D \qquad z = 0 \tag{3.9}$$

An advantage of the N-K linearization is its simplicity and the possibility to derive explicit elementary solutions known as Wave Green Functions in steady flow, the

frequency or time domains. The N-K model can be rationally justified only for ships with very small beam or draft. For conventional ships with finite beam and draft of comparable magnitude, a more accurate basis-flow model exists which accounts for the effects of the ship thickness.

The Double-Body Linearization, first proposed by Gadd [3] and Dawson [4], models the flow past the ship and its positive image above the free surface may be selected as the basis-flow. The resulting basis wave elevation ζ_0 follows from the Bernoulli's equation in the form:

$$\zeta_0 = \frac{U}{g}\frac{\partial \varphi_0}{\partial x} - \frac{1}{2}\nabla\varphi_0.\nabla\varphi_0 \qquad z = 0 \tag{3.10}$$

With substitution in the nonlinear free-surface conditions and use of the linearization assumptions, the following conditions for (φ_D, ζ_D) over the $z = 0$ plane can be derived:

$$\left[\frac{\partial}{\partial t} - \left(\vec{U} - \nabla\varphi_0\right).\nabla\right]\zeta_D = \frac{\partial^2 \varphi_0}{\partial z^2}\zeta_D + \frac{\partial \varphi_D}{\partial z} \qquad \text{on} \qquad z = 0 \tag{3.11}$$

$$\left[\frac{\partial}{\partial t} - \left(\vec{U} - \nabla\varphi_0\right).\nabla\right]\varphi_D = -g\zeta_D + \left[\vec{U}.\nabla\varphi_0 - \frac{1}{2}\nabla\varphi_0.\nabla\varphi_0\right] \text{ on } z = 0 \tag{3.12}$$

Several variations of the double-body linearization have been suggested in the literature for steady and unsteady ship flows. A popular version of (3.11)-(3.12) is that of Dawson [xx], because he was the first to implement it in a Rankine Panel Method.

3. Linearization of the Body Boundary Condition

Linear theory allows the decomposition of the wave disturbance into independent incident, radiated and diffracted components. The linearization of the exact body boundary condition entails its statement over the mean translating position of the ship hull; assuming that it's oscillatory displacement is small. Adopting the decomposition of the total velocity potential Φ into basis and disturbance components, φ_0 and φ_D, the former offsets the normal flux due to the forward translation of the ship, or:

$$\frac{\partial \varphi_0}{\partial n} = \vec{U}.\vec{n} = Un_1 \qquad \text{on } \bar{S} \tag{3.13}$$

where $\bar{n} = (n_1, n_2, n_3)$ is the unit vector normal to the ship hull pointing out of the fluid domain.

The corresponding body boundary condition for the radiation disturbance potential, linearized about the mean surface of the hull, takes the form:

$$\frac{\partial \varphi_D}{\partial n} = \sum_{j=1}^{6}\left(\frac{\partial \varsigma_j}{\partial t} n_j + \varsigma_j m_j\right) \qquad \text{on } \bar{S} \tag{3.14}$$

where $\varsigma_j(t)$, $j = 1, 2, ..., 6$ is the ship oscillatory motions in six degrees of freedom.

$$(n_1, n_2, n_3) = \vec{n} \tag{3.15}$$

$$(n_4, n_5, n_6) = \vec{x}.\vec{n} \tag{3.16}$$

$$(m_1, m_2, m_3) = (\vec{n}.\nabla)(\vec{U} - \nabla\varphi_0) \tag{3.17}$$

$$(m_4, m_5, m_6) = (\vec{n}.\nabla)\left[\vec{x} \times (\vec{U} - \nabla\varphi_0)\right] \tag{3.18}$$

The m terms, m_j provide a coupling between the steady basis flow and the unsteady body motion.

B. PANEL METHOD

Panel methods are developed to solve open form, complex, three-dimensional fluid dynamic problems where greater accuracy is required. Panel methods are based on potential flow theory where oscillating amplitudes of the fluid and the body are small relative to the dimensions of the body cross-section.

Panel method relies on the assumption that any irrotational, incompressible flow can be represented by a proper distribution of sources, sinks or doublets over its bounding surfaces. A source is defined as a point from which a fluid is imagined to follow out uniformly in all directions. A sink is a ‘negative’ source, where fluid is ‘sucked’ in

uniformly. A doublet is a combination of source and sink. G represent the potential of a source at an arbitrary point inside a control volume such that:

$$G = -\mu \frac{1}{4\pi} . \frac{1}{r} \tag{3.19}$$

r is the distance from the source to the arbitrary point where the potential is to be evaluated and μ is the 'strength' of the source, defined as the total flux outwards (or inwards) across a small closed surface surrounding the arbitrary point. Green's second identity is a governing mathematical identity utilized to solve fluid hydrodynamic problems. It is derived from the divergence line:

$$\int_{\substack{control \\ volume}} \nabla . \bar{U} . dV = \int_{\substack{control \\ surface}} \bar{n} . \bar{U} . dS \tag{3.20}$$

where $\bar{U}$ is a vector. $\bar{U}$ can be replaced by the vector $\varphi \nabla G - G \nabla \varphi$, where φ is the velocity potential inside control volume such that $\bar{V} = \nabla \varphi$ ($\bar{V}$ is the body velocity) and G is the source potential. The Green's second identity becomes:

$$\int_{\substack{control \\ volume}} \nabla . \left(\varphi \nabla G - G \nabla \varphi \right) . dV = \int_{\substack{control \\ surface}} \bar{n} . \left(\varphi \nabla G - G \nabla \varphi \right) . dS$$

$$\int_{\substack{control \\ volume}} \left(\varphi \nabla^2 G - G \nabla^2 \varphi \right) . dV = \int_{\substack{control \\ surface}} \left(\varphi \frac{\partial G}{\partial n} - G \frac{\partial \varphi}{\partial n} \right) . dS \tag{3.21}$$

This identity basically relates the governing equation of the physical problem to the velocity potential on the bounding surfaces of the boundary value problem. On the left hand side of the identity the term $-\int_{\substack{control \\ volume}} G \nabla^2 \varphi . dV$ turns into zero due to Laplace Equation (3.1). This fact indicates that an infinite control volume problem in space is reduced to a finite closed form problem over the bounding surfaces of the body.

1. Rankine Panel Method

Rankine Source potential with unit strength takes the form of:

$$G(\bar{x},\bar{\xi}) = -\frac{1}{4\pi}.\frac{1}{r} = -\frac{1}{4\pi}\frac{1}{|\bar{x}-\bar{\xi}|} = -\frac{1}{4\pi}\frac{1}{\left[(x_1-\xi_1)^2+(x_2-\xi_2)^2+(x_3-\xi_3)^2\right]^{\frac{1}{2}}} \tag{3.22}$$

$\bar{x}$ is the vector aiming to an arbitrary point and $\bar{\xi}$ is the vector aiming to the source point. Figure 2 demonstrates the coordinate system and the distances from the origin satisfying equation (3.22). The simple Rankine Source is used to model free surface flows since it is difficult to evaluate the wave Green Function. The penalty for using this source is the necessity to discretize also the free surface in addition to the body surface.

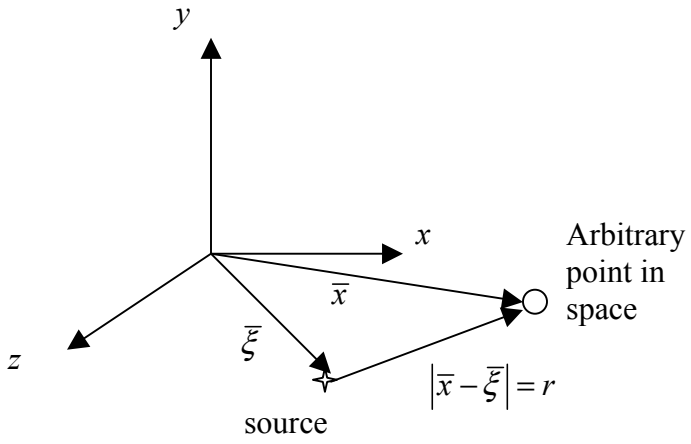

Figure 2. Rankine Source and an arbitrary point coordinate system

Using the Rankine Source as the Green Function in equation (3.21), the Green Identity becomes:

$$-\frac{1}{2}\Phi(\bar{\xi},t) + \iint_{S_B+S_F} \Phi(\bar{x},t)\frac{\partial G(\bar{x},\bar{\xi})}{\partial n}dS - \iint_{S_B+S_F} G(\bar{x},\bar{\xi})\frac{\partial \Phi(\bar{x},t)}{\partial n}dS = 0 \tag{3.23}$$

$\Phi(\bar{x},t)$ is the unknown velocity potential of the problem, S_B is the surface plane of the body, S_F is the free surface and $\bar{\xi}$ is the position of the Rankine Source.

The contributions from a closing surface at infinity vanishes due to the decay of $\Phi(\bar{x})$ and $G(\bar{x},\bar{\xi})$ as $\bar{x} \to \infty$ for fixed values of $\bar{\xi}$ and t. Over S_B, Φ_n is known and can

be found using the body boundary conditions. Over S_F the linearized boundary conditions establish $\Phi_z = \Phi_n$. Substitution of these boundary conditions reduces (3.23) into two integro-differential equations for Φ over S_B and (Φ, ξ) over S_F which solved by SWAN and described on the next. [5]

C. SWAN (SHIP WAVE ANALYSIS)

SWAN-2 is a computational fluid dynamic program for the analysis of the steady and unsteady zero-speed and forward-speed free surface flows past ships which are stationary or cruising in water of infinite or finite depth or in a channel.

Program solves the steady and unsteady free-surface potential flow problems around ships using a three-dimensional Rankine Panel Method in the time domain by distribution of quadrilateral panels over the ship hull and the free surface. The free surface conditions presented in section III.A.2 and implemented in SWAN-2 linearize the steady and unsteady wave disturbances about the double-body flow. SWAN-2 calculates the vessels ideal fluid resistance; sinkage and trim motions while translating at calm water, by invoking the boundary conditions presented in section III.A.3 and solving the equations of motion.

The use of SWAN-2 does not require access to a Computer Aided Design (CAD) program for the generation of the panel meshes over the ship hull and the free surface. The panel mesh is generated by routines internal to SWAN-2, which are designed to ensure that all stability criteria are met. The ship hull is input to SWAN-2 in the form of offsets generated by any CAD program. Output from SWAN-2 may be viewed by the TECHPLOT package licensed by AMTEC Engineering.

The reference coordinate system illustrated in Figure 3 and used by SWAN-2 must be selected such that the $z = 0$ plane coincides with the calm water surface, the $z > 0$ axis points upwards and the x-axis points upstream with the origin near mid-ships.

The free surface flows are solved about the reference coordinate system fixed at the ship mean position. A uniform stream with velocity U flows in the negative x-direction.

The internal panel mesh generation routine of SWAN-2 distributes panels over the mean free surface and the body surface of the ship hull. The mesh density and the extent of the free surface discretization may be specified by the user, but must be selected carefully. The internal stability analysis routine of SWAN-2 provides the optimal time step for the time integration of equation of free surface and body motion so that the mesh specified by the user meets the SWAN-2 stability criteria.

The hull offset file (PLN) is converted into the spline sheet geometry file (SSG) that contains the panel mesh distribution on the free surface and the body surface of the hull. This is done via the program MAKESSG.EXE.

The panel density and domain size are specified by the user via the job control parameters input file (INP). Presently the mesh generation routine supports monohulls, catamarans, trimarans and SES vessels.

D. SHIP RESISTANCE

The resistance of a ship at a given speed U is the force required to tow the ship at that speed in calm water, assuming no interference from the towing ship. If the hull has no appendages, this is called 'The bare-hull resistance'. The power necessary to overcome this resistance is called the towrope or effective power and is usually notated as EHP (Effective Horse Power). The total resistance is sum of a number of different components, which are caused by a variety of factors and which interact with each other in a rather complicated way. In order to deal with the question more efficiently, it is usual to consider the total calm water resistance as being made up of three major components.

1. Frictional (viscous) Resistance

Frictional resistance is usually the most significant component of the total ship resistance and caused due to the movement of the ship through a viscous fluid. Frictional resistance is basically the result of the tangential fluid force exerted from the ships movement in water. For relatively slow ships with high block coefficients it contributes to about 85% of the total resistance, whereas for high speed streamlined displacement hulls it may drop to about 50%. These values may become higher in time due to the

increased roughness of the ship surface. Frictional resistance depends on the roughness of the surface, on the overall wetted area of the ship and on the ships speed. The frictional resistance is usually presented by:

$$R_F = \frac{1}{2}.C_f.\rho.S_B.U^2 \tag{3.24}$$

where R_F is the frictional resistance, C_f is the frictional resistance coefficient, ρ is the mass density of water, S_B is the static wetted surface area of the ship and U is the ships speed.

For many years, lots of model and full-scale experiments had been performed in order to calculate the magnitude of the frictional resistance and the frictional resistance coefficient. The International Towing Tank Conference (ITTC) adopted the following formula which is known as "ITTC 1957 model-ship correlation line" for the frictional resistance coefficient for a flat plate in 1957:

$$C_f = \frac{0.0075}{\left(\log_{10} \mathrm{Re} - 2\right)^2} \tag{3.25}$$

in the formula; Re is a non-dimensional value and is known as the Reynolds Number:

$$\mathrm{Re} = \frac{U.L}{\nu} \tag{3.26}$$

U is the ships speed, L is the ships length and ν is the kinematic viscosity of the water.

2. Calm Water Wave Making Resistance

The wave making resistance of a ship is the net fore-and-aft force upon the ship due to the fluid pressures acting normally on all parts of the hull. If the body is traveling on or near the free surface this pressure variation causes waves which radiate away from the body and carry with them a certain amount of energy that is dissipated in the ocean. The wave making resistance can also be characterized by the energy expended by the ship that is necessary to maintain the wave system. Theoretical determination of the wave making requires knowledge of the wave system generated by a moving ship.

The most general wave elevation distribution in three dimensions, transformed to a reference system, moving with a vessel in the positive x-direction with velocity U, is given by:

$$\zeta(x,y,t) = \mathrm{Re}\left\{\int_0^{\infty} dw \int_0^{2\pi} d\theta . A(w,\theta) . e^{\left[-ik(x\cos\theta + y\sin\theta) + i(w - kU\cos\theta)t\right]}\right\} \tag{3.27}$$

this formulation shows oblique wave (with angle θ) distribution in the ships wake. For steady motion the second exponential term disappears, hence:

$$kU\cos\theta - w = 0 \tag{3.28}$$

The wave phase velocity becomes:

$$V_p = \frac{w}{k} = U\cos\theta \tag{3.29}$$

For a steady wake pattern behind a moving ship, the wave elevation distribution expression becomes:

$$\zeta(x,y) = \mathrm{Re}\left\{\int_{-\frac{\pi}{2}}^{\frac{\pi}{2}} d\theta . A(\theta) . e^{\left[-ik(x\cos\theta + y\sin\theta)(\theta)\right]}\right\} \tag{3.30}$$

This expression is known as the free-wave distribution and can be simplified and the classic ship-wave pattern can be obtained as derived by Lord Kelvin for a very large distance downstream from the location of the ship. The following figure describes the Kelvin wave pattern in the wake of a moving vessel.

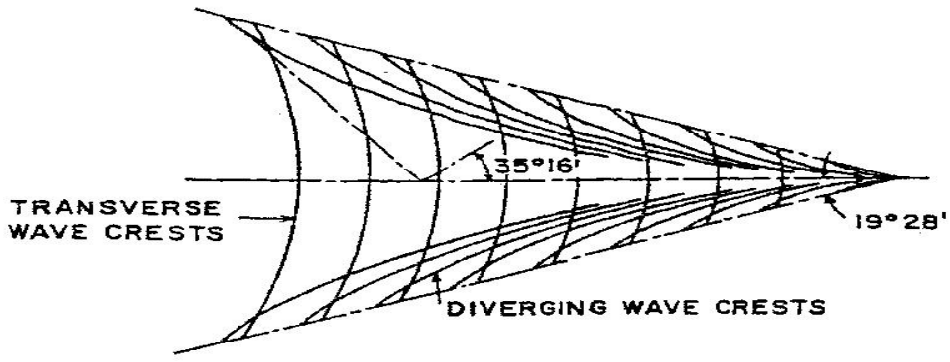

Figure 3. Kelvin wave pattern in a ship wake (From: TS4001 Course Notes)

The waves generated in the wake of a ship are confined to a symmetrical sector about the negative x-axis, which includes semiangles of $y/x = \pm 19^{\circ}28'$. At this maximum, the wave is directed with corresponding angle of $\theta = \pm 35^{\circ}16'$ above or below the x-axis. For all other y/x angles in the wake between $-19^{\circ}28'$ to $+19^{\circ}28'$ there are two corresponding values of the wave angle θ. One represents a transverse wave pattern; the other represents a diverged wave.

The waves both contain both potential and kinetic energy. By considering the wave energy per wavelength, per unit breadth:

$$P.E. = \int_0^T \int_0^{\lambda} \frac{1}{T} \frac{\rho g}{2} \zeta^2 dx dt \tag{3.31}$$

$$K.E. = \int_0^T \int_0^{\lambda} \int_{-H}^{0} \frac{1}{2} \frac{1}{T} \rho |\nabla \varphi|^2 \, dz dx \tag{3.32}$$

the x-axis coincides with the direction of the waves so the y- dependence is dropped. After integration the following results are obtained:

$$P.E. = \frac{1}{4} \rho g A^2 \tag{3.33}$$

$$K.E. = \frac{1}{4} \rho g A^2 \tag{3.34}$$

and the total energy density is given by:

$$E = \frac{1}{2} \rho g A^2 \tag{3.35}$$

The traveling energy is best expressed as wave power per unit width averaged over a wave period and can be found to be:

$$P = \frac{1}{2} \rho g A^2 V_p \frac{1}{2} \left(1 + \frac{2kH}{\sinh(2kH)} \right) \tag{3.36}$$

where V_p is the wave phase velocity as defined earlier and the term $\frac{1}{2} V_p \left(1 + \frac{2kH}{\sinh(2kH)} \right)$

is known as the group velocity, V_g. Group Velocity is defined as the velocity, which the energy of the wave travels. In a fixed reference frame, the energy of each plane wave component moves in direction θ with a group velocity V_g. The velocity of energy transfer across the control surface, which moves through the fluid with velocity U, is given by $V_g \cos\theta - U$. The total energy flux can be found by multiplying the energy density with the velocity of energy transfer across the control surface and integrating along the width of the control surface:

$$\frac{\partial E}{\partial t} = \frac{1}{2}\rho g \int_{-\infty}^{\infty} A^2 \left(V_g \cos\theta - U\right) dz \tag{3.37}$$

The total wave resistance of a moving vessel can be found by using the method of stationary phase approximation, as shown in Newman chapter 6 [6]:

$$R_w = \frac{1}{2}\pi\rho U^2 \int_{-\pi/2}^{\pi/2} \left|A(\theta)\right|^2 .\cos^3\theta .d\theta \tag{3.38}$$

This equation expresses the wave resistance of a moving vessel as the weighted integral of the square of the wave amplitude $A(\theta)$. The factor $\cos^3\theta$ implies that the dominant portion of the resistance will be associated with the transverse waves where the angle θ is smaller. We can see that $R_w \sim U^2 A^2$, and since $A \sim U$ (at least), it follows that $R_w \sim U^4$ (or higher). Since the frictional increases like U^2 or less we can see that at high speed (or high Fn) the wave making resistance will dominate the total ship resistance.

The wave amplitude $A(\theta)$ must be predicted from theory or measured in suitable experiment. One way of evaluating $A(\theta)$ is based on the thin ship theory, which was introduced by J.H. Mitchell in 1898 as a purely analytic approach for predicting the wave resistance of ships. The essential assumption is that the hull is thin and the beam is small compared to all other characteristic lengths of the problem. The resulting solution can be expressed in terms of a distribution of sources and sinks on the center line of the hull, with the local source strength proportional to the longitudinal slope of the hull. Using this

theory, the wave resistance of a thin ship can be expressed in the form of the so called Mitchell's integral:

$$R_w = \frac{4\rho g^2}{\pi U^2} \int_0^{\pi/2} \sec^3\theta \left| \iint \frac{\partial \xi}{\partial x} e^{\left[\left(g/U^2\right)\sec^2\theta(z - ix\cos\theta)\right]} dx dz \right|^2 d\theta \qquad (3.39)$$

where $\xi(x, y)$ defines the local half-beam of the hull surface.

More recent numerical studies of wave making resistance do away with the thin ship assumption and follow the panel method, which was presented in section 3.B. In this method, the surface of the ship is approximated by a series of panels with distributed sources and sinks. The method is similar to the thin ship approximation with the difference that source/sink distribution is on the actual ship surface instead of the centerplane. This allows for actual geometry of the hull to be taken into account, and therefore, minor modifications can be inflicted in order to minimize the wave making resistance.

3. Eddy Resistance, Viscous Pressure Drag and Separation Resistance

Besides the frictional and wave making resistance, there are several other components contribute to the resistance of a ship such as eddy resistance, viscous pressure drag, separation resistance, and wave breaking resistance.

The turbulent frictional belt around a ship consists of eddies or vortices, so that all forms of frictional resistance are really due to eddy making. However, the term is usually applied to the resistance due to eddy formation or distributed streamline flow caused by abrupt changes of form, appendages or other projections, and excludes tangential skin friction. When the total model resistance R_{TM} is measured over a range of speeds and plotted as the coefficient $C_{TM} = R_{TM} \Big/ \left(\frac{1}{2}\rho S_B U^2\right)$ against log Re, the curve will be of the general shape in Figure 6. Also shown is a curve of the coefficient of frictional resistance C_{FOM} for a smooth plate in fully turbulent flow. The intercept C_{RM} between the curves of C_{FOM} for the flat plate and C_{TM} for the total model resistance is so called residuary resistance coefficient. In a typical case the C_{TM} curve at the very low values of Re is

almost parallel to the C_{FOM} curve but some distance above it. Since the primary component of the coefficient C_w varies roughly as the fourth power of the speed, the wave making resistance at very low values of Re must be vanishingly small, so the intercept C_{RM} can not be attributed this case. If a curve is drawn parallel to the curve of C_{FOM}, the intercept FG represents the wave making resistance coefficient $C_w = R_w \Big/ \left(\frac{1}{2} \rho S_B U^2 \right)$. On this assumption, the intercept FE (=BC) must be due to some other cause, and this is the form resistance.

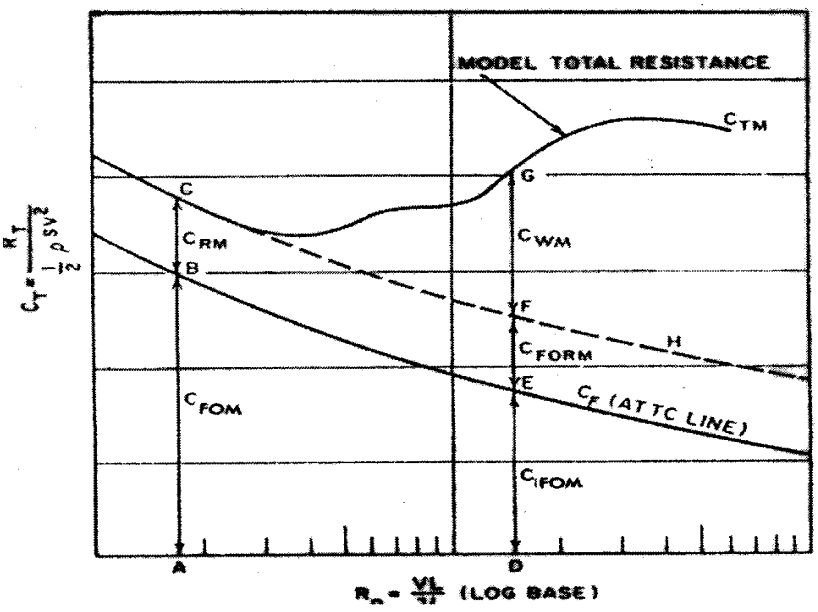

Figure 4. Elements of Model Resistance (From: TS4001 Course Notes)

There are three main causes of this form resistance. The ordinate of the C_{FOM} curve applies to a flat surface having the same length and wetted area as the model and so neglects any effects due to curvature of the hull. This curvature affects the pressure distribution along the length, causing the velocity to increase along most of the middle part and to decrease at the ends. The former effect outweighs the latter. Also, since the path along a streamline from bow to stern is longer on a shaped body than on a flat plate, the average velocity must be higher. Thus, the real skin friction of a ship must be greater than that of the equivalent flat plate. Since the pressure and the velocity

changes and the extra path lengths are greater the fuller and stumpier the form, such shapes would be expected to have greater form drag.

The existing boundary layer has virtual effect of lengthening the form and reducing the slopes of the after waterlines. This is a region where the normal pressure on the hull is higher than the static pressure and the forward components of these excess pressures will exert a forward thrust overcoming some of the ship's resistance. The presence of the boundary layer reduces these forward components, resulting in an increase in resistance as compared with that which would be experienced in a nonviscous fluid, and is called the viscous pressure drag.

If the curvature near the stern becomes too abrupt, the water may no longer be able to follow the hull and breaks away, and the space between the hull and the smooth flowing water is filled with vortices. A point at which this happens is called a separation point, and the resulting resistance is the third element of the form drag, called separation resistance. In addition to form and separation resistance, eddy making resistance is also caused by struts, shafts, bossing and other appendages.

IV. RESULTS

A. INTRODUCTION

The results of the parametric runs are presented in this chapter for a typical trimaran hull. This ship has the following characteristics:

Characteristic	**Main Hull**	**Side Hull**
Length (L_{BP})	400 ft	125 ft
Beam (B)	30.8 ft	7.5 ft
Draft (T)	12 ft	10 ft
L/B	13.0	16.7
$L/\nabla^{1/3}$	9.39	7.54
Block Coefficient (C_B)	0.53	0.50
Midship Coefficient (C_M)	0.84	0.68
Waterplane Coefficient (C_W)	0.81	0.79
Volume	77226 ft^3	4558ft^3
Displacement	2206 LT	130 LT
Total Volume	86343 ft^3	
Total Displacement	2466 LT	
Total Beam for $Y_{out}/L_{pp} = 0.1$	89.5 ft	
Total Beam for $Y_{out}/L_{pp} = 0.15$	129.5 ft	
Total Beam for $Y_{out}/L_{pp} = 0.2$	169.5 ft	

Table 1. Ship Characteristics

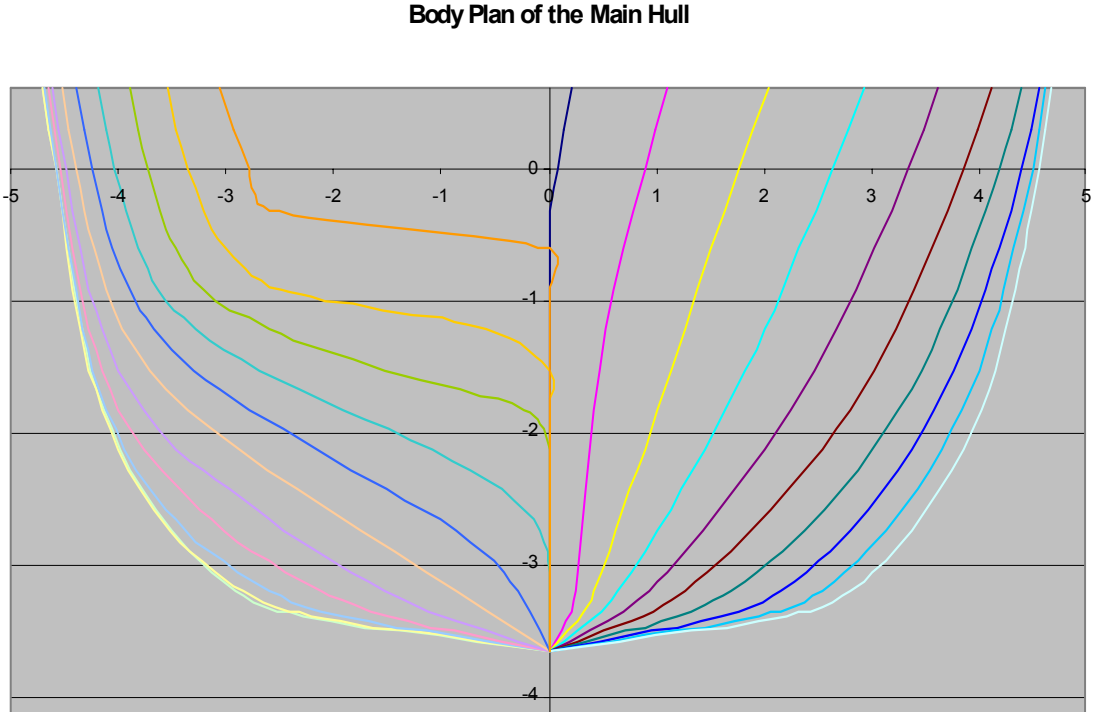

Figure 5. Body Plan of the Main Hull

Figure 6. Body Plan of the Side Hull

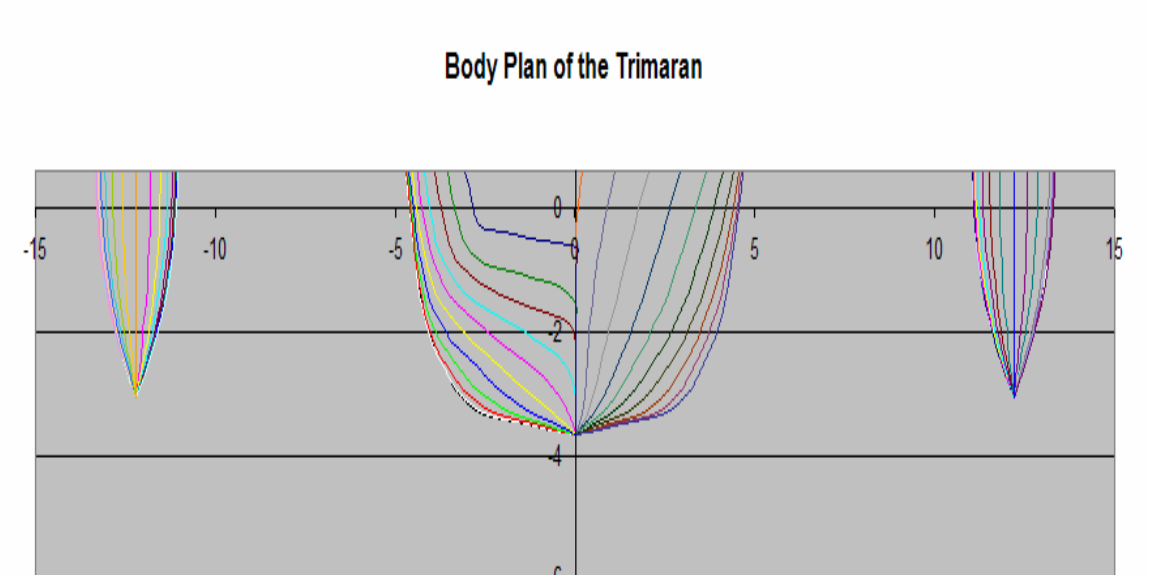

Figure 7. Body Plan of the Trimaran

B. EFFECTS OF SIDE TO MAIN HULL SEPARATION

Figures 8 through 27 present the wave making resistance coefficient versus the ship's Froude number for several transverse and longitudinal positions of the side hulls. We can see that a bigger side-main hull separation distance produces a beneficial effect on wave making resistance, particularly for low Froude numbers and aft placement of the side hulls. For higher Froude numbers the effect of the separation distance is minimal. These results are not as consistent, and in fact the trend may be reversed, as the side hulls are moved forward towards the middle and in front of the center of the main hull.

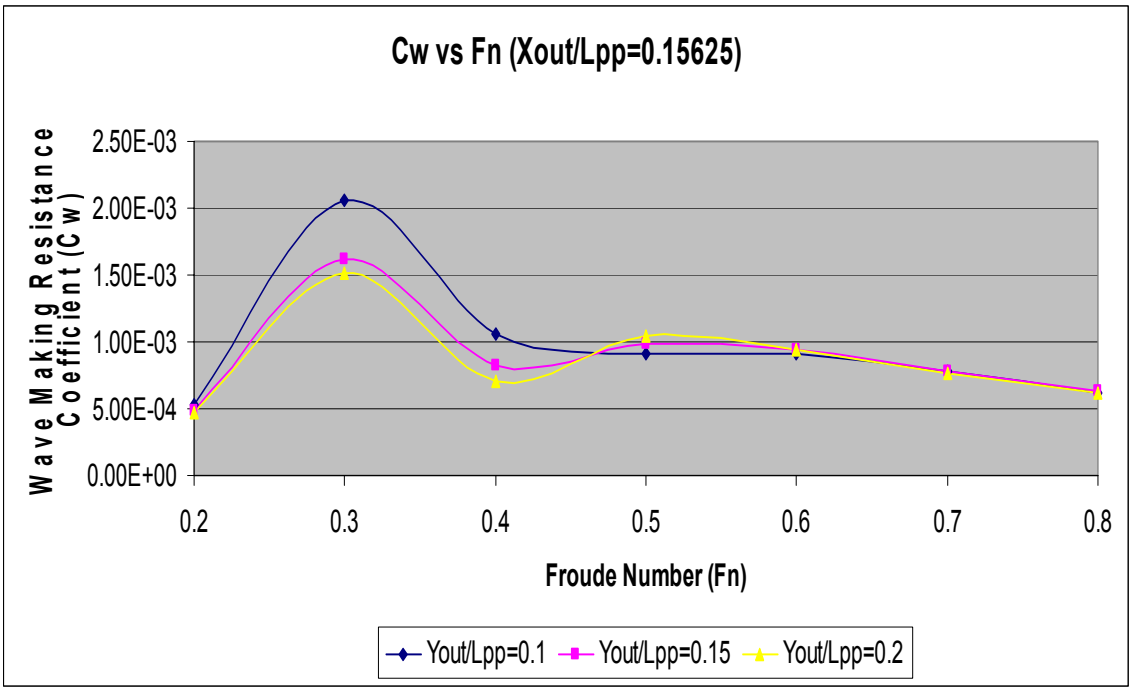

Figure 8. Wave Making Resistance Coefficient Results for $X_{out} / L_{pp} = 0.15625$

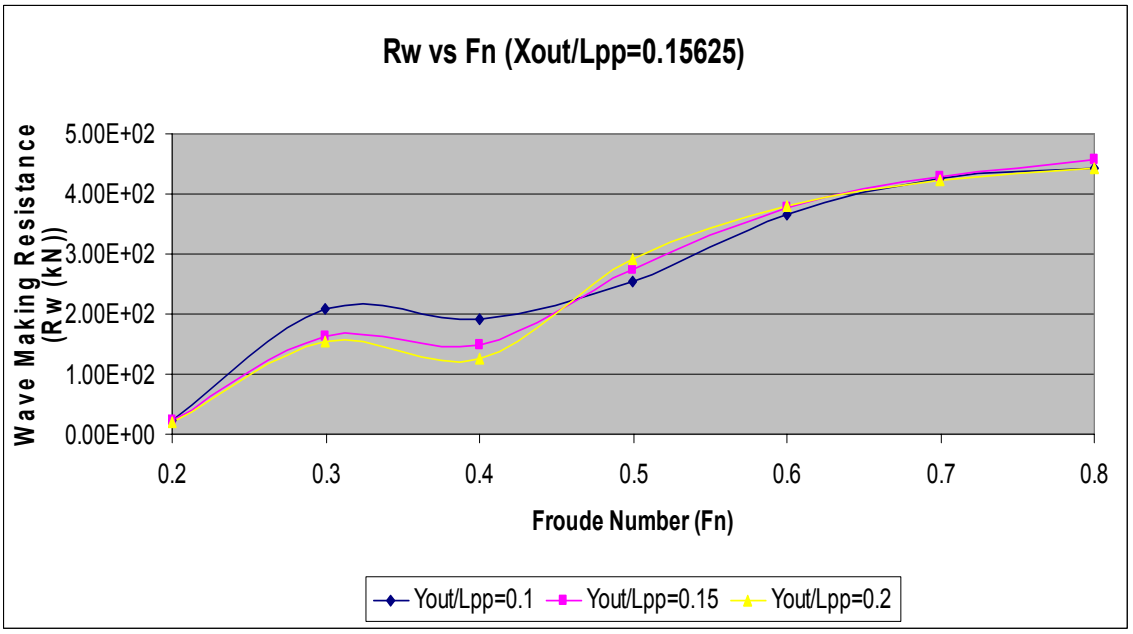

Figure 9. Wave Making Resistance Results for $X_{out} / L_{pp} = 0.15625$

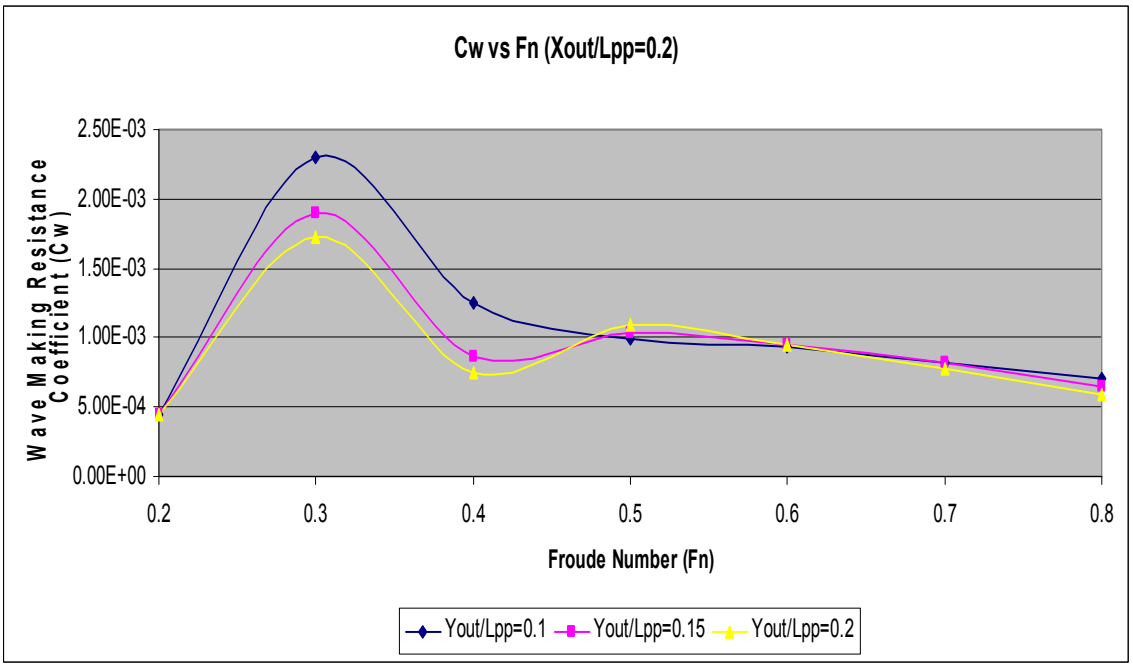

Figure 10. Wave Making Resistance Coefficient Results for $X_{out} / L_{pp} = 0.2$

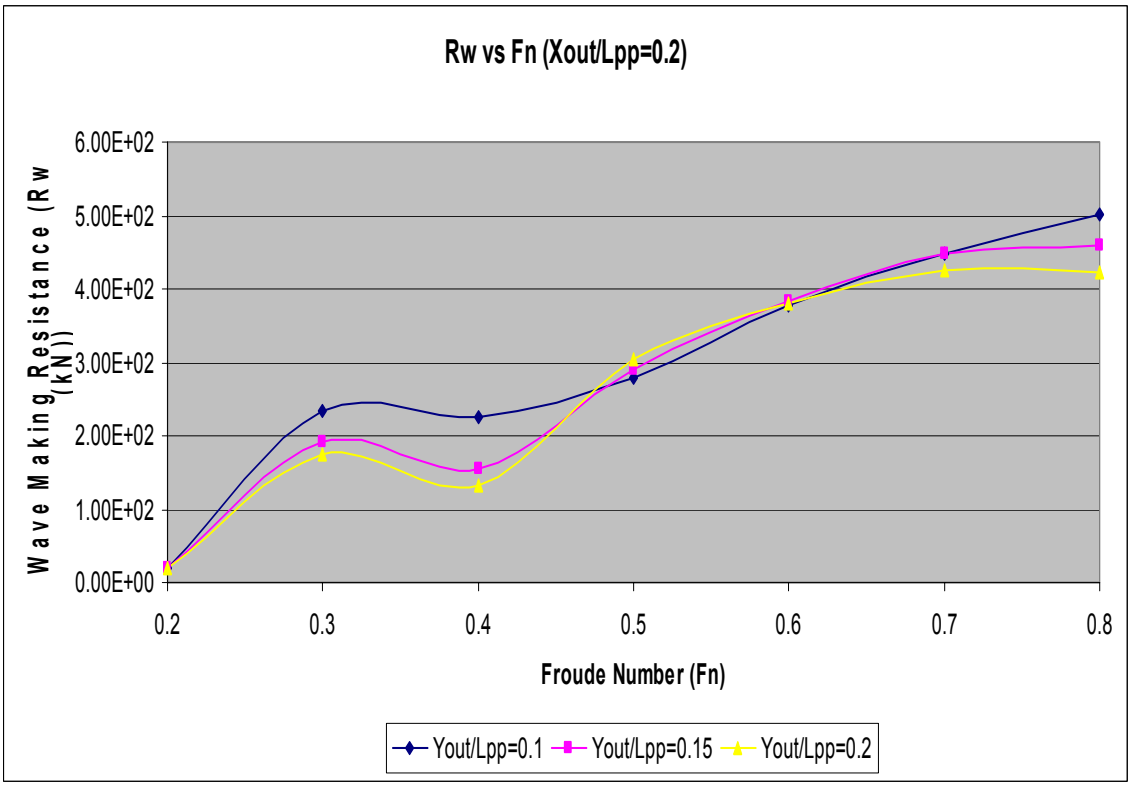

Figure 11. Wave Making Resistance Results for $X_{out} / L_{pp} = 0.2$

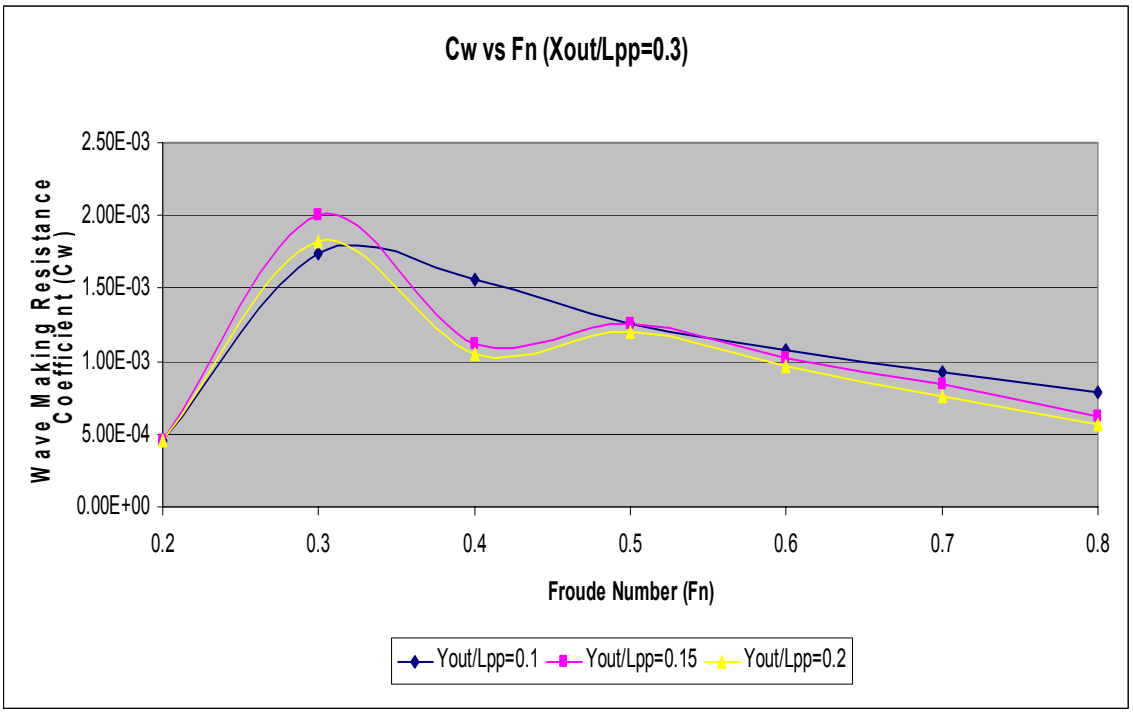

Figure 12. Wave Making Resistance Coefficient Results for $X_{out} / L_{pp} = 0.3$

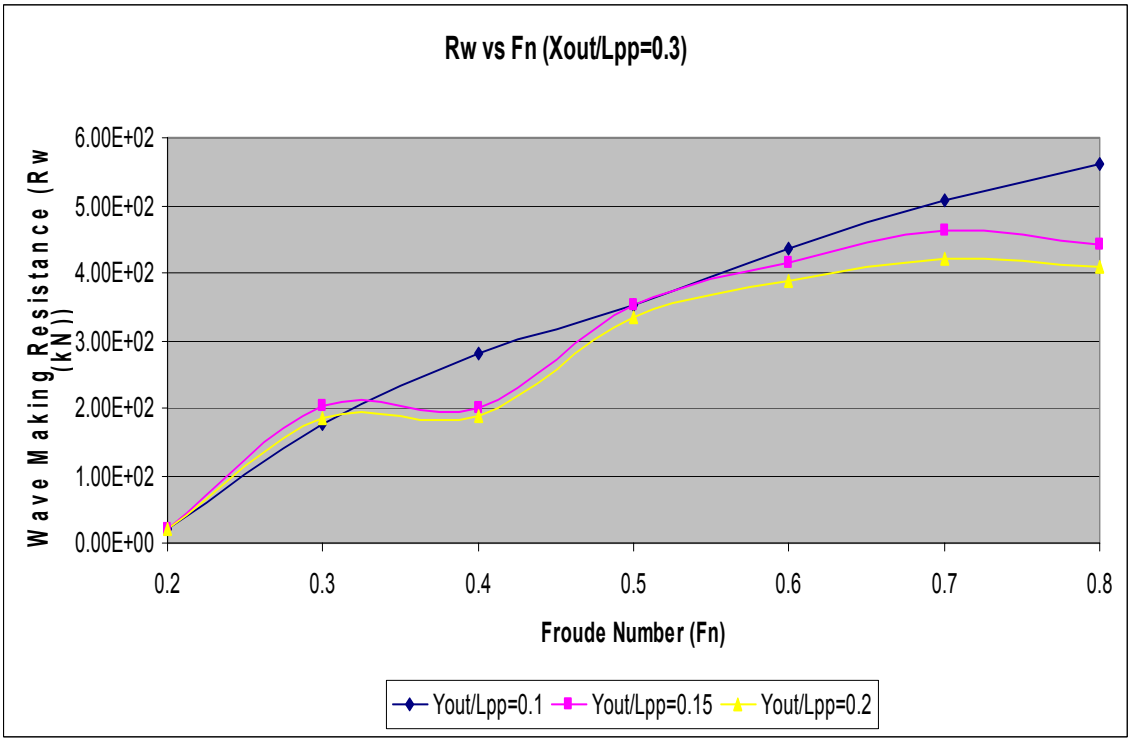

Figure 13. Wave Making Resistance Results for $X_{out} / L_{pp} = 0.3$

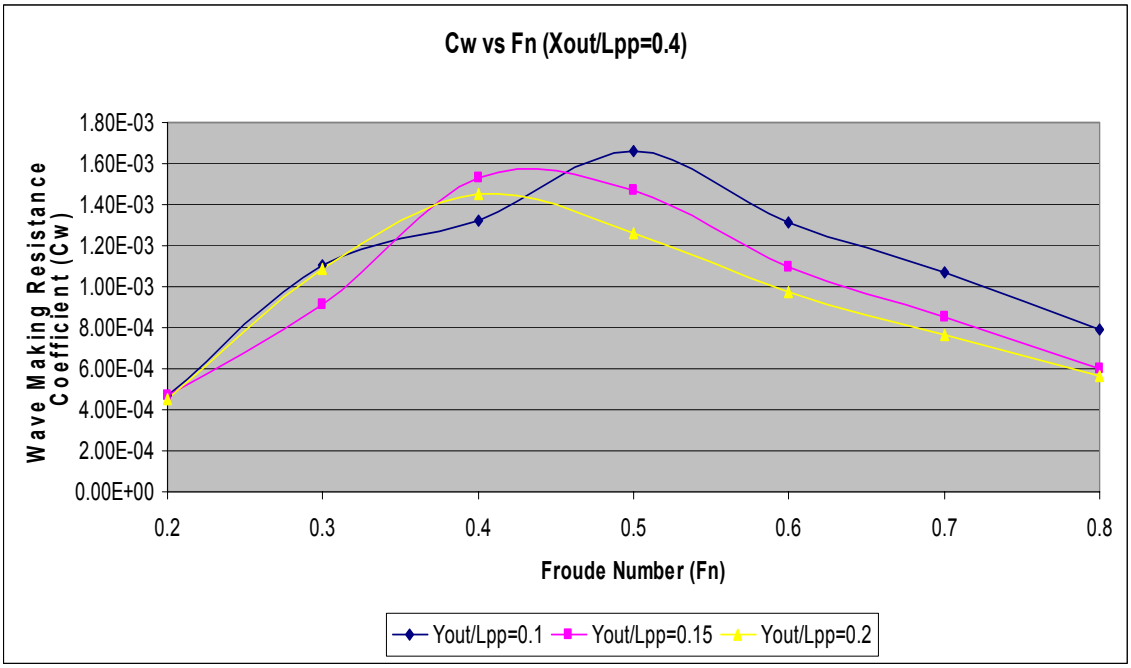

Figure 14. Wave Making Resistance Coefficient Results for $X_{out} / L_{pp} = 0.4$

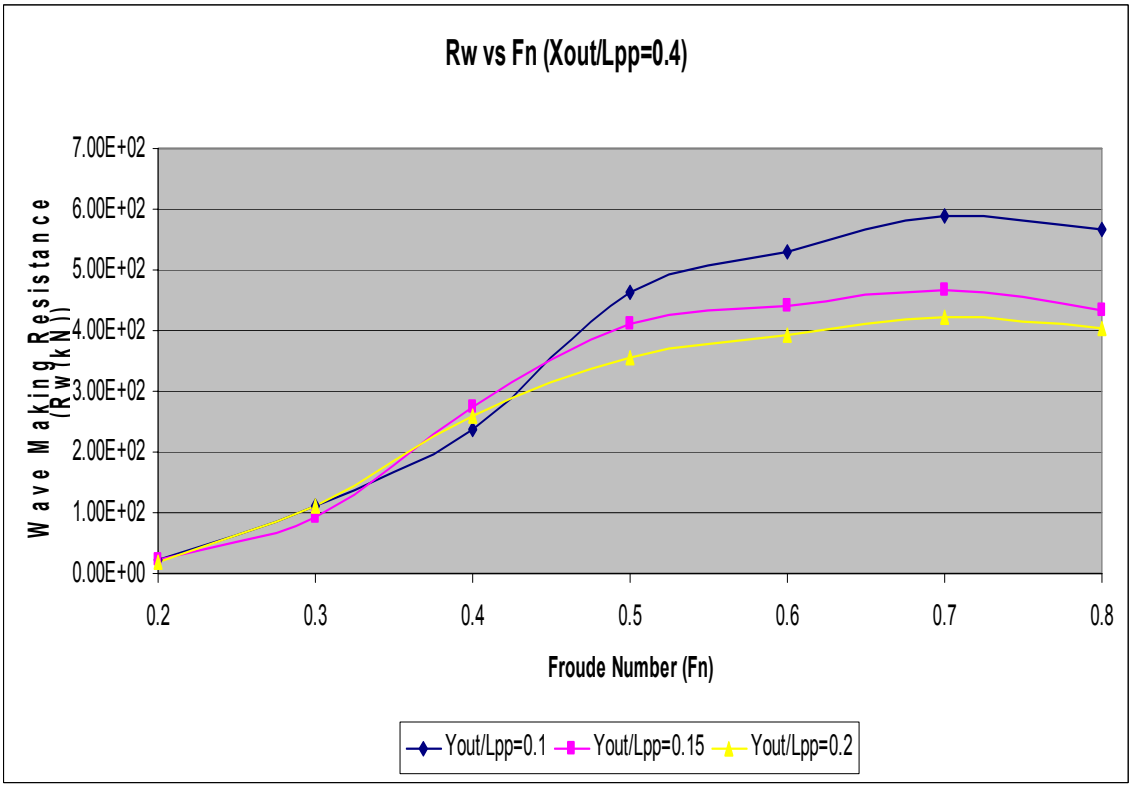

Figure 15. Wave Making Resistance Results for $X_{out} / L_{pp} = 0.4$

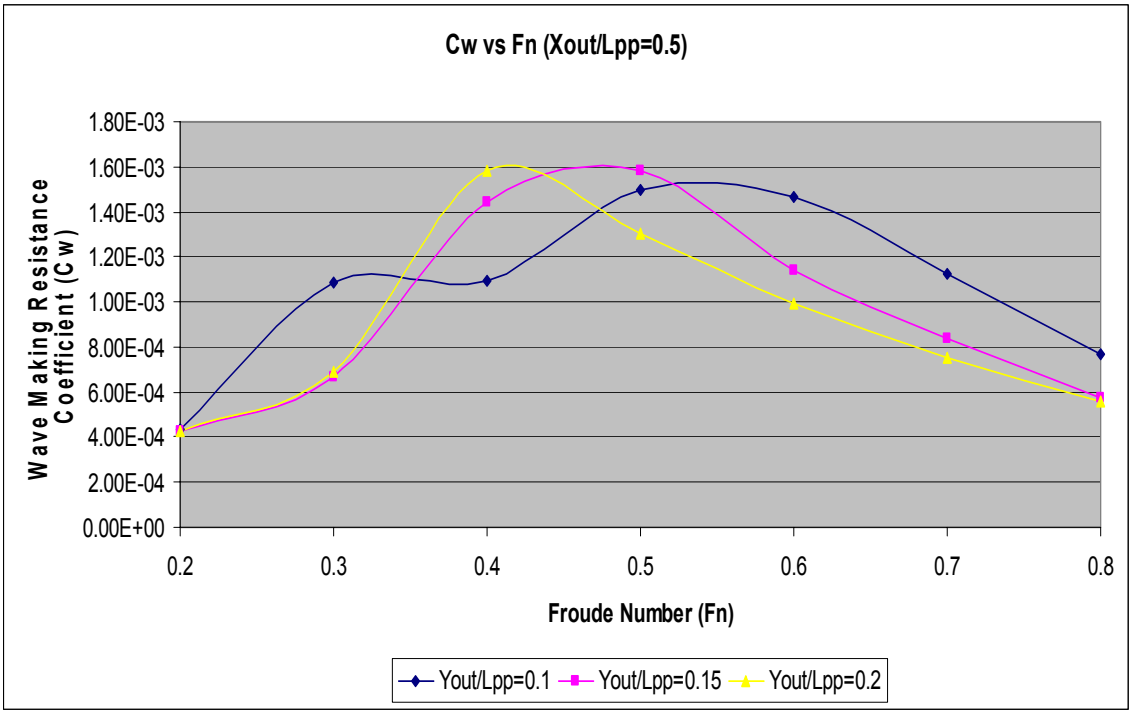

Figure 16. Wave Making Resistance Coefficient Results for $X_{out} / L_{pp} = 0.5$

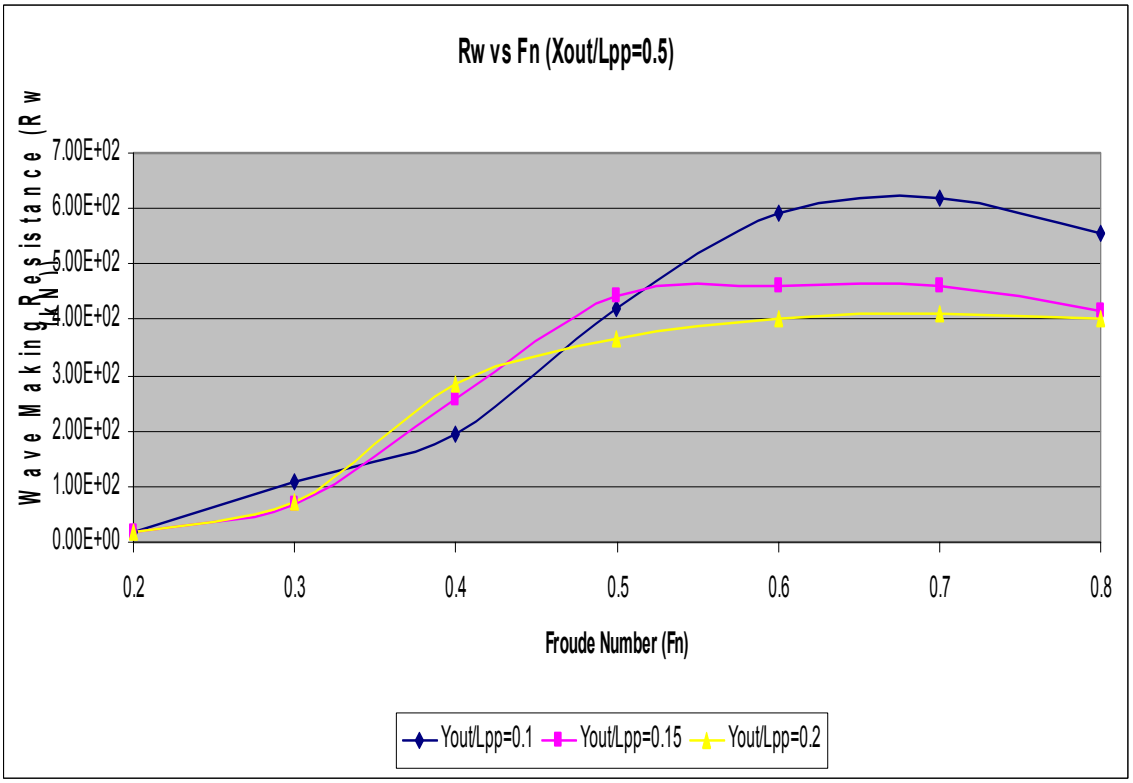

Figure 17. Wave Making Resistance Results for $X_{out} / L_{pp} = 0.5$

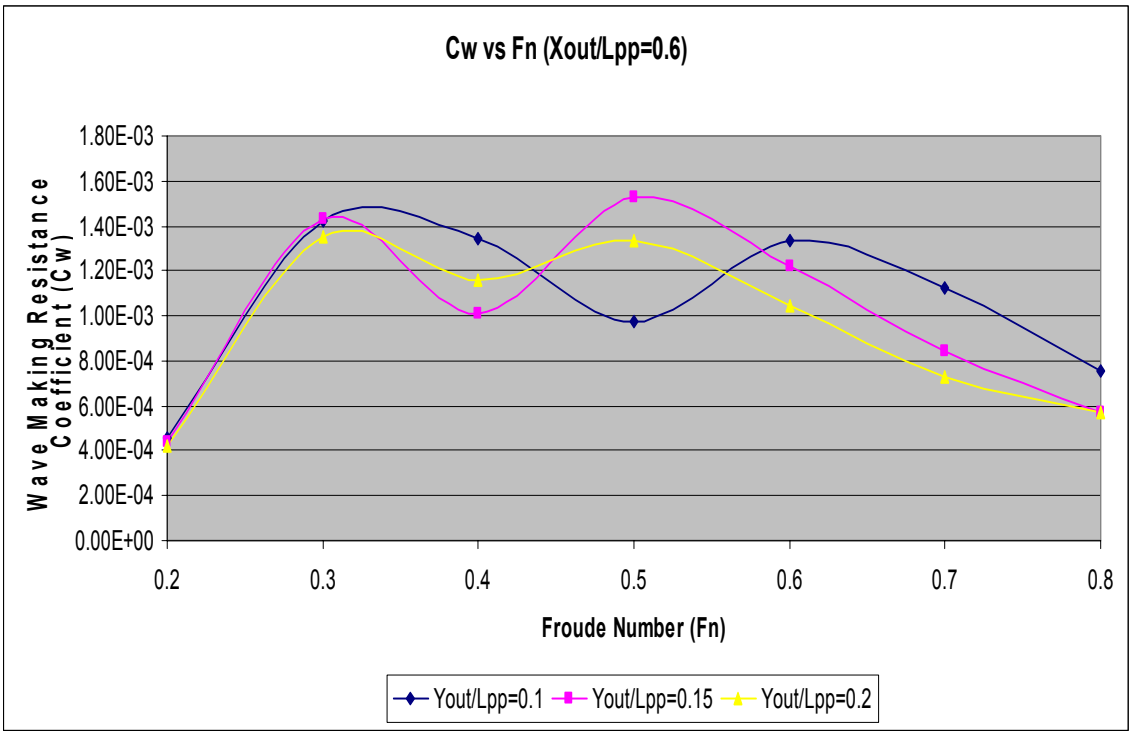

Figure 18. Wave Making Resistance Coefficient Results for $X_{out} / L_{pp} = 0.6$

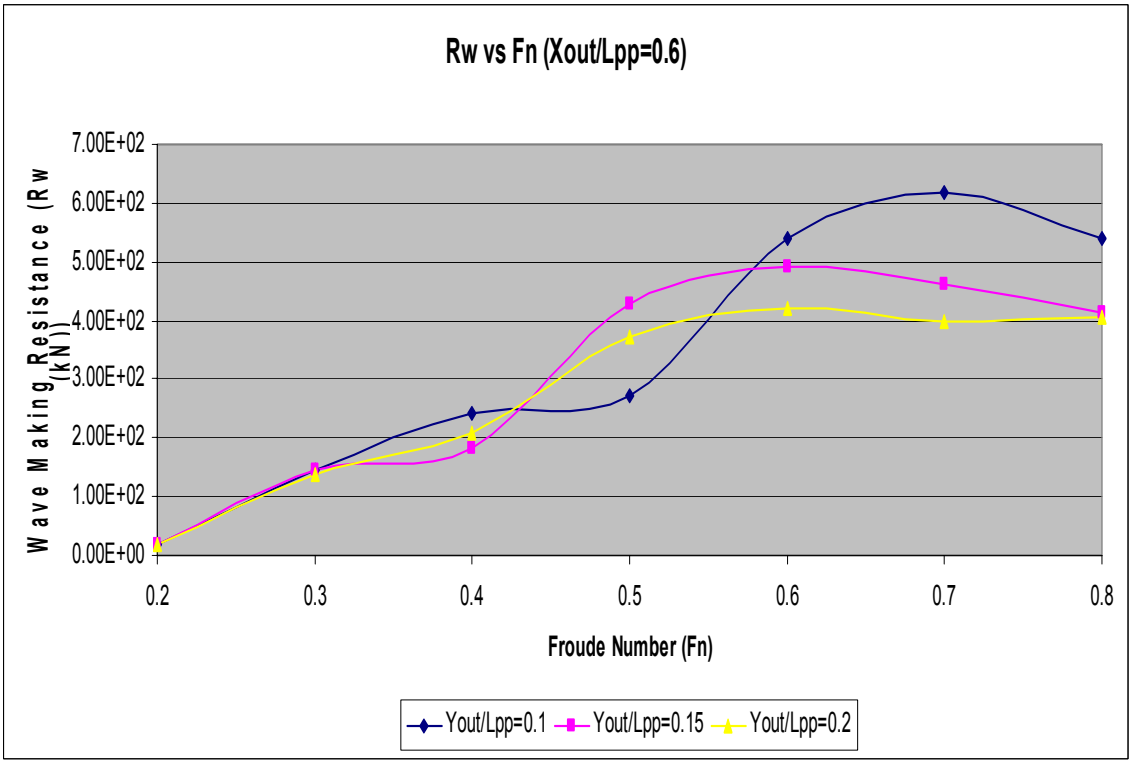

Figure 19. Wave Making Resistance Results for $X_{out} / L_{pp} = 0.6$

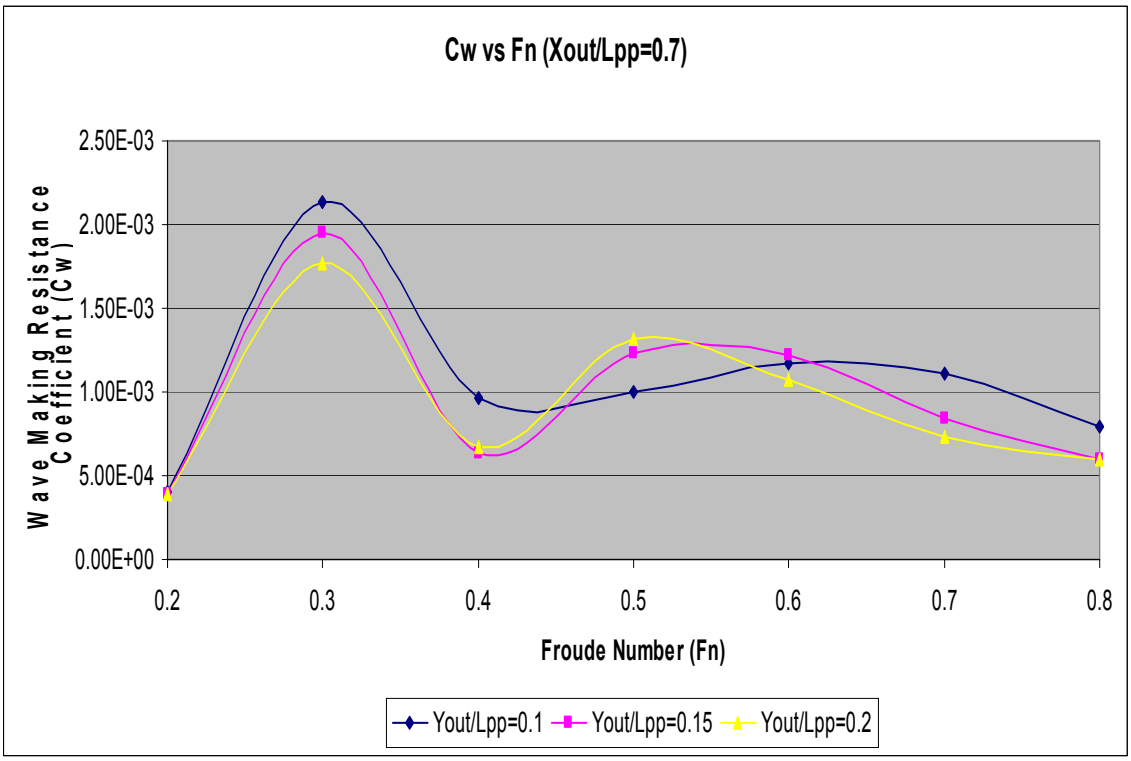

Figure 20. Wave Making Resistance Coefficient Results for $X_{out} / L_{pp} = 0.7$

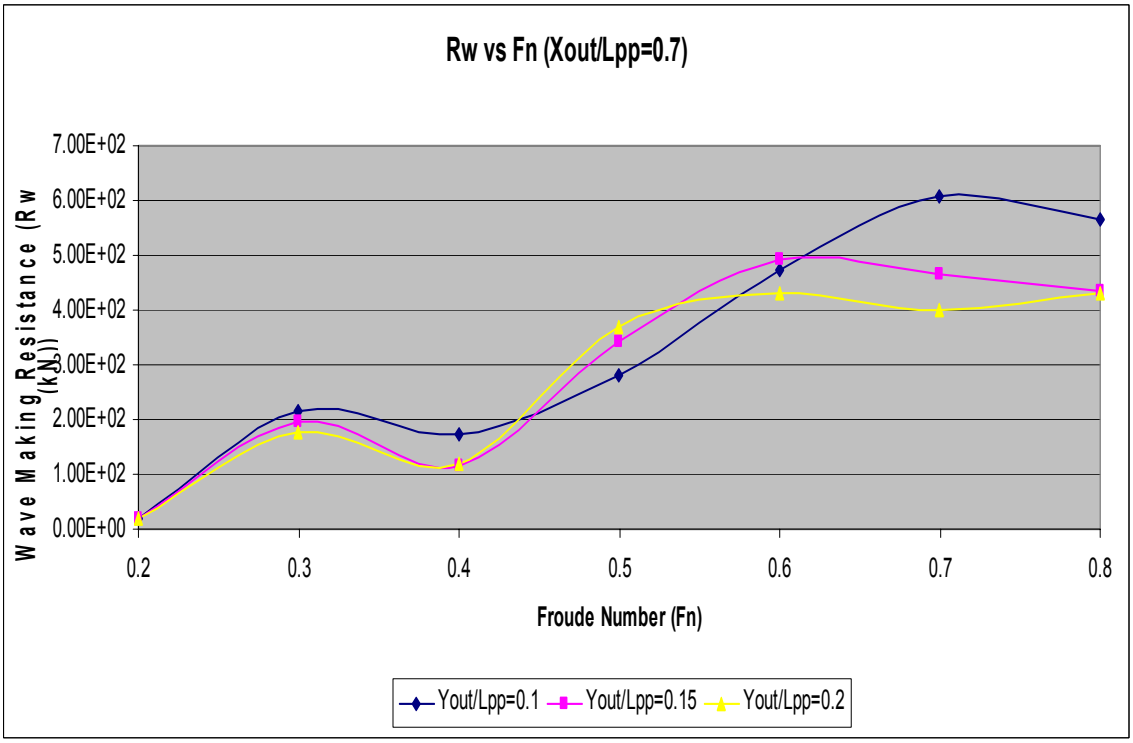

Figure 21. Wave Making Resistance Results for $X_{out} / L_{pp} = 0.7$

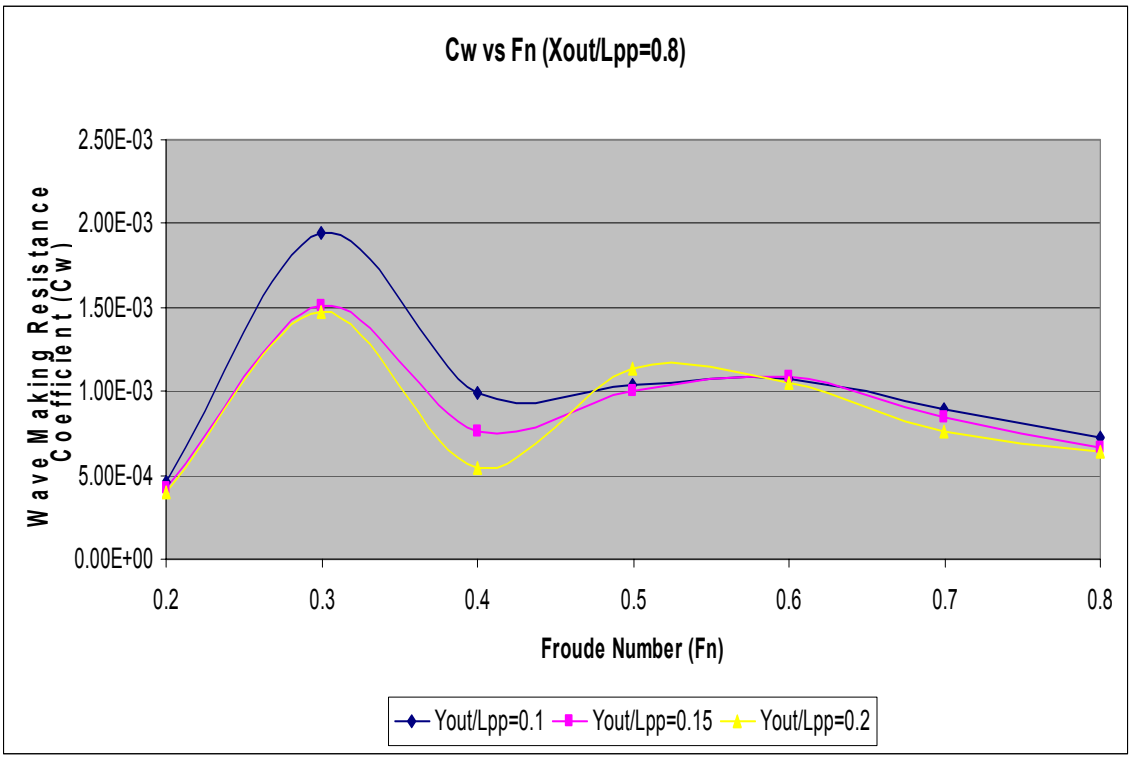

Figure 22. Wave Making Resistance Coefficient Results for $X_{out} / L_{pp} = 0.8$

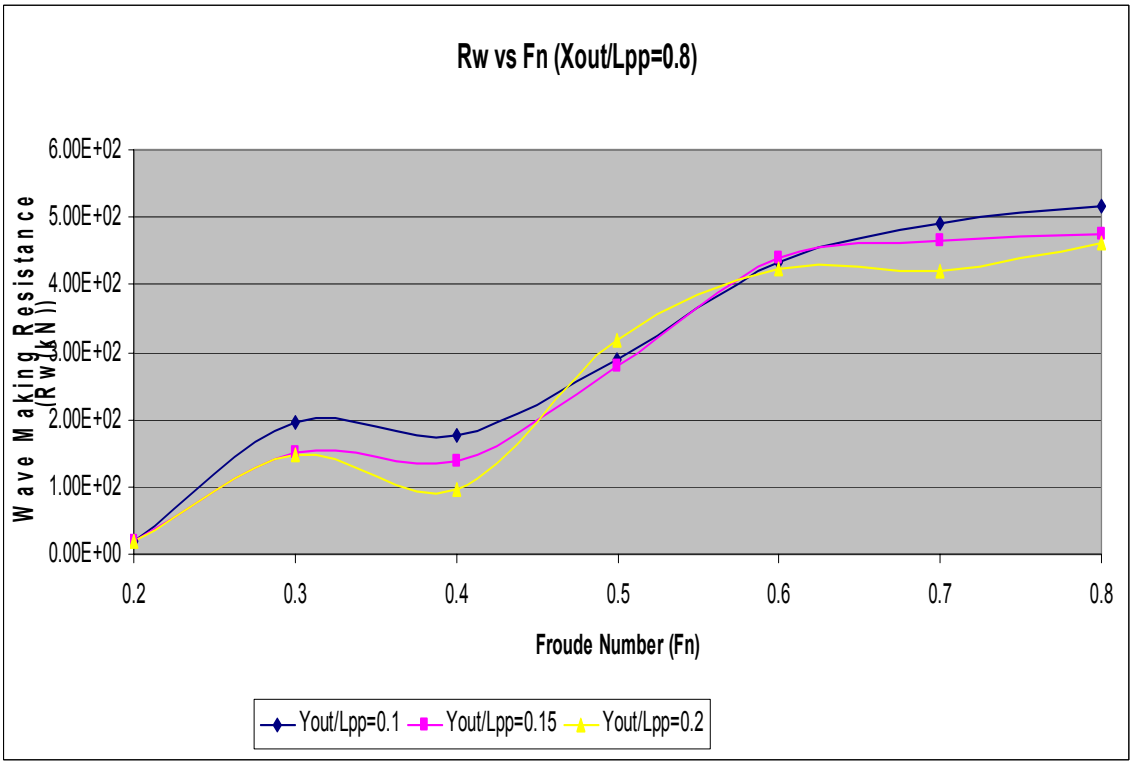

Figure 23. Wave Making Resistance Results for $X_{out} / L_{pp} = 0.8$

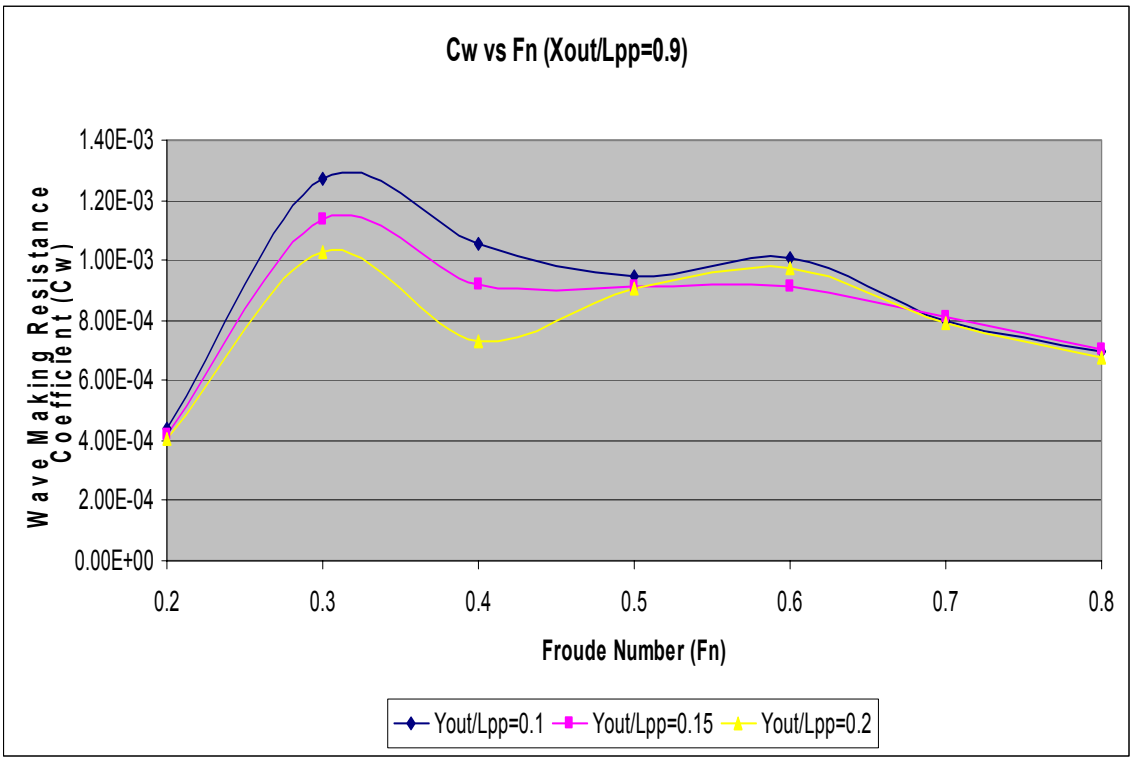

Figure 24. Wave Making Resistance Coefficient Results for $X_{out} / L_{pp} = 0.9$

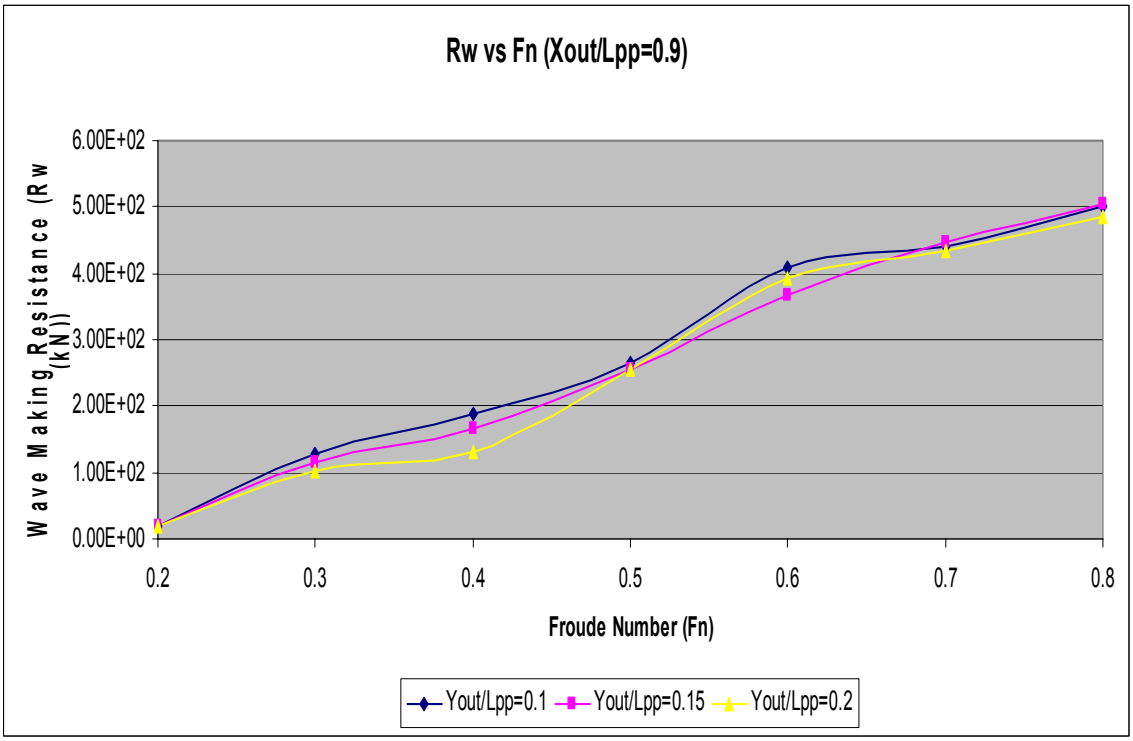

Figure 25. Wave Making Resistance Results for $X_{out} / L_{pp} = 0.9$

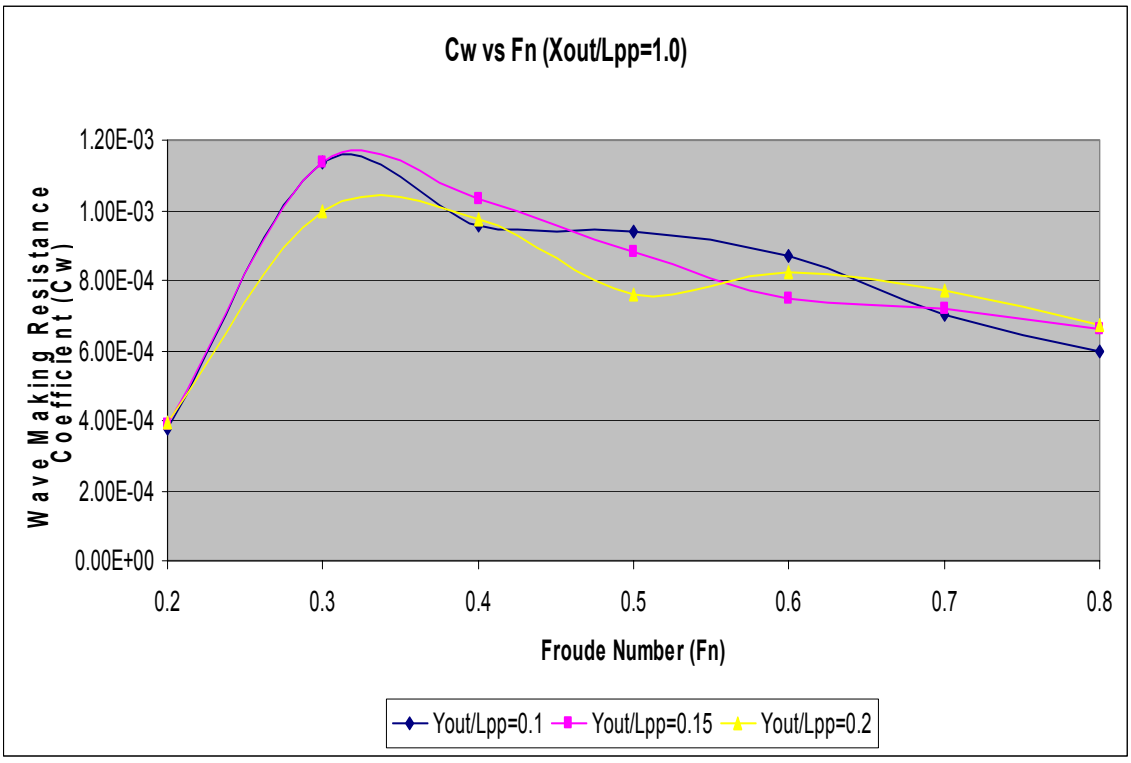

Figure 26. Wave Making Resistance Coefficient Results for $X_{out} / L_{pp} = 1.0$

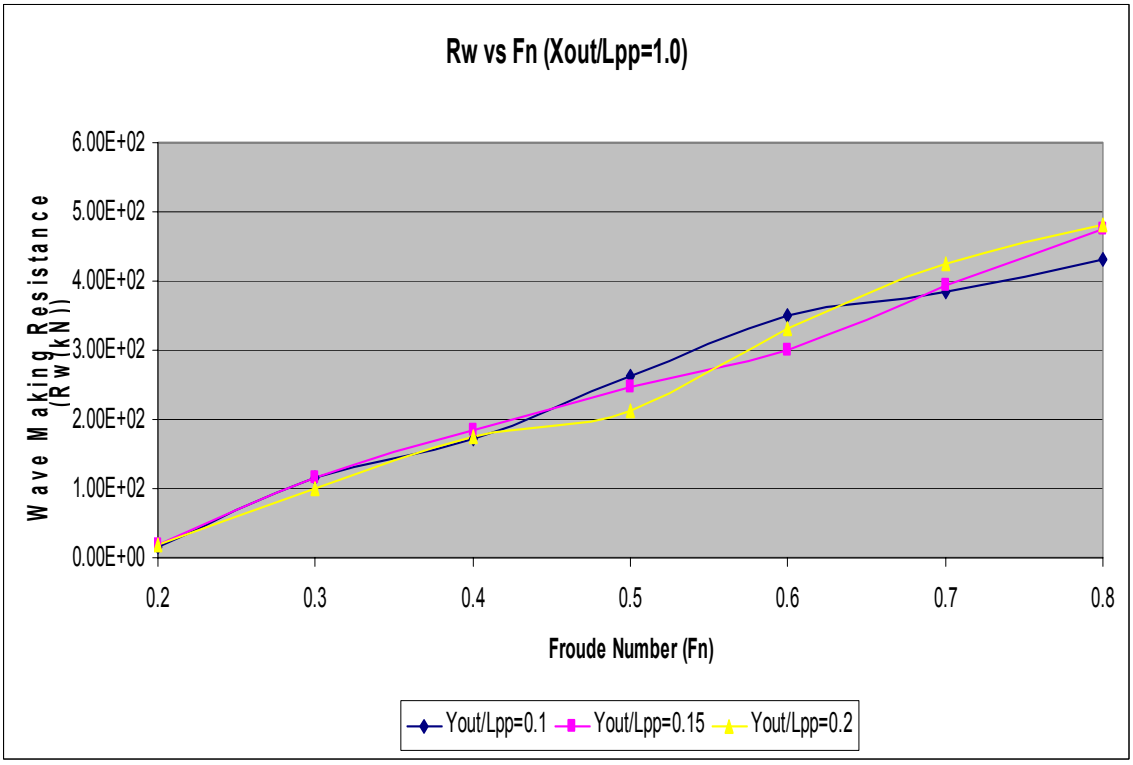

Figure 27. Wave Making Resistance Results for $X_{out} / L_{pp} = 1.0$

C. EFFECTS OF SIDE HULL LONGITUDINAL PLACEMENT

Figures 28 through 33 show the effects of longitudinal placement of the side hulls in terms of Froude number. We can see that, in general, the results depend highly on the Froude number. It is possible to optimize wave making resistance by suitable positioning of the side hulls, but such an optimization needs to be tuned to a specific operating speed.

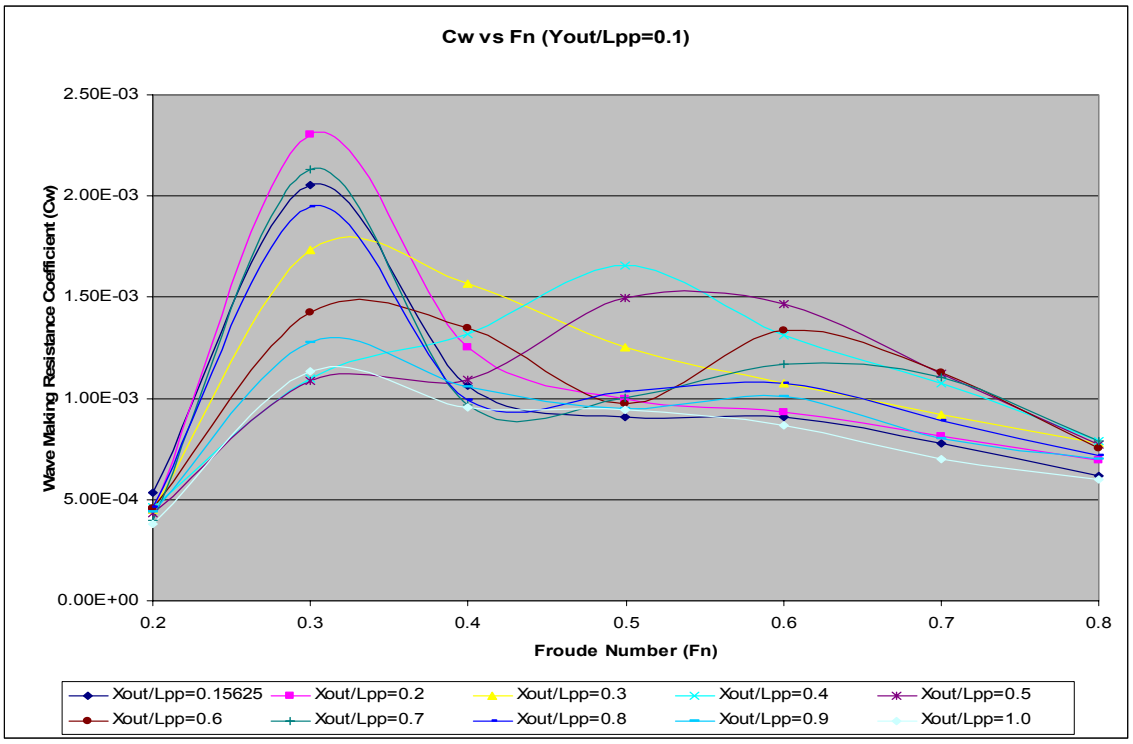

Figure 28. Wave Making Resistance Coefficient Results for $Y_{out} / L_{pp} = 0.1$

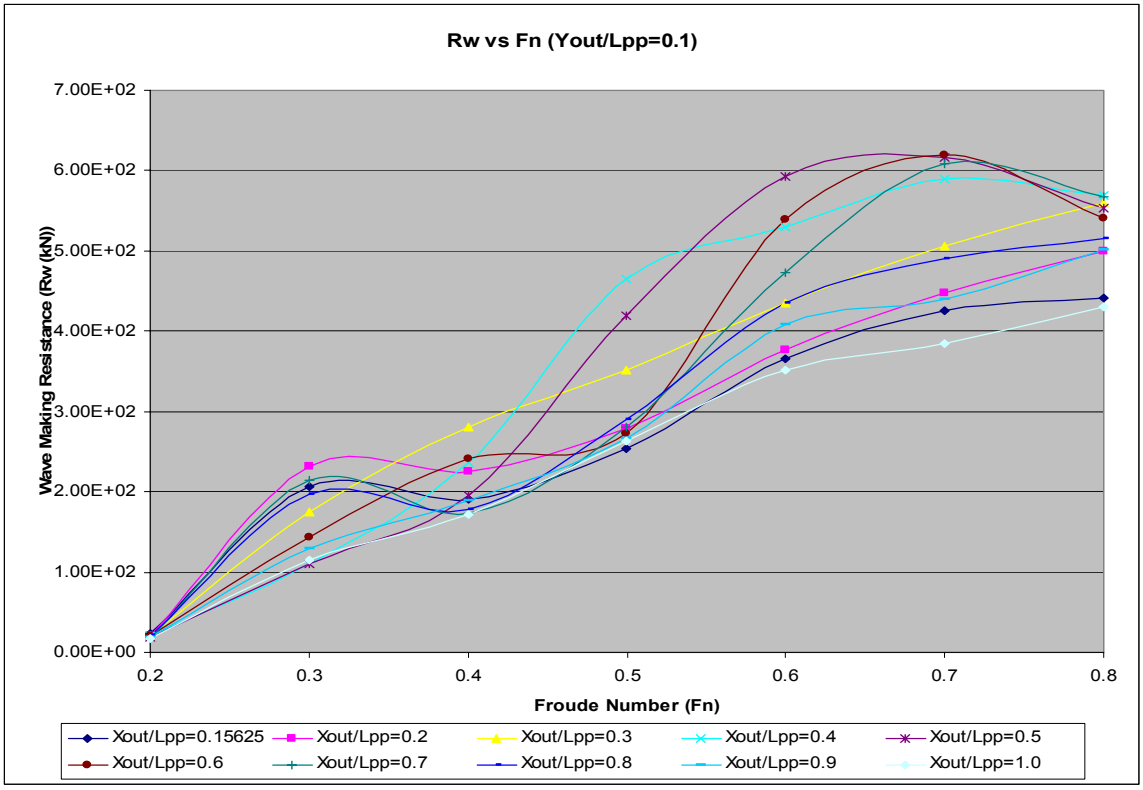

Figure 29. Wave Making Resistance Results for $Y_{out} / L_{pp} = 0.1$

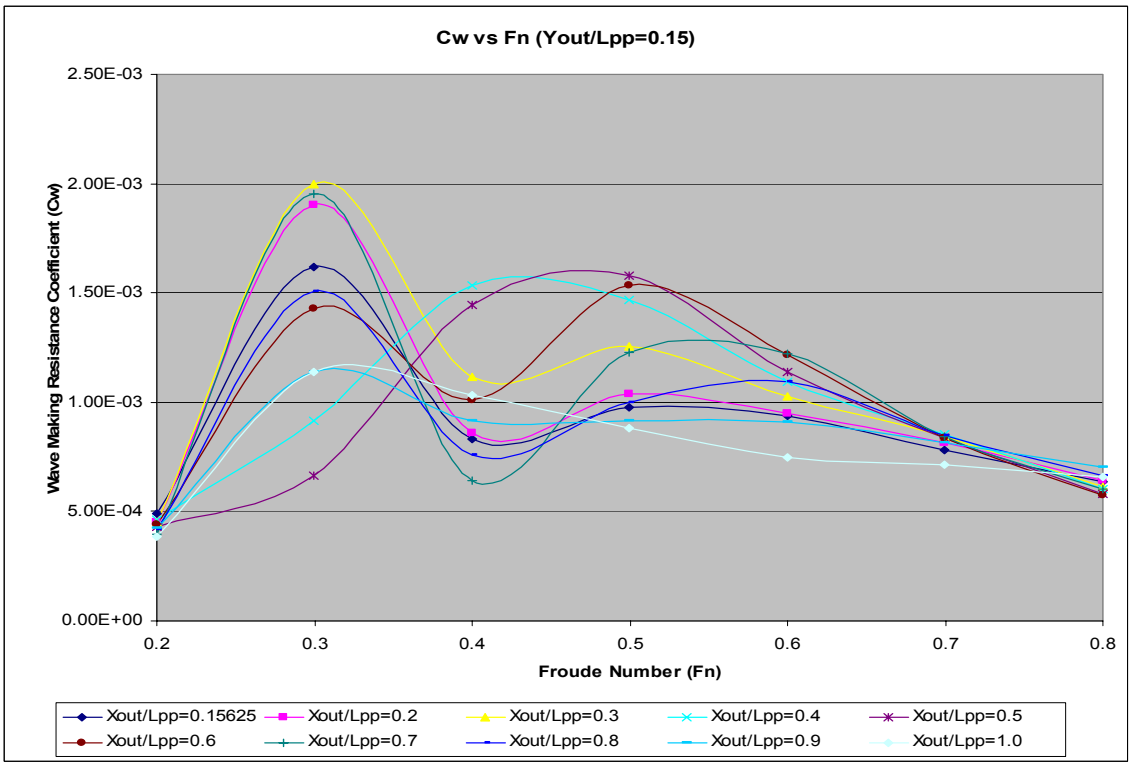

Figure 30. Wave Making Resistance Coefficient Results for $Y_{out} / L_{pp} = 0.15$

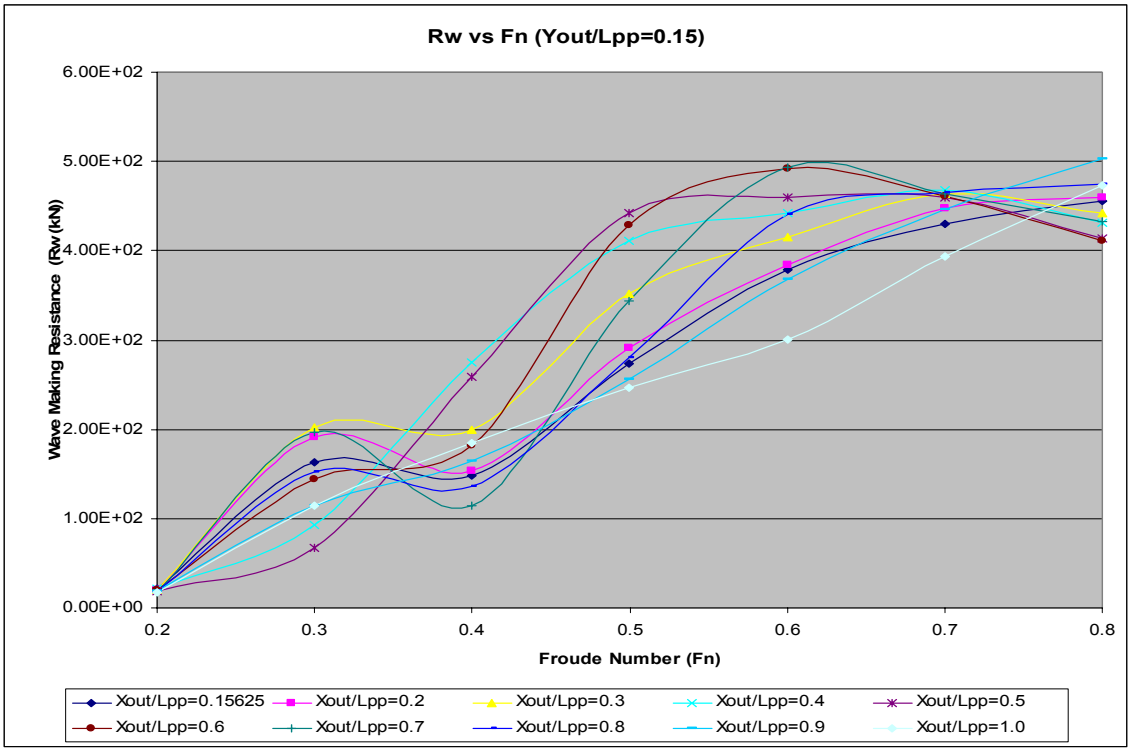

Figure 31. Wave Making Resistance Results for $Y_{out} / L_{pp} = 0.15$

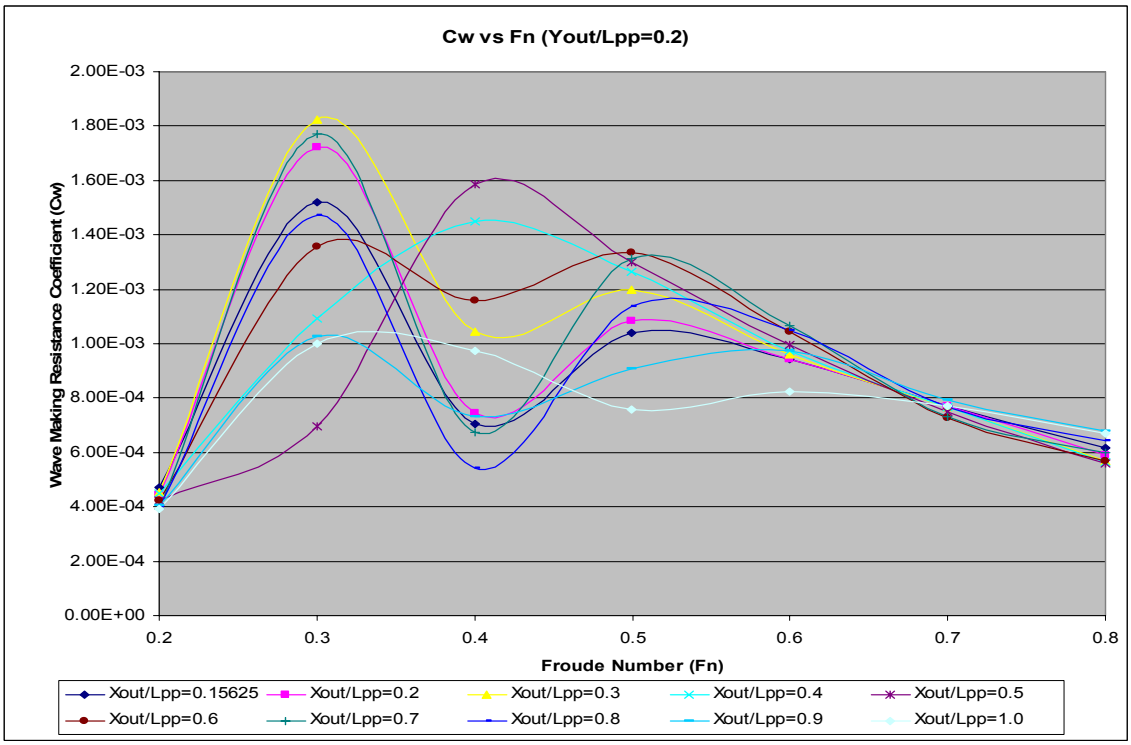

Figure 32. Wave Making Resistance Coefficient Results for $Y_{out} / L_{pp} = 0.2$

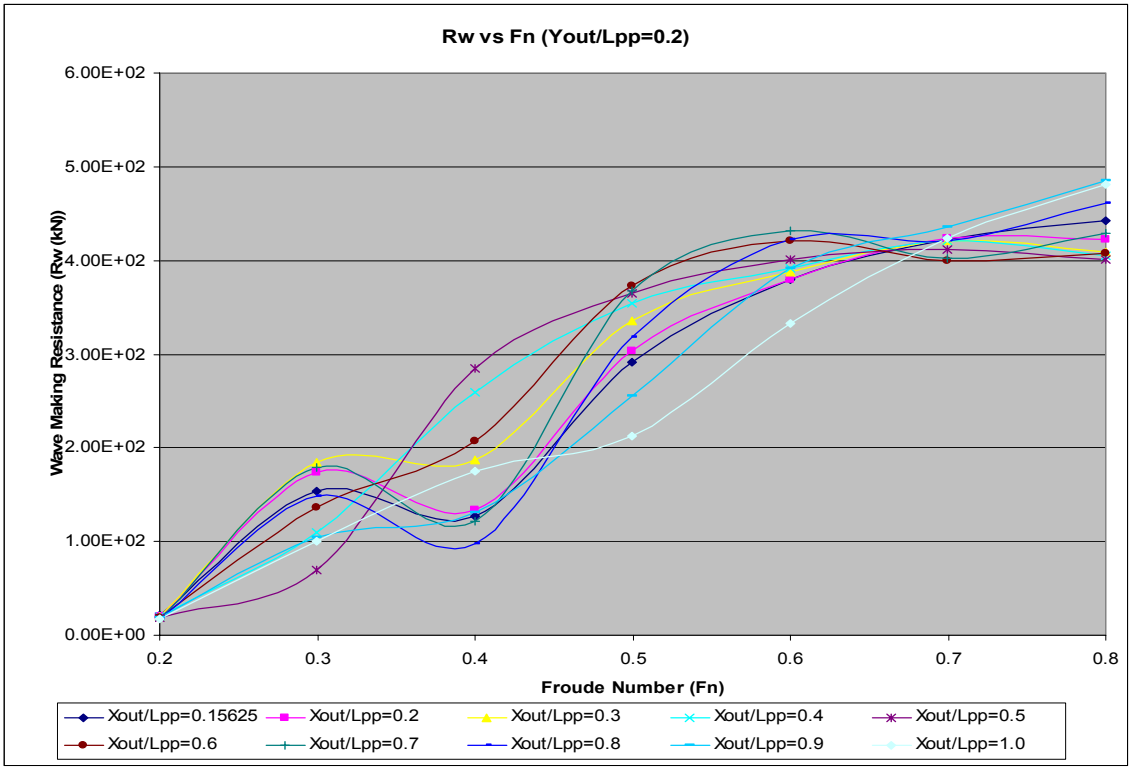

Figure 33. Wave Making Resistance Results for $Y_{out} / L_{pp} = 0.2$

D. WAVE PATTERN PREDICTIONS

The steady wave patterns for all three side-main hull separation ratios, at all speeds were predicted. Some of these patterns are presented in the following figures. We can see the interference increases as the separation ratio decreases due to increasing proximity between the hulls. The wave patterns are all within the Kelvin Wave Pattern sector as described previously. From the figures it can be seen that as the vessel speed increases, more diverging waves are seen. For lower speeds, more transverse waves exist. The figures describe Kelvin Wave Pattern for three transverse and three longitudinal positions of side hulls at seven different forward speeds, which comply with Froude Numbers 0.2, 0.3, 0.4, 0.5, 0.6, 0.7, and 0.8.

Green portions of the figure present free surface with zero elevation or a very low elevation. Yellow to red spots describe positive elevation, where the darker color stands for higher waves. Light blue and blue present negative elevation, i.e. wave troughs. As the color becomes darker the trough is deeper.

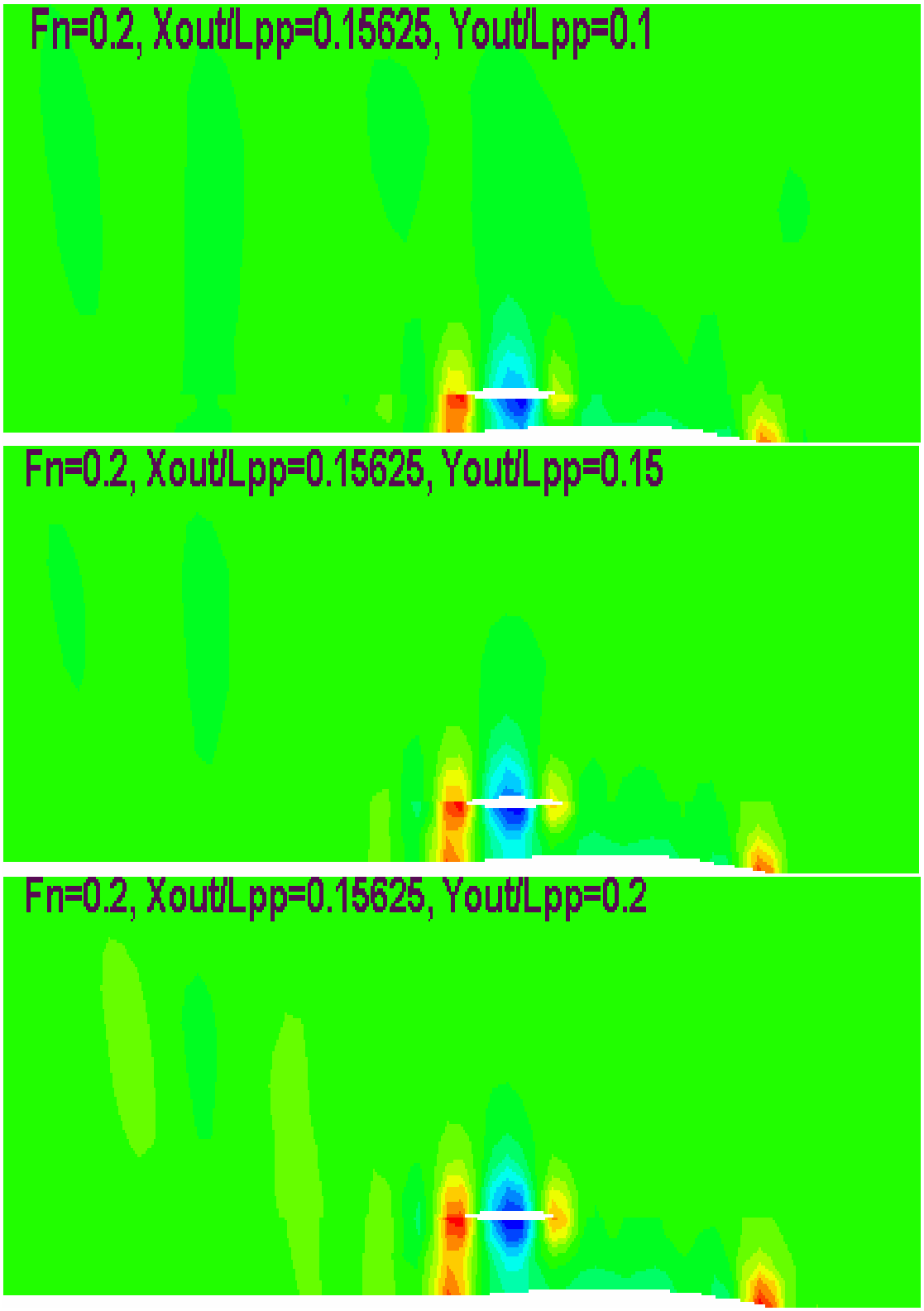

Figure 34. Wave Pattern for $X_{out} / L_{pp} = 0.15625$, at Froude Number 0.2

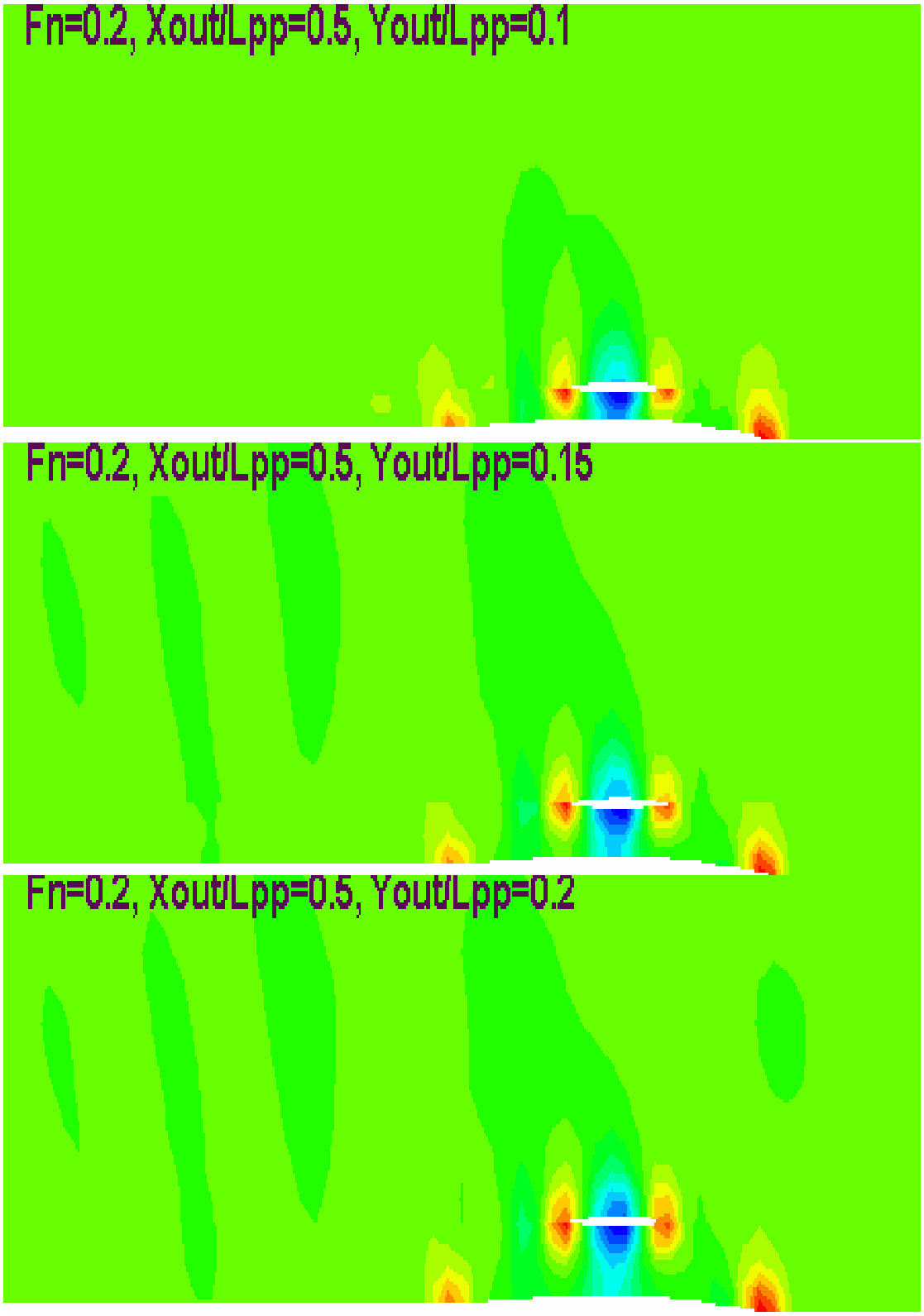

Figure 35. Wave Pattern for $X_{out} / L_{pp} = 0.5$, at Froude Number 0.2

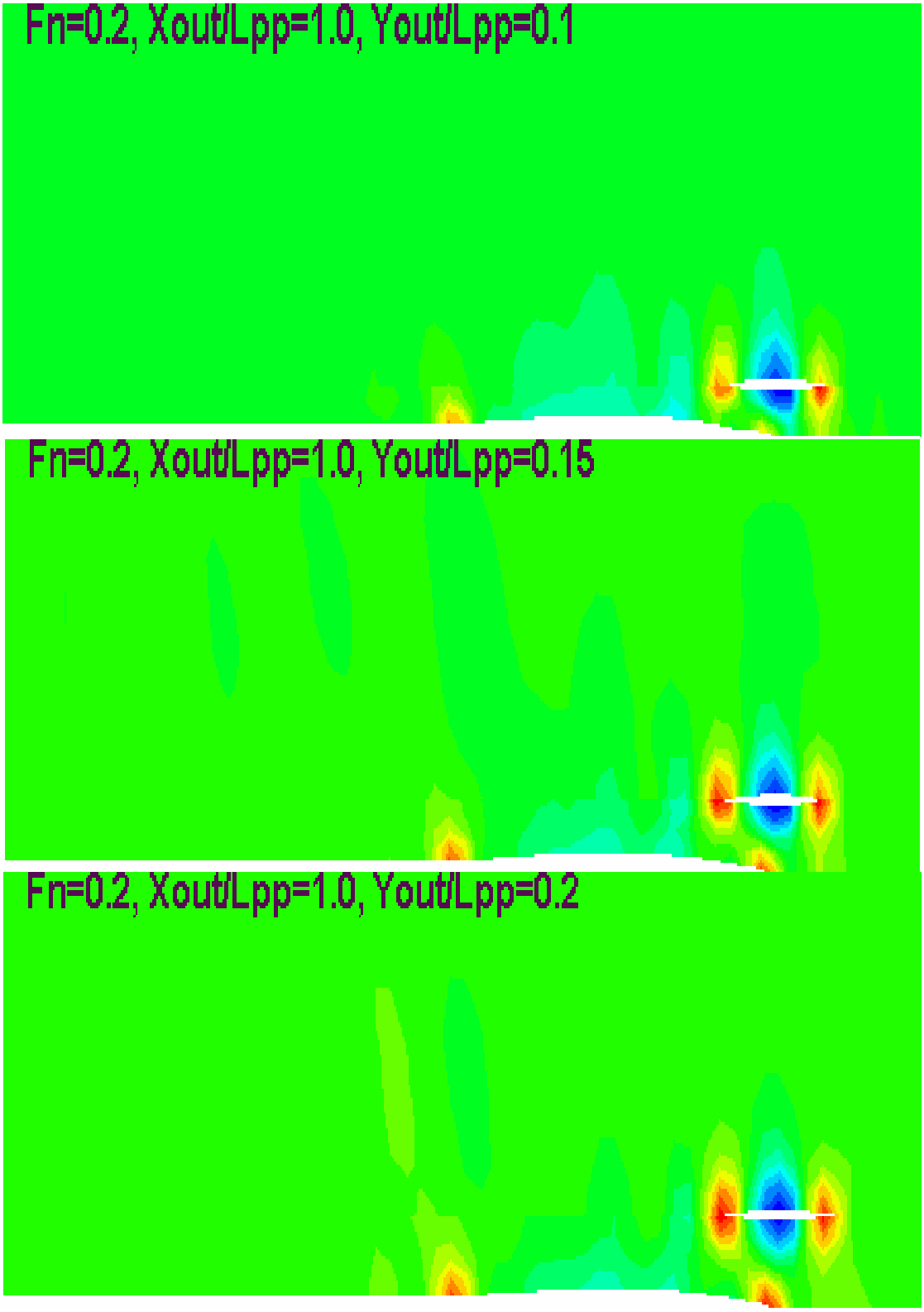

Figure 36. Wave Pattern for $X_{out} / L_{pp} = 1.0$, at Froude Number 0.2

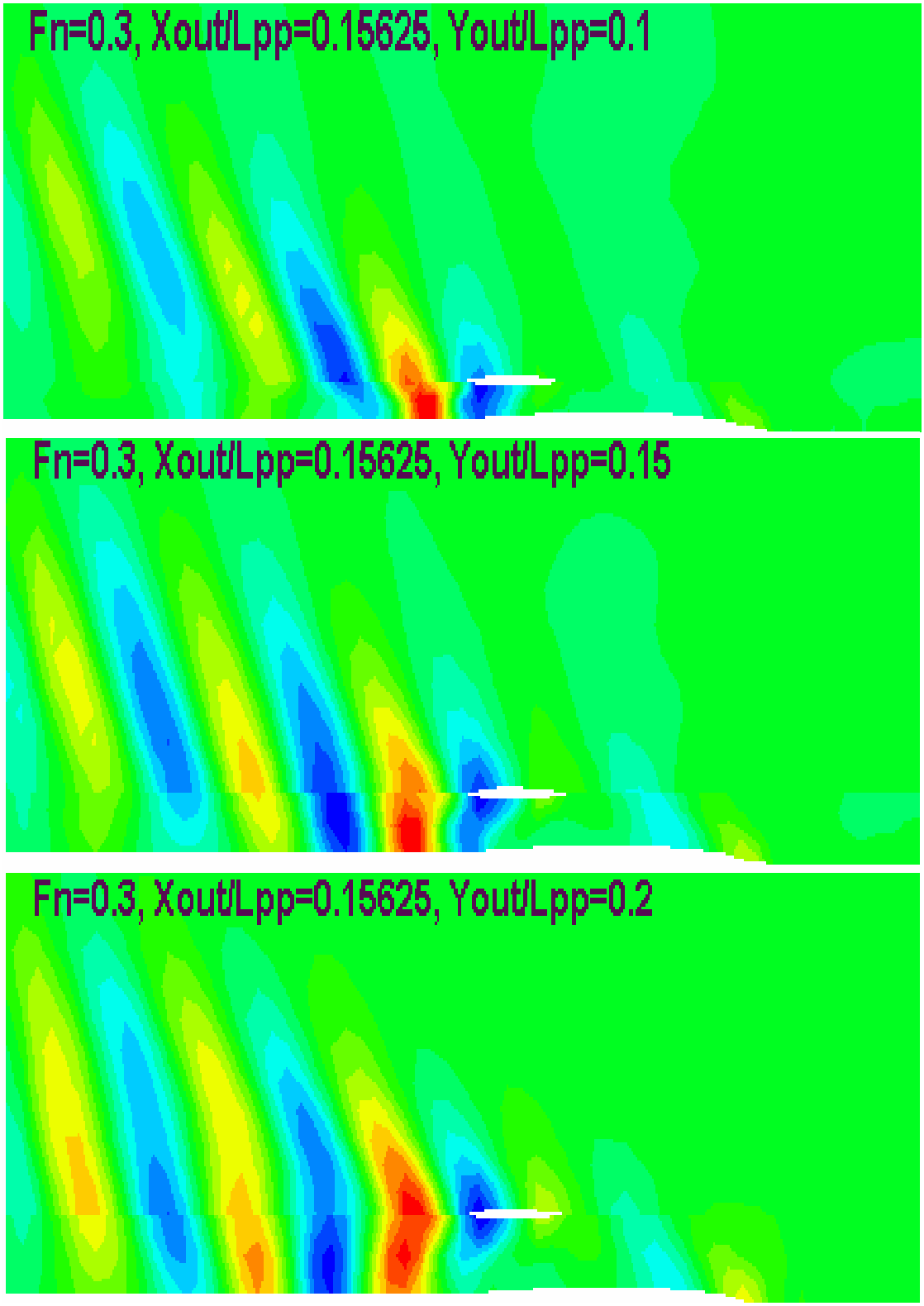

Figure 37. Wave Pattern for $X_{out} / L_{pp} = 0.15625$, at Froude Number 0.3

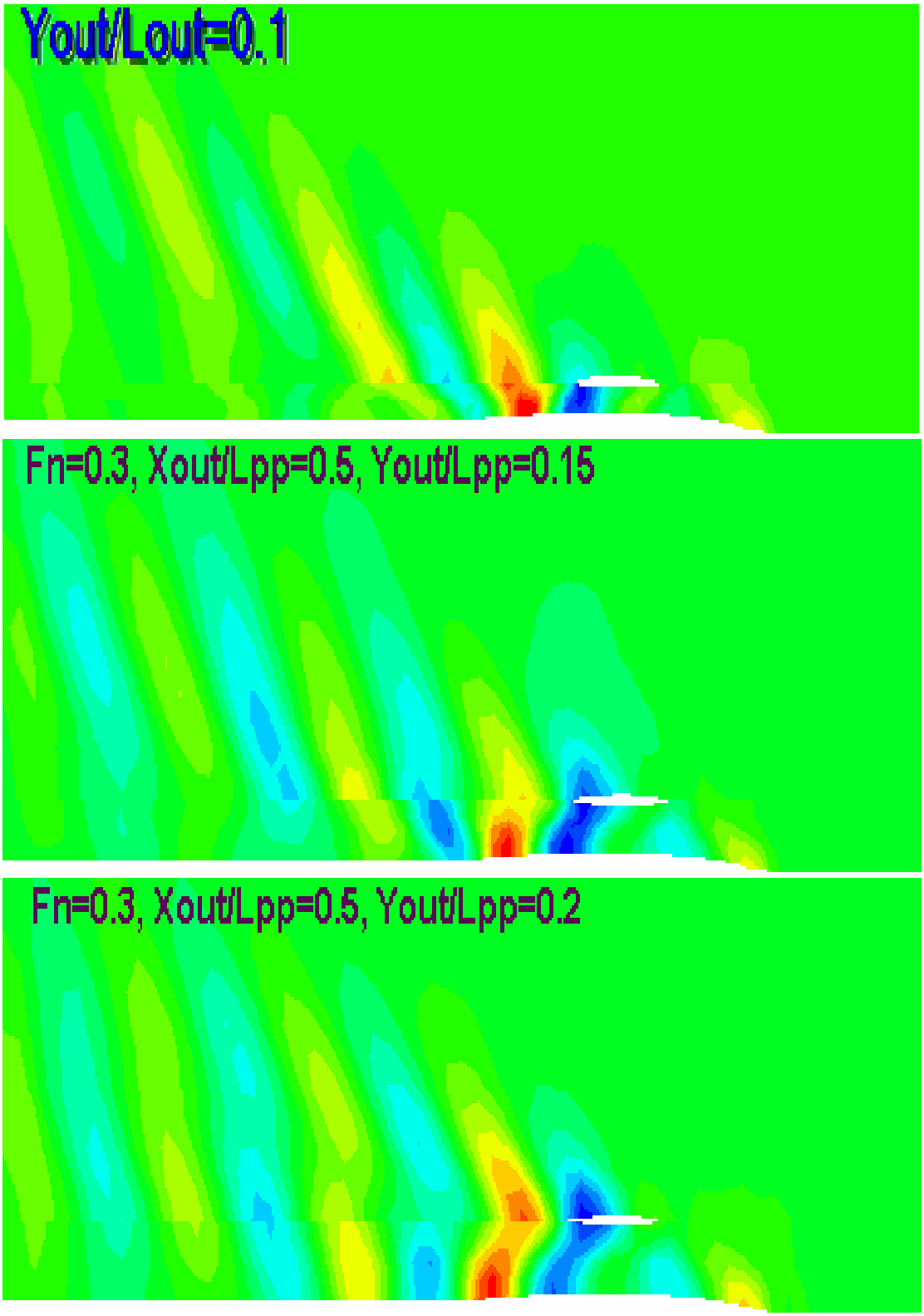

Figure 38. Wave Pattern for $X_{out} / L_{pp} = 0.5$, at Froude Number 0.3

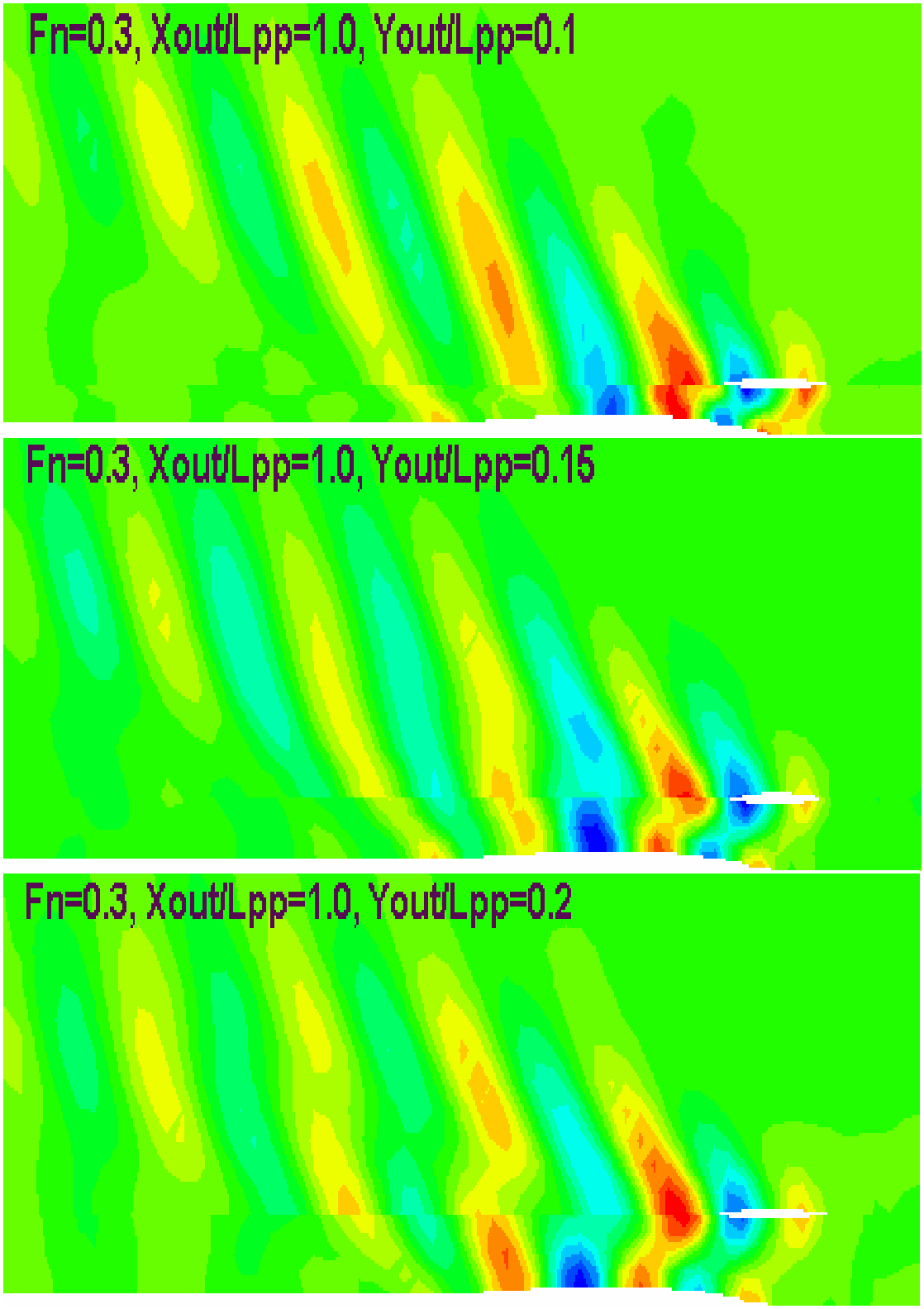

Figure 39. Wave Pattern for $X_{out} / L_{pp} = 1.0$, at Froude Number 0.3

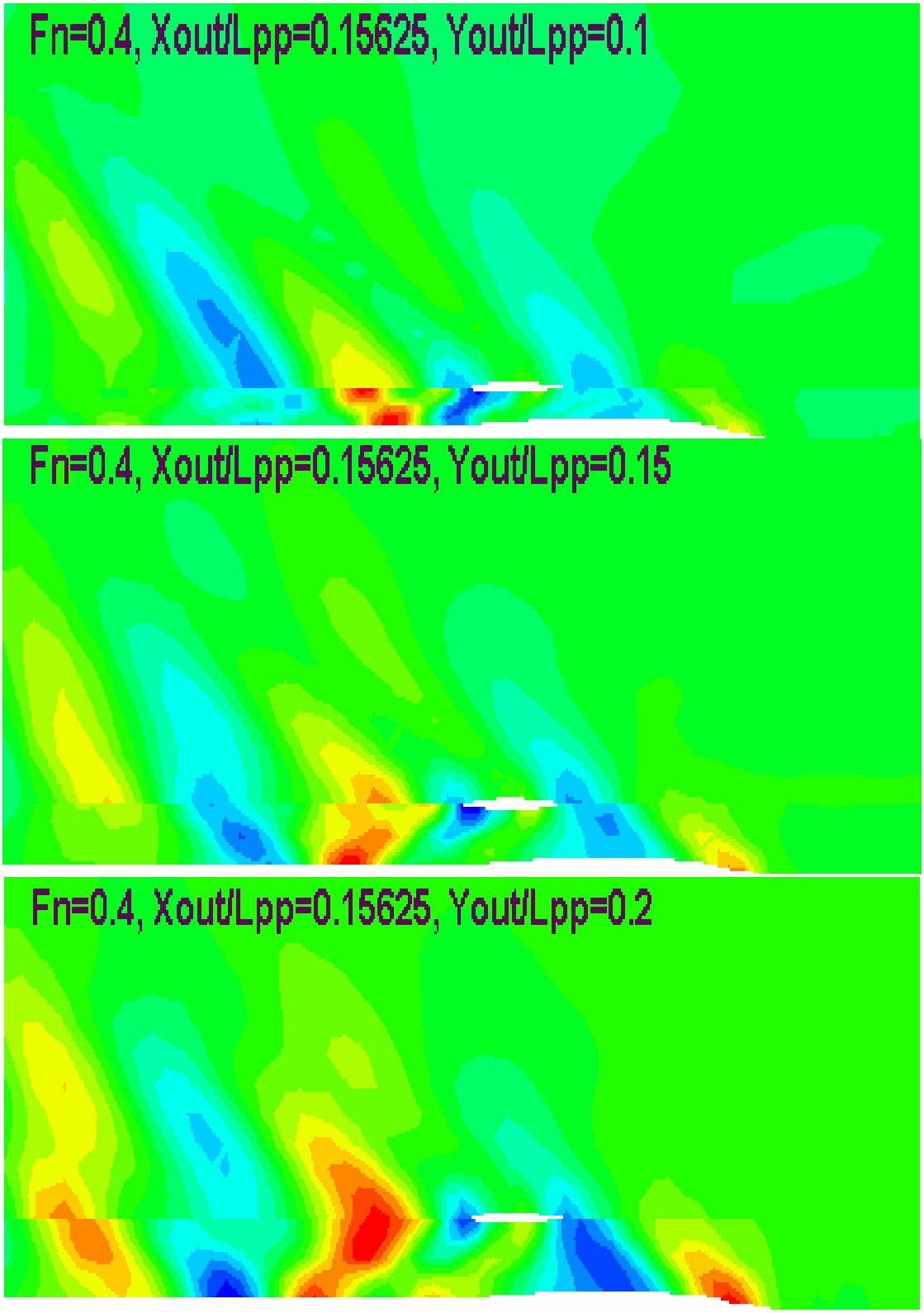

Figure 40. Wave Pattern for $X_{out} / L_{pp} = 0.15625$, at Froude Number 0.4

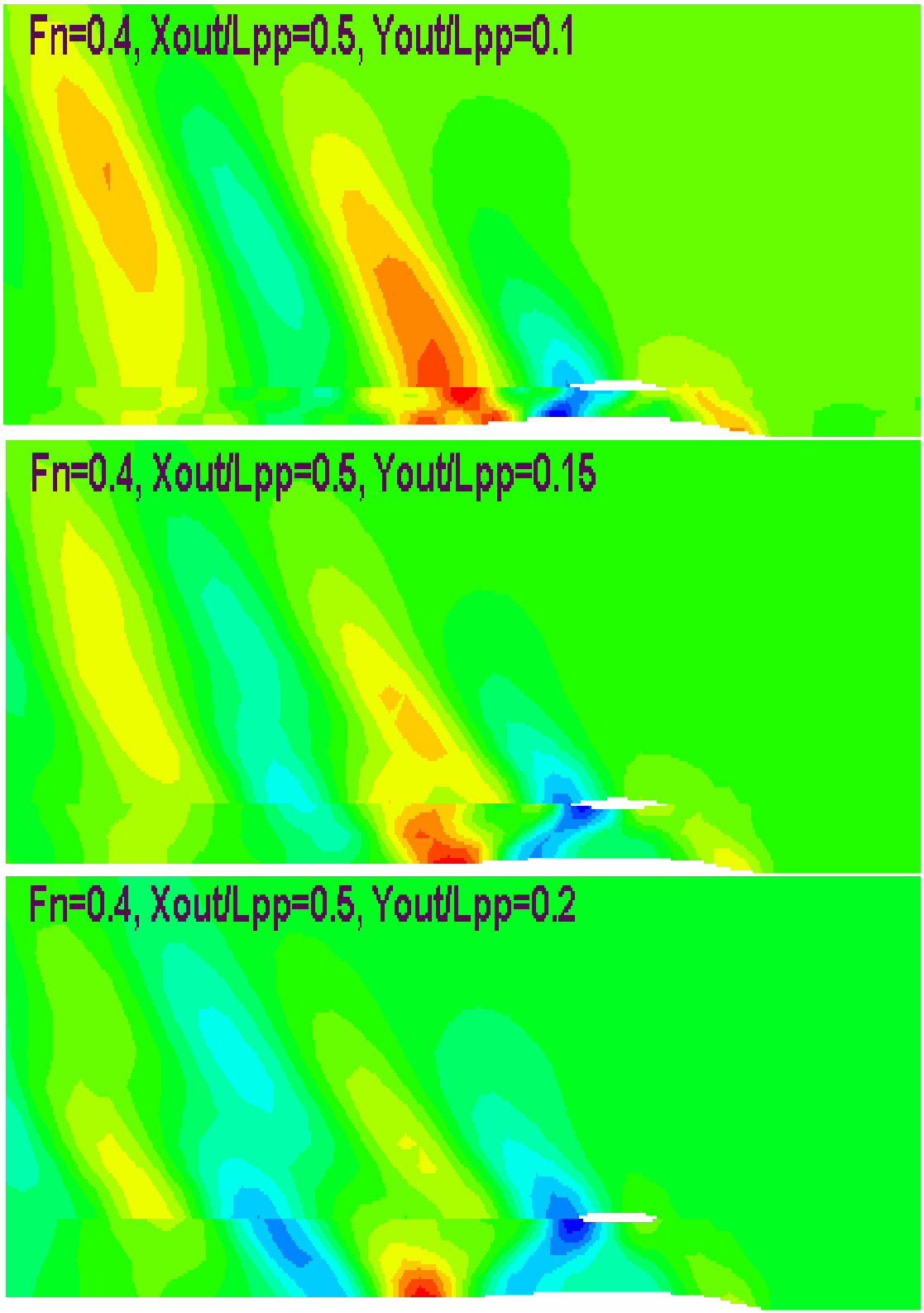

Figure 41. Wave Pattern for $X_{out} / L_{pp} = 0.5$, at Froude Number 0.4

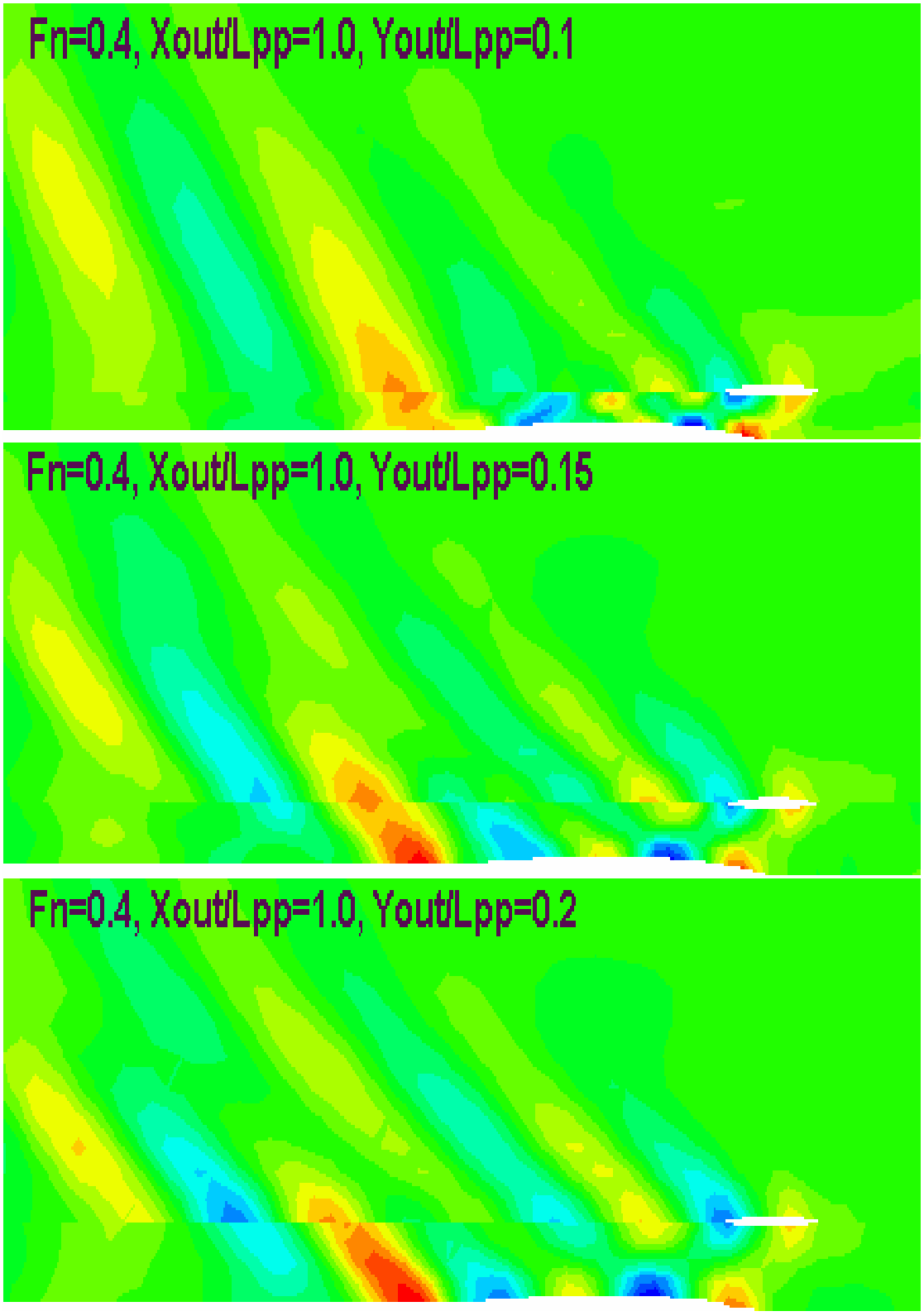

Figure 42. Wave Pattern for $X_{out} / L_{pp} = 1.0$, at Froude Number 0.4

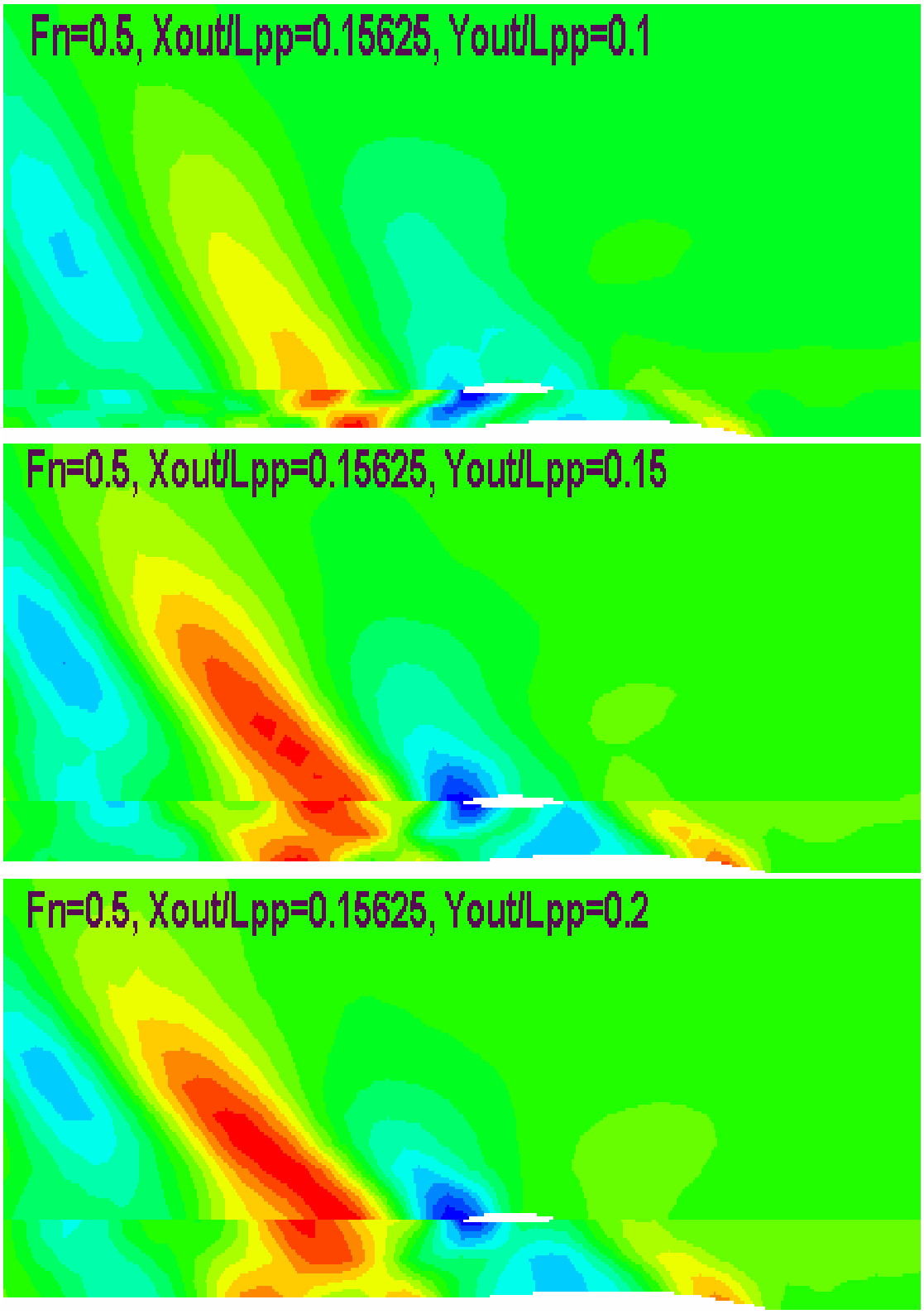

Figure 43. Wave Pattern for $X_{out} / L_{pp} = 0.15625$, at Froude Number 0.5

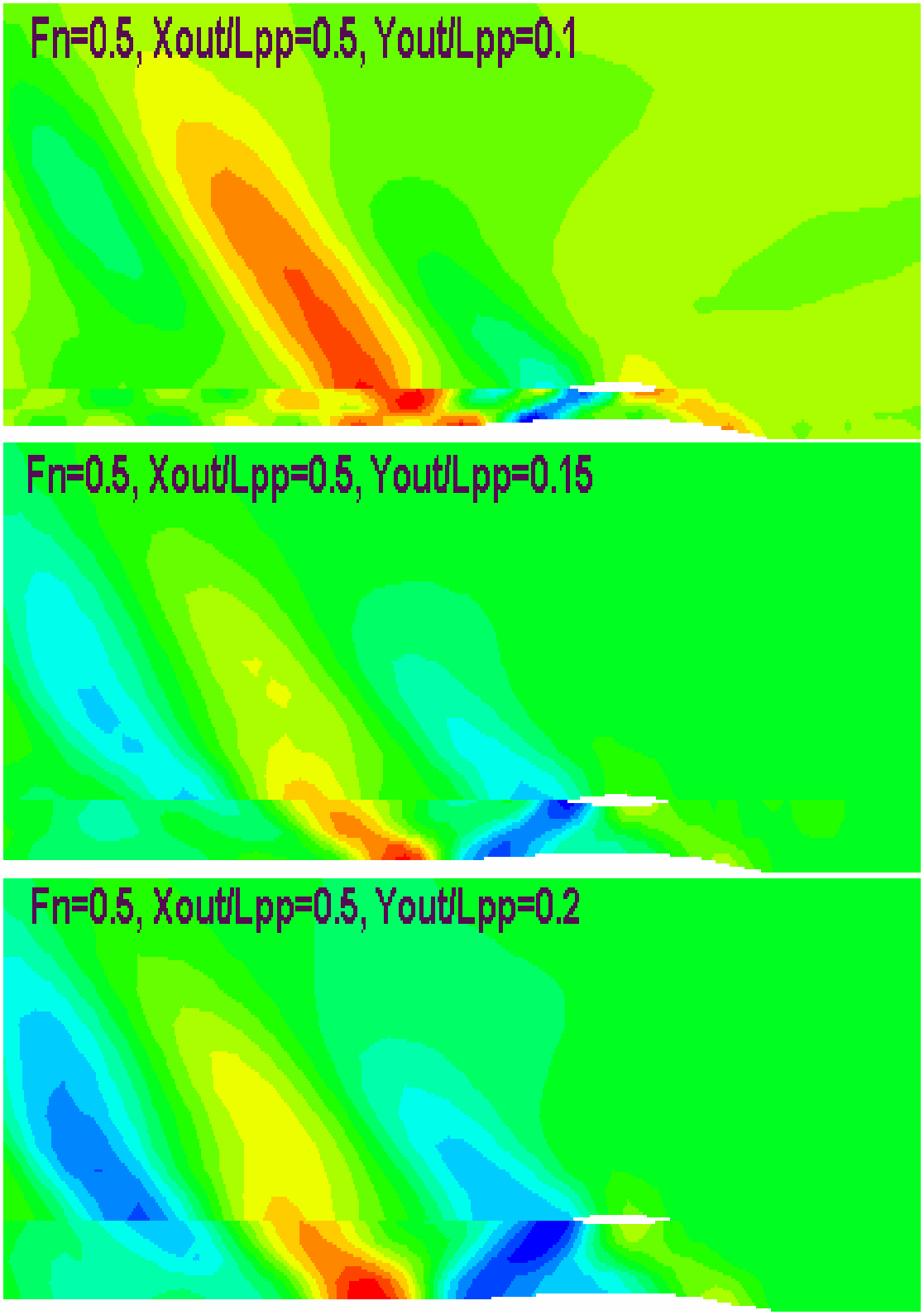

Figure 44. Wave Pattern for $X_{out} / L_{pp} = 0.5$, at Froude Number 0.5

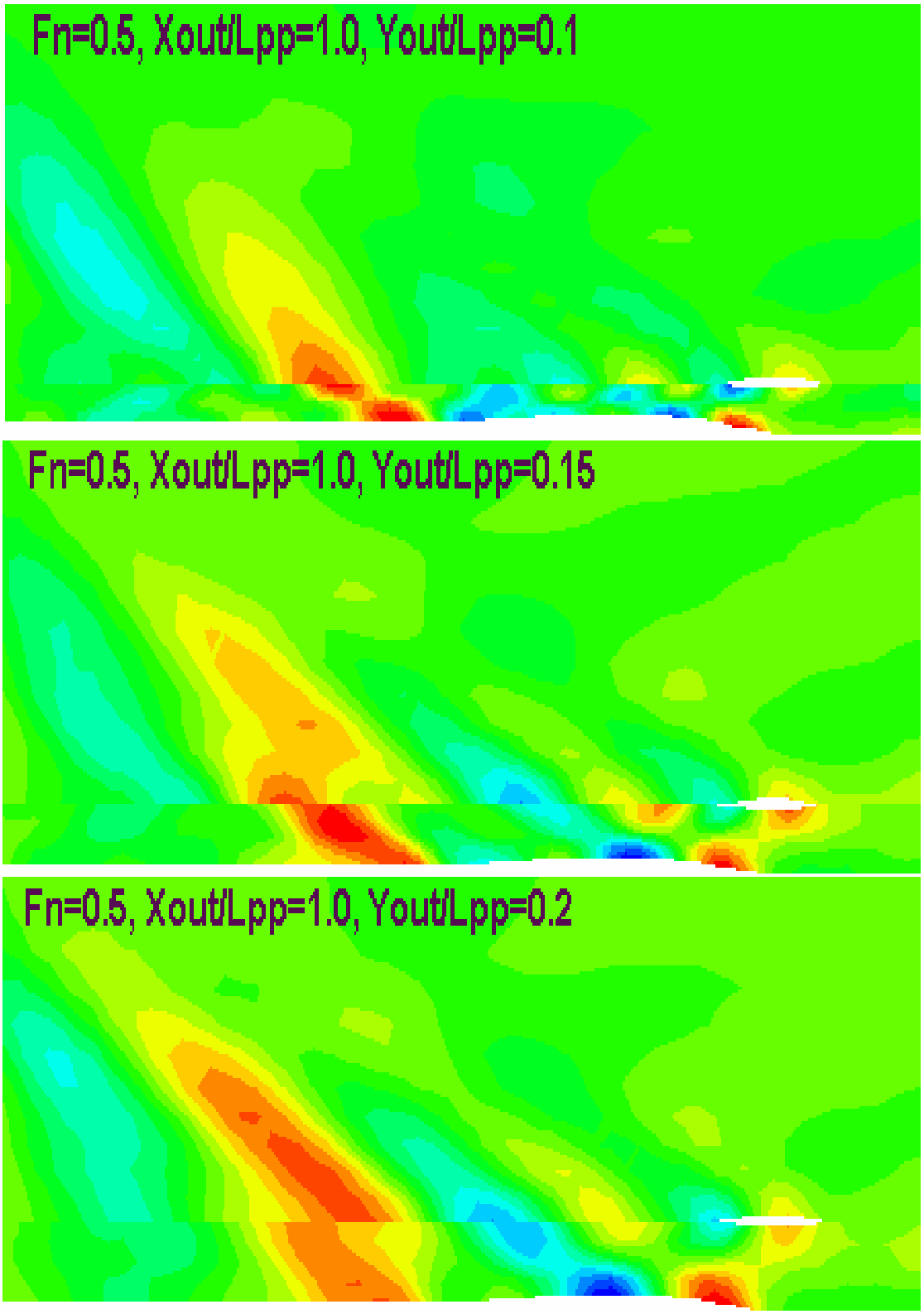

Figure 45. Wave Pattern for $X_{out} / L_{pp} = 1.0$, at Froude Number 0.5

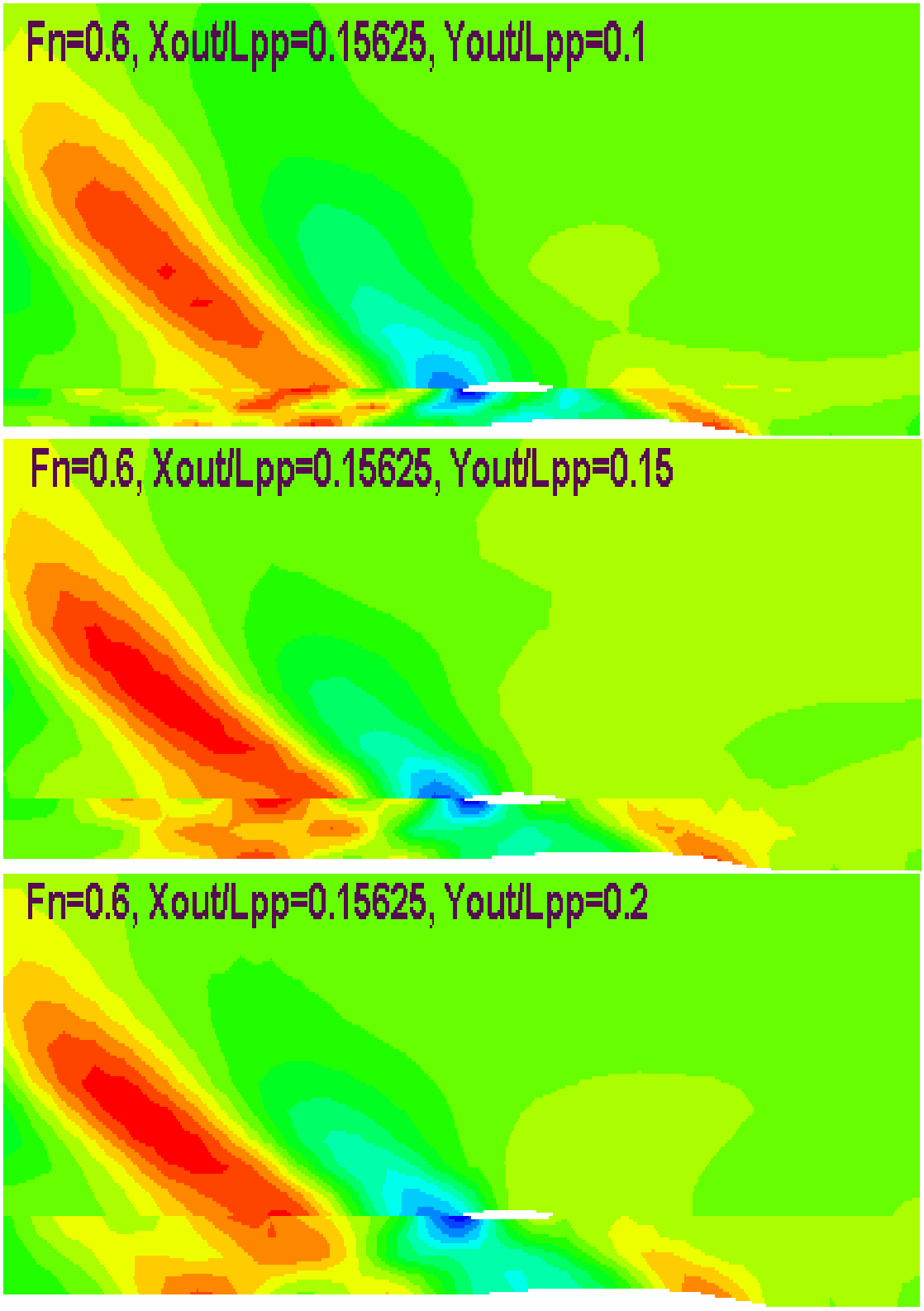

Figure 46. Wave Pattern for $X_{out} / L_{pp} = 0.15625$, at Froude Number 0.6

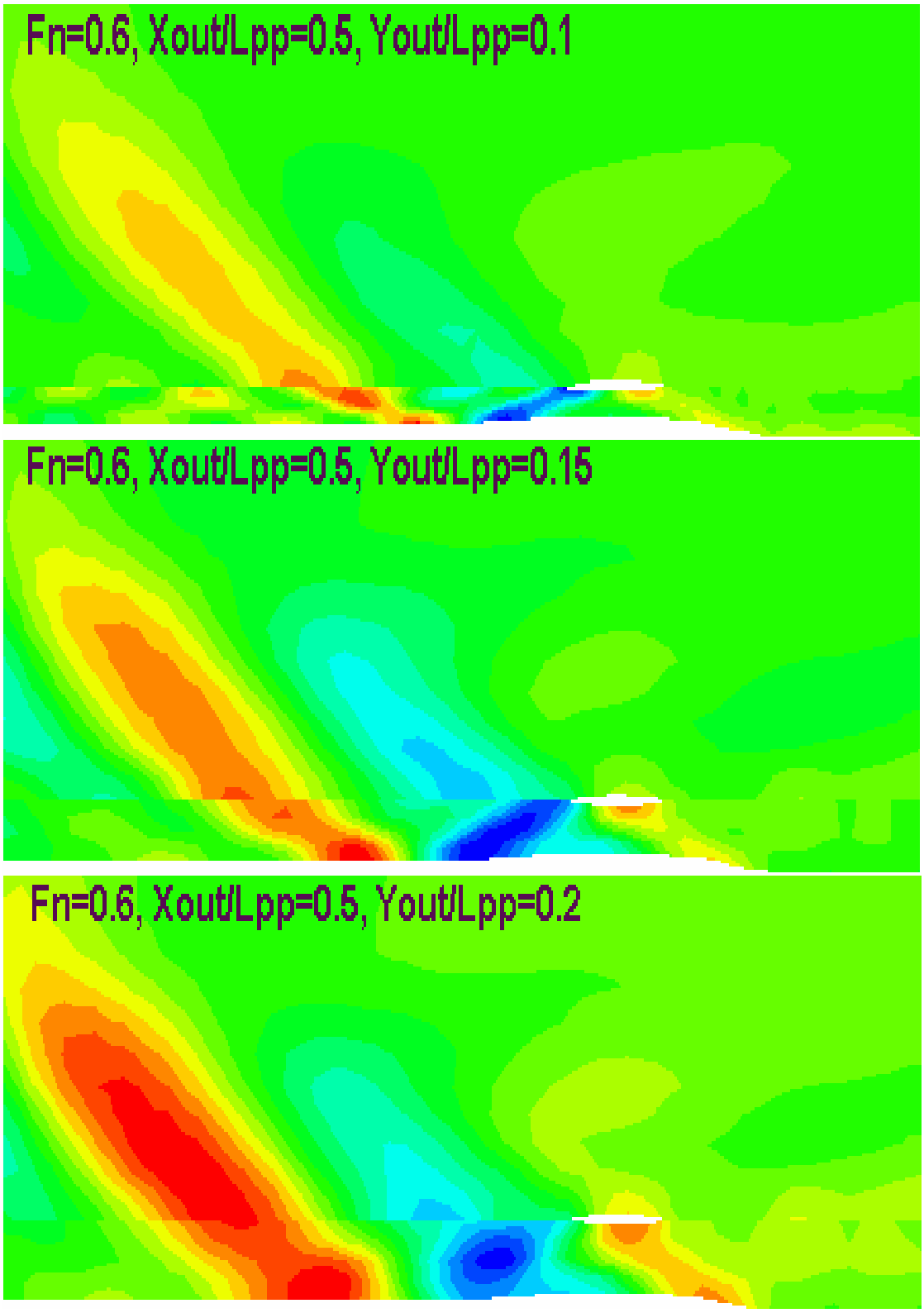

Figure 47. Wave Pattern for $X_{out} / L_{pp} = 0.5$, at Froude Number 0.6

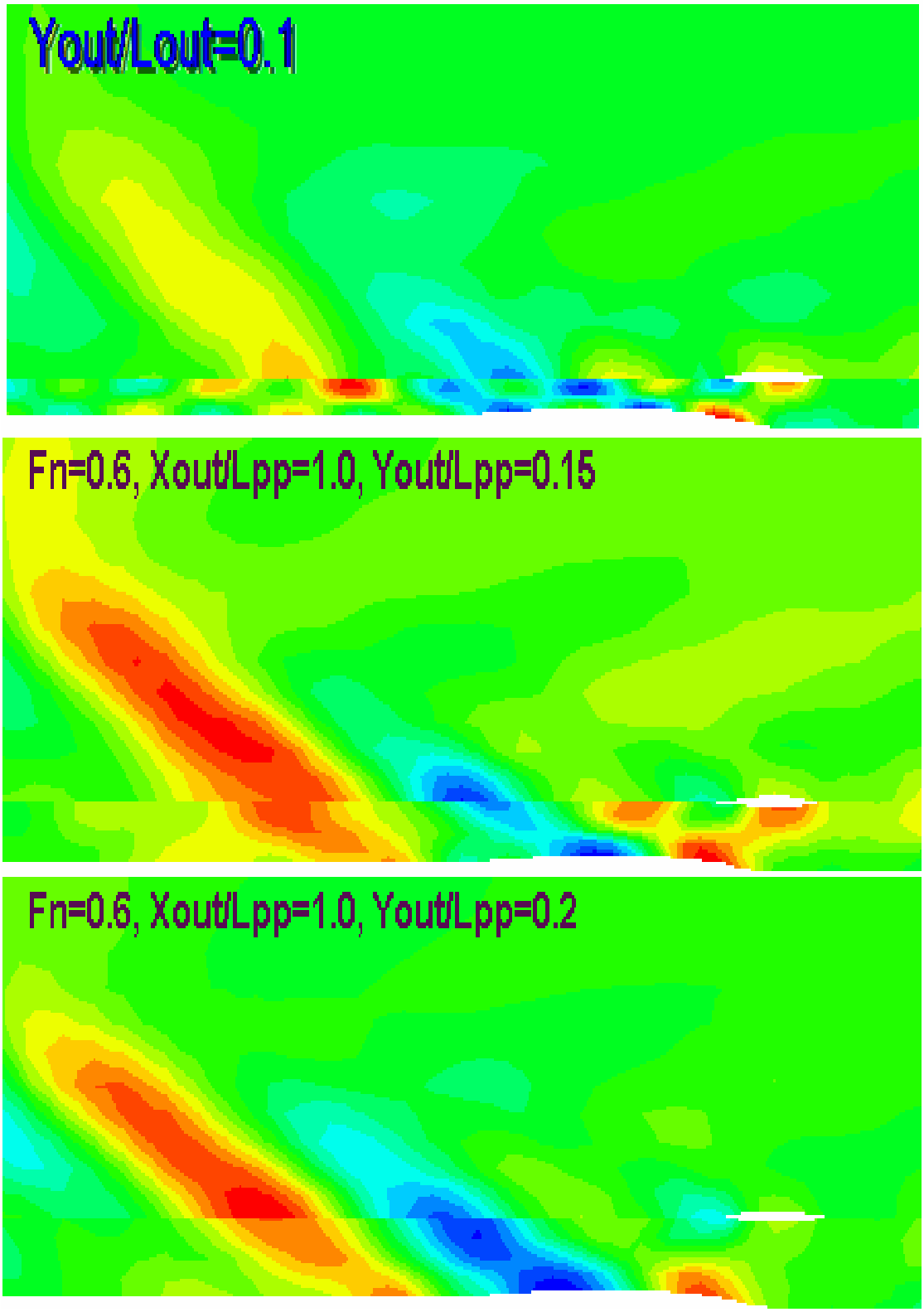

Figure 48. Wave Pattern for $X_{out} / L_{pp} = 1.0$, at Froude Number 0.6

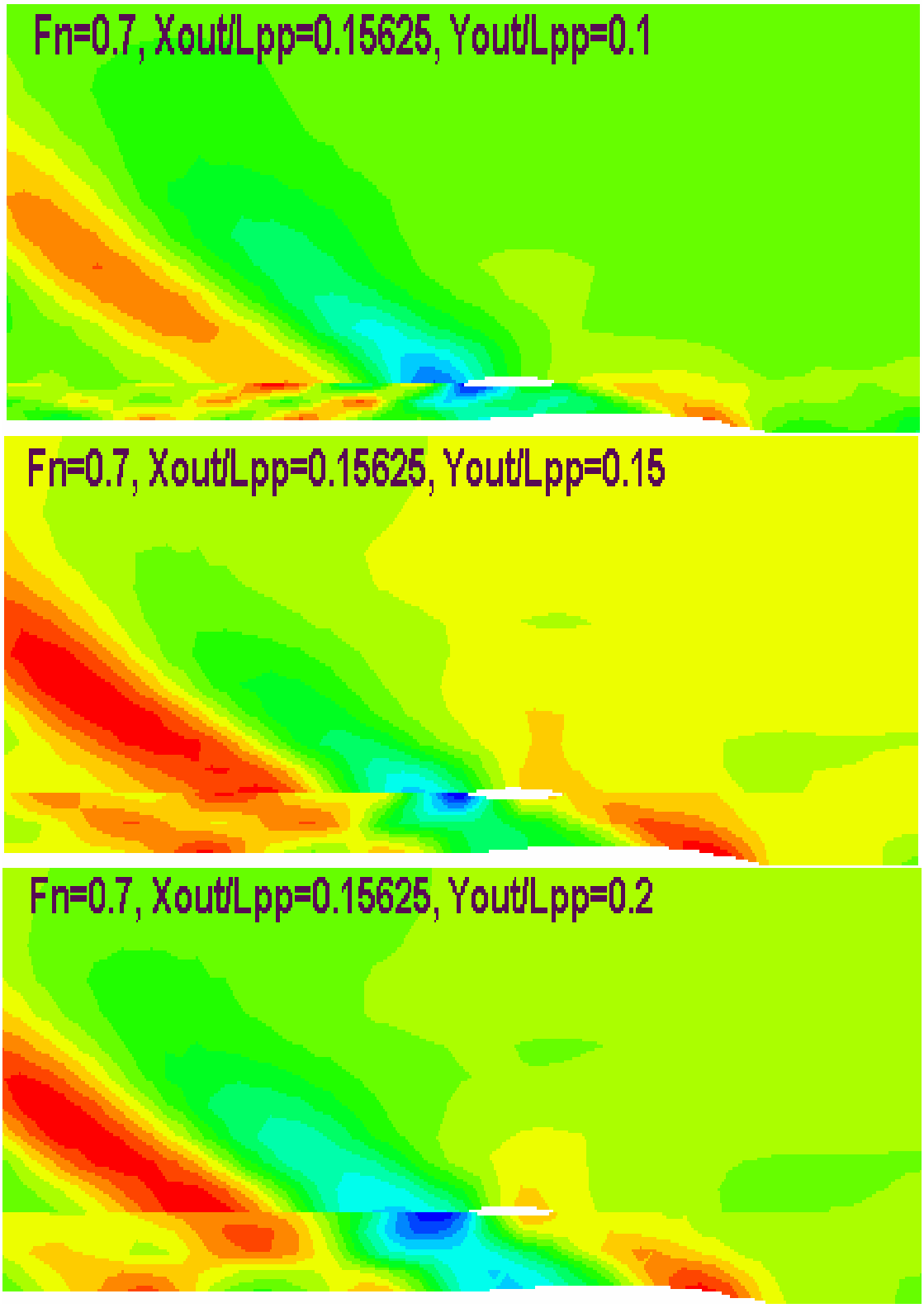

Figure 49. Wave Pattern for $X_{out} / L_{pp} = 0.15625$, at Froude Number 0.7

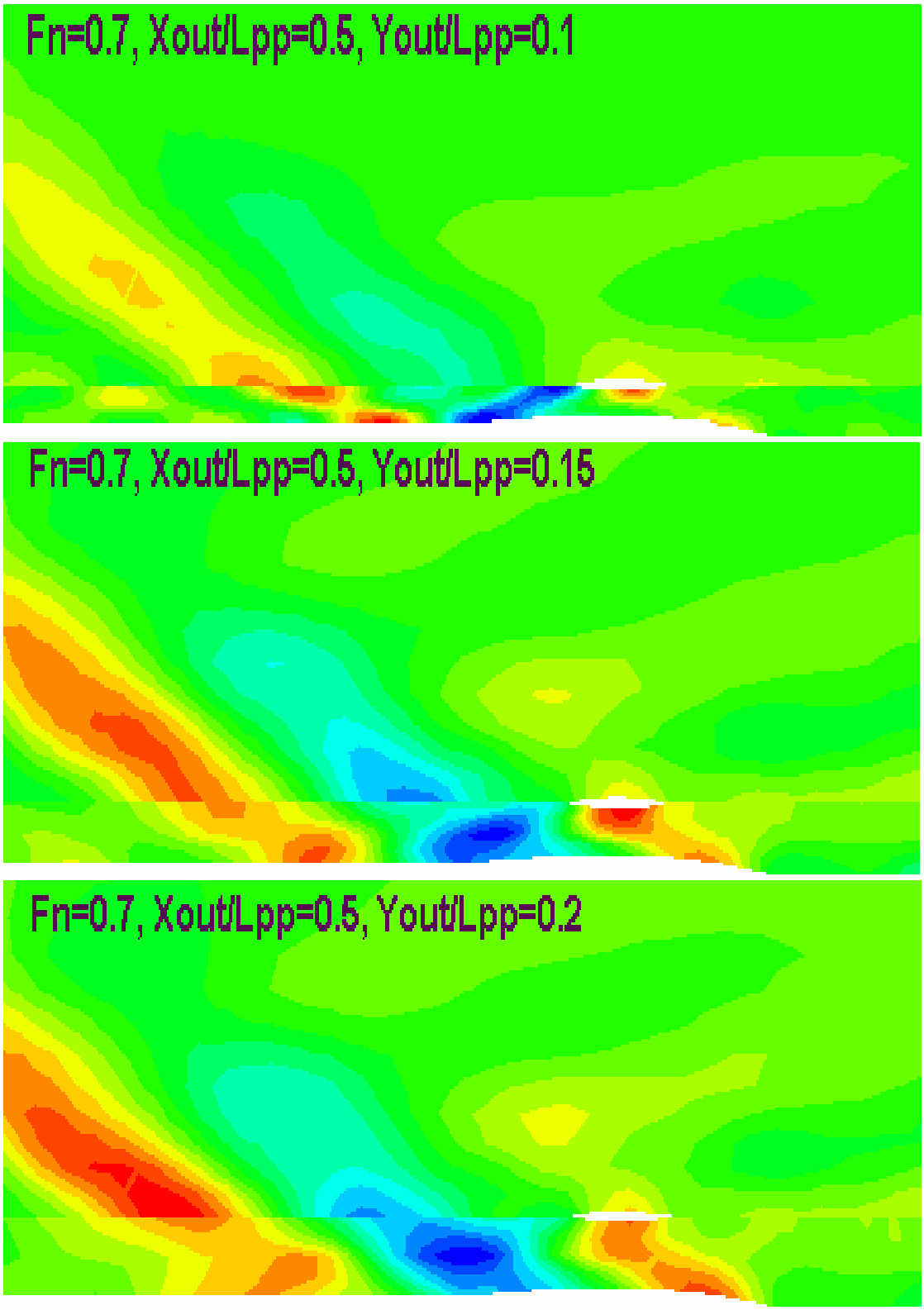

Figure 50. Wave Pattern for $X_{out} / L_{pp} = 0.5$, at Froude Number 0.7

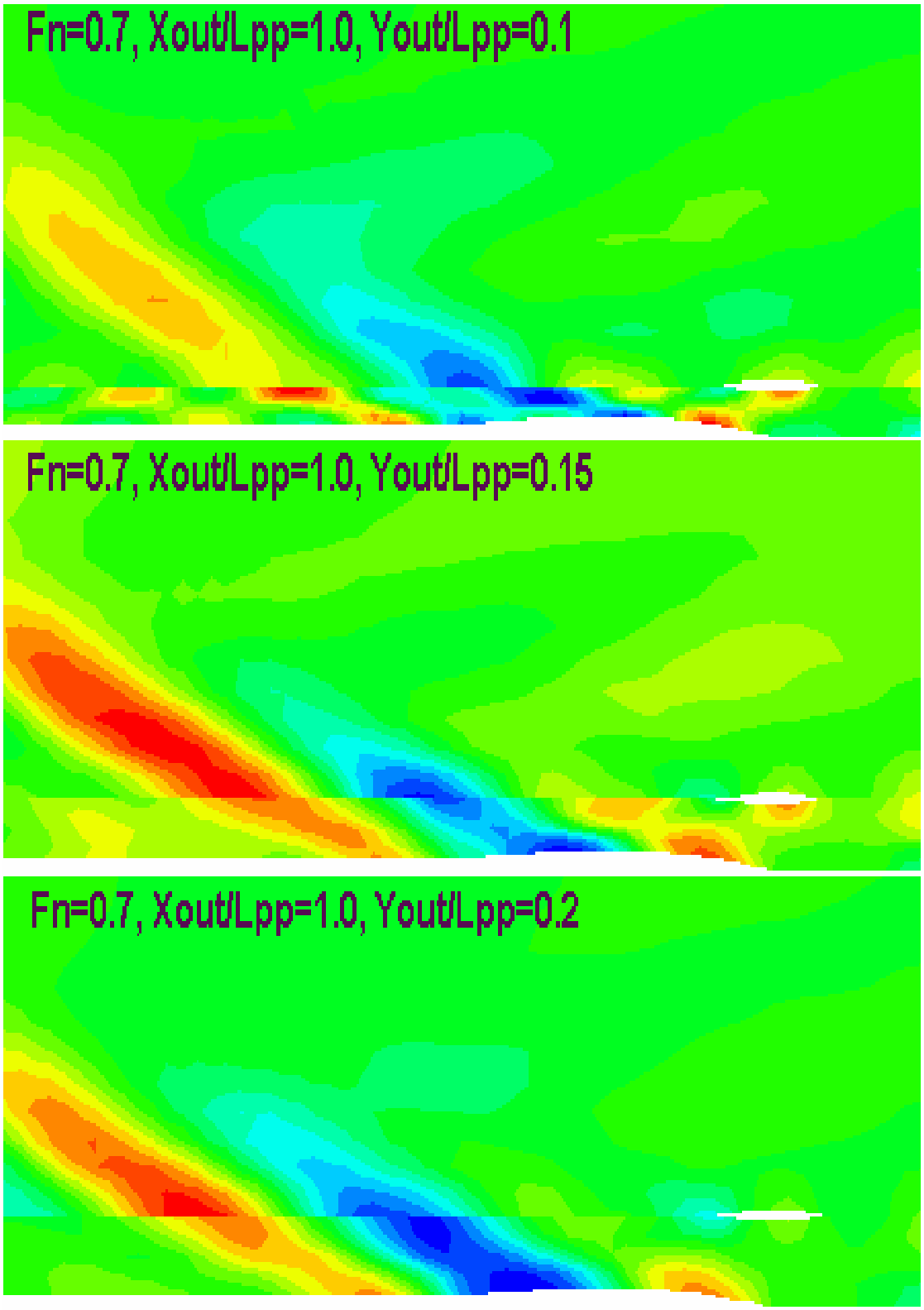

Figure 51. Wave Pattern for $X_{out} / L_{pp} = 1.0$, at Froude Number 0.7

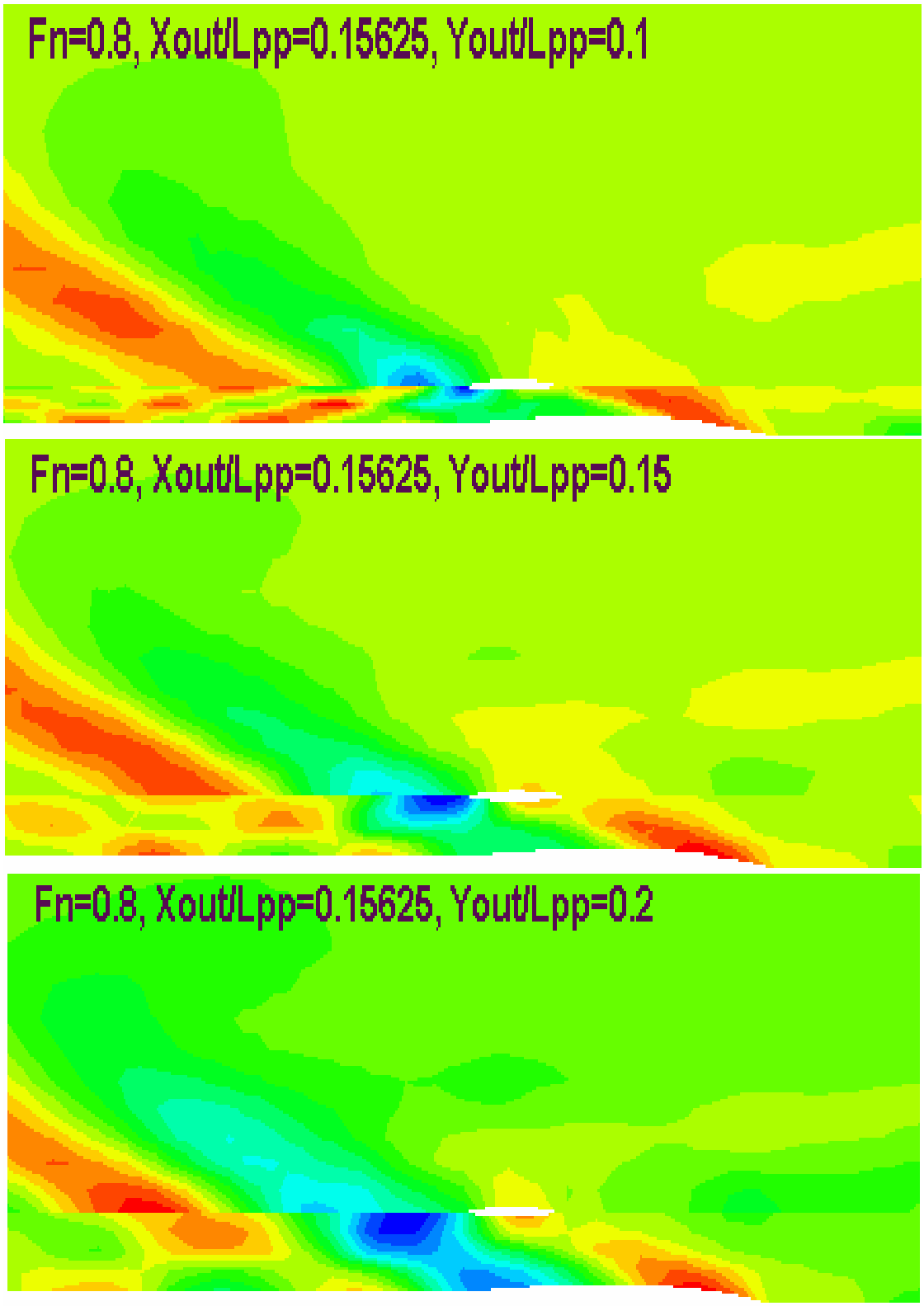

Figure 52. Wave Pattern for $X_{out} / L_{pp} = 0.15625$, at Froude Number 0.8

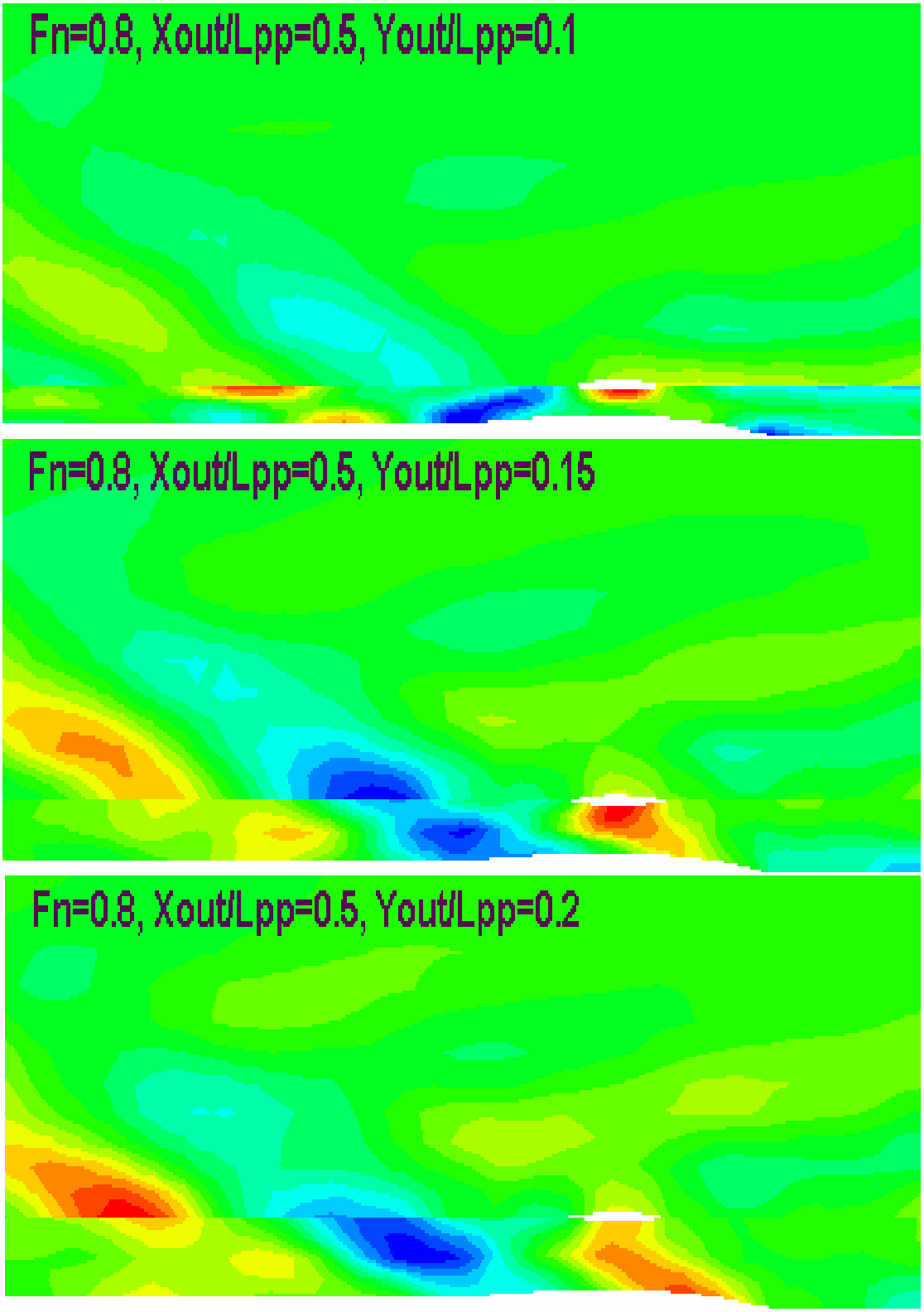

Figure 53. Wave Pattern for $X_{out} / L_{pp} = 0.5$, at Froude Number 0.8

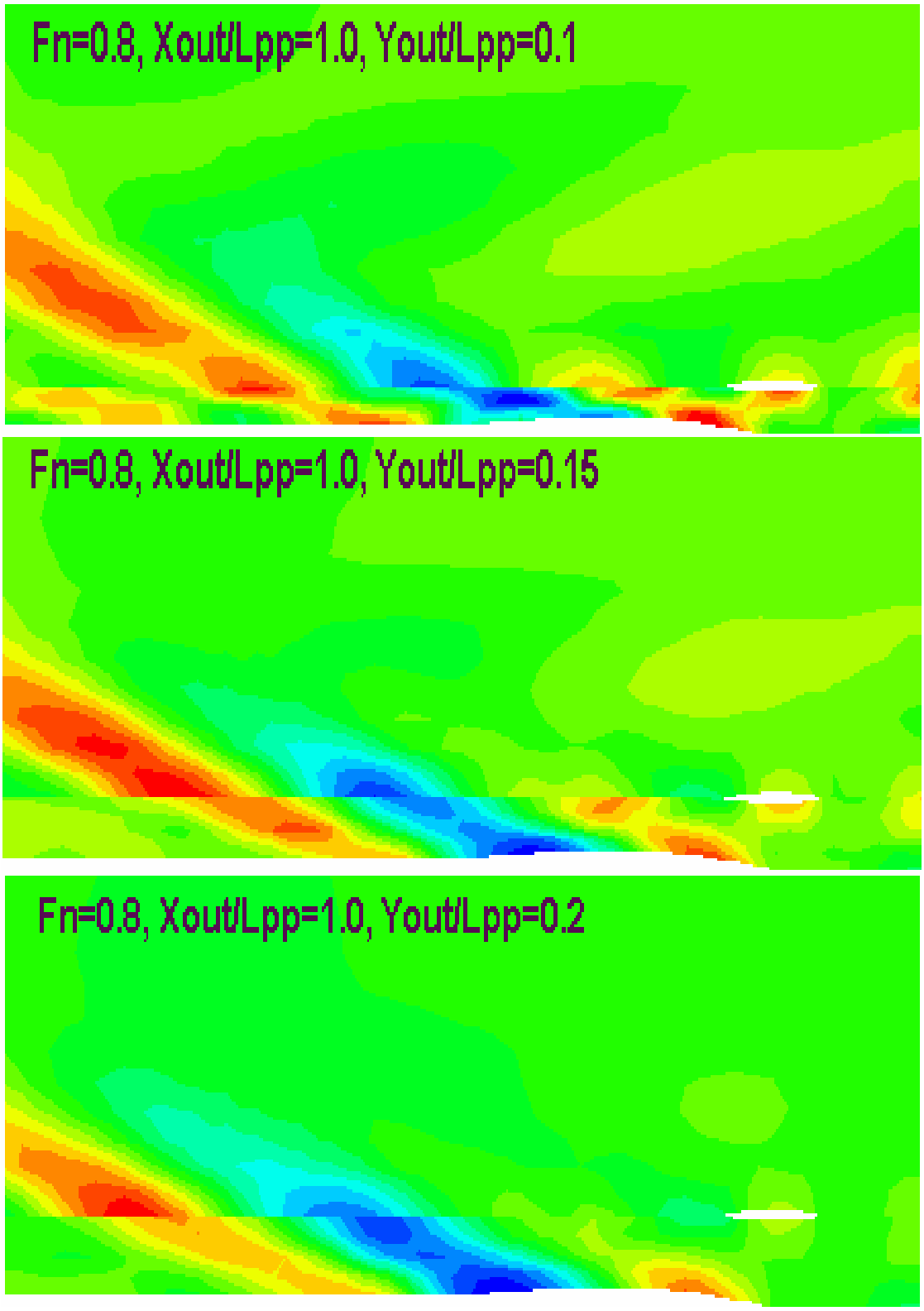

Figure 54. Wave Pattern for $X_{out} / L_{pp} = 1.0$, at Froude Number 0.8

E. SUMMARY OF RESULTS

The previous results are summarized in the following figures. We can clearly see the fundamental effect that the Froude number has. It is also clear that there is no consistent trend with regards to side hull longitudinal placement. For some Froude numbers, the wave making resistance varies very little in terms of side hull placement. For other Froude numbers, most notably between 0.3 and 0.5 in the present case, there is significant fluctuation of the wave making resistance coefficient in terms of either the longitudinal or the transverse side hull position. In such cases, it is possible to arrive at significant fuel saving by properly selecting the above design variables.

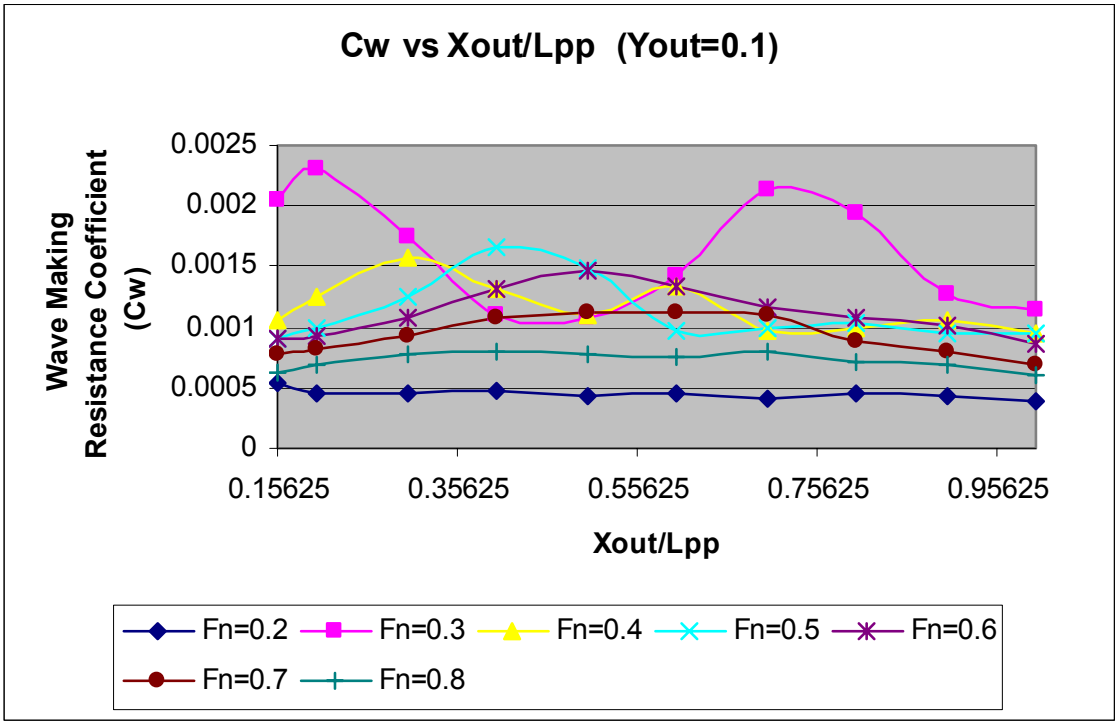

Figure 55. Wave Making Resistance Coefficient Results for $Y_{out} / L_{pp} = 0.1$

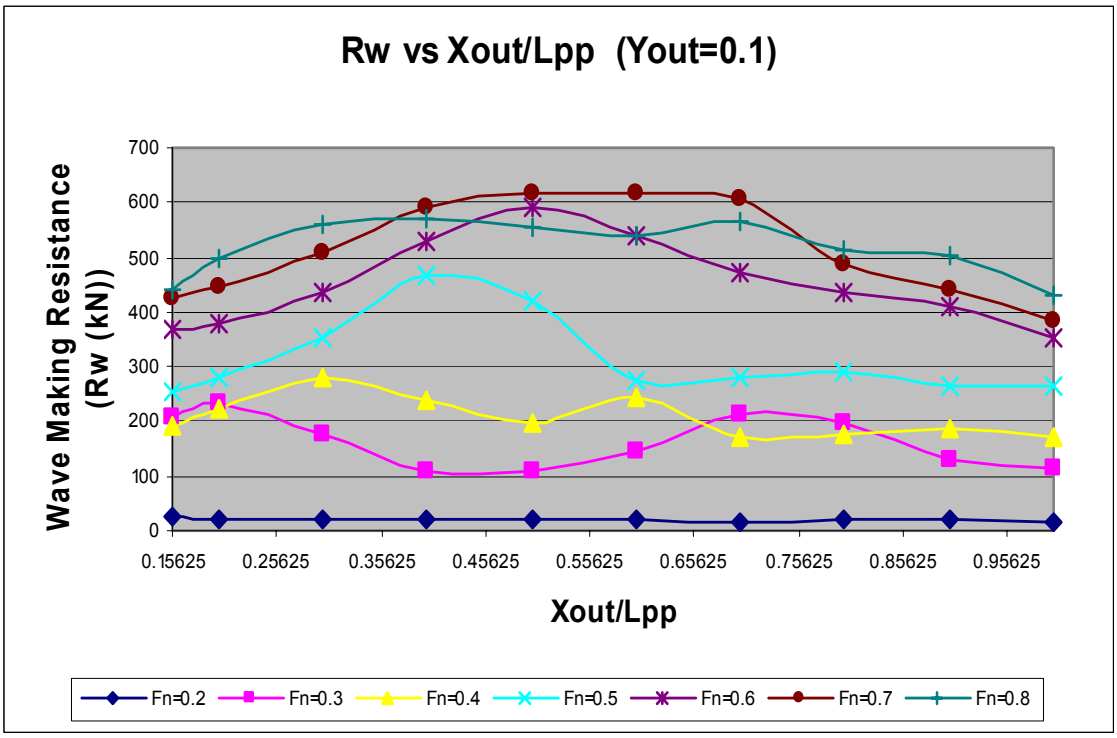

Figure 56. Wave Making Resistance Results for $Y_{out} / L_{pp} = 0.1$

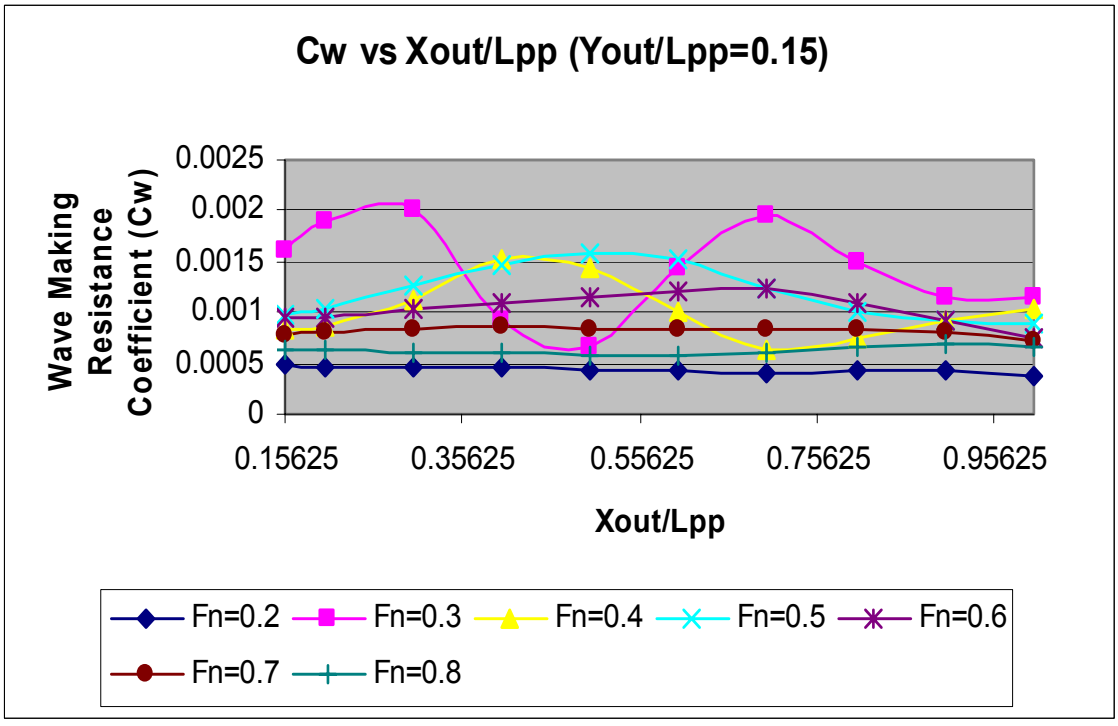

Figure 57. Wave Making Resistance Coefficient Results for $Y_{out} / L_{pp} = 0.15$

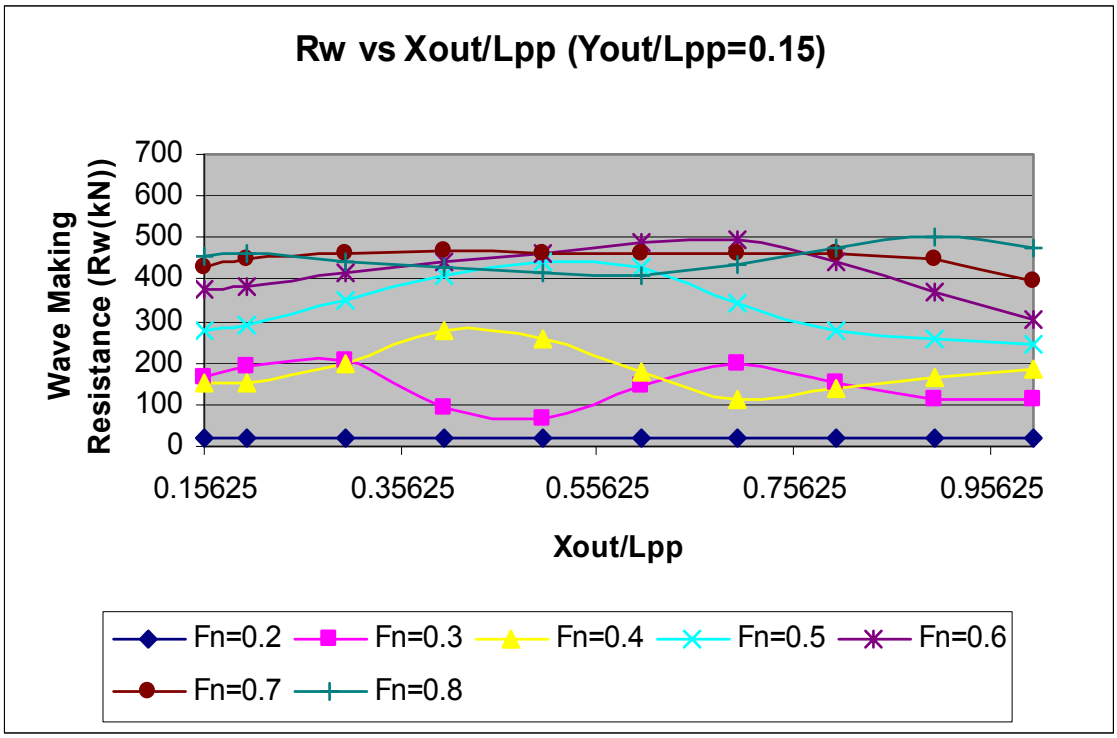

Figure 58. Wave Making Resistance Results for $Y_{out} / L_{pp} = 0.15$

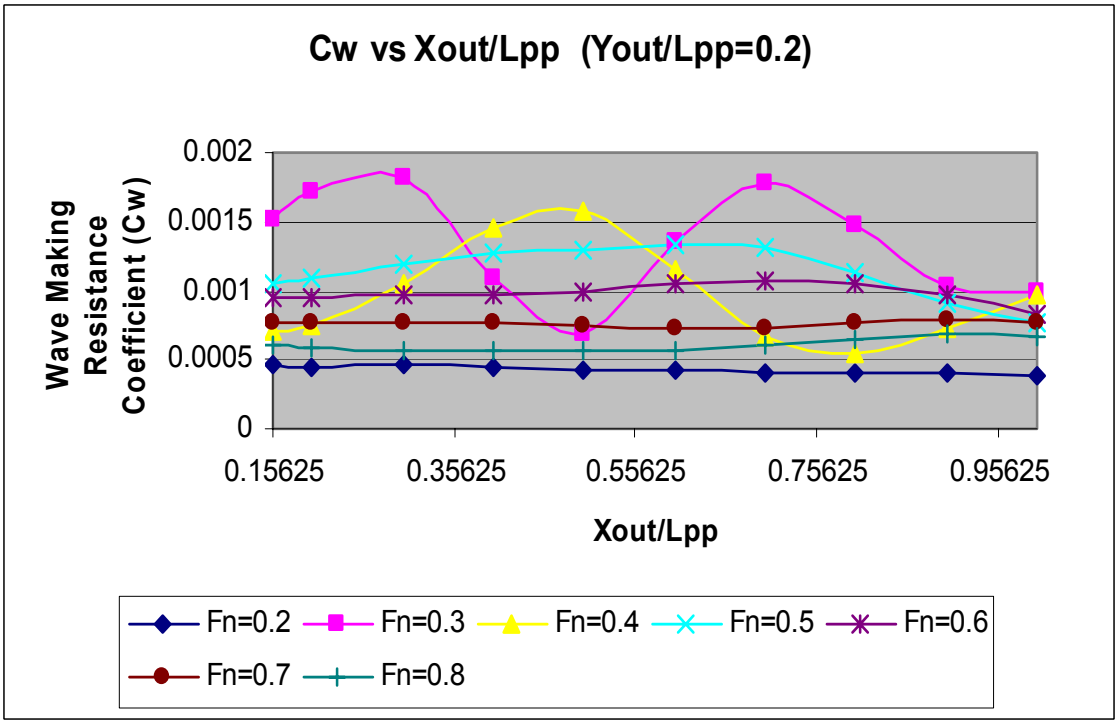

Figure 59. Wave Making Resistance Coefficient Results for $Y_{out} / L_{pp} = 0.2$

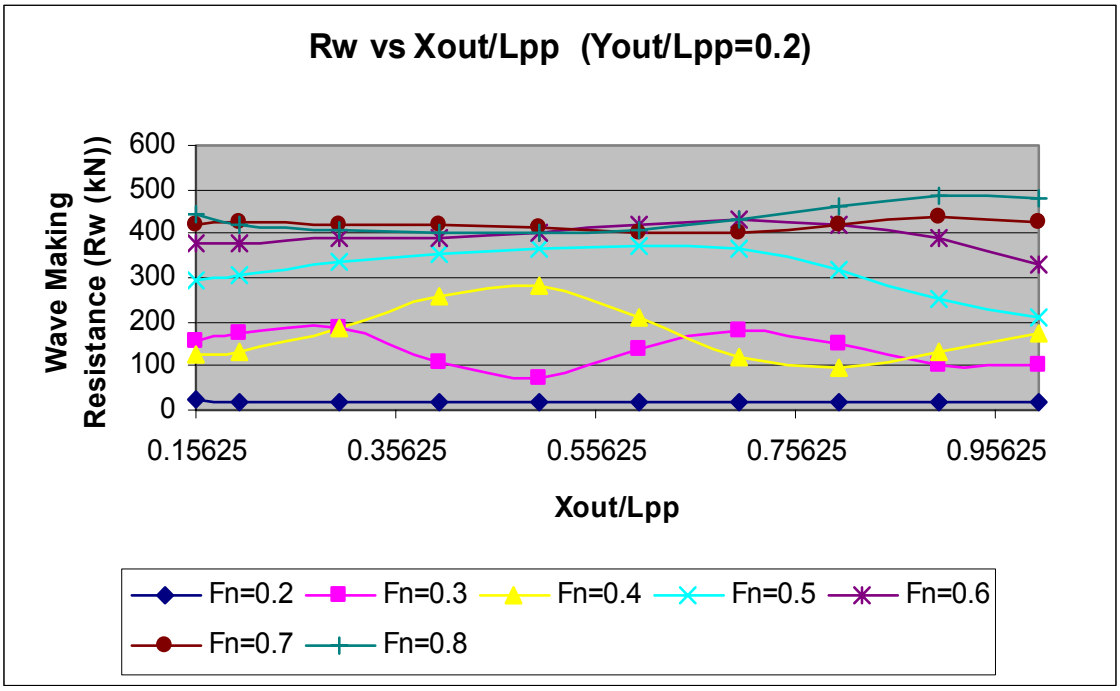

Figure 60. Wave Making Resistance Results for $Y_{out} / L_{pp} = 0.2$

V. CONCLUSIONS AND RECOMMENDATIONS

A. CONCLUSIONS

This thesis presented a comprehensive study on the effects of side hull position on the wave making resistance characteristics of powered trimarans. The simulation results show that side hull position is very important factor affecting trimaran resistance. While there is no single optimum configuration for the entire speed range, the results of this study can be directly utilized in design, in order to minimize ship resistance, and maximize available payload.

It can be clearly seen the fundamental effect that the Froude number has. It is also clear that there is no consistent trend with regards to side hull longitudinal placement. For some Froude numbers, the wave making resistance varies very little in terms of side hull placement. For other Froude numbers, most notably between 0.3 and 0.5 in the present case, there is significant fluctuation of the wave making resistance coefficient in terms of either the longitudinal or the transverse side hull position. In such cases, it is possible to arrive at significant fuel saving by properly selecting the above design variables. Generally, the lowest interference values at low speeds occur at aft, outboard locations. At higher Froude numbers, the lowest interference occurs aft and outboard, generally moving inboard as Froude number increases further.

We can see that, in general, the results depend highly on the Froude number. It is possible to optimize wave making resistance by suitable positioning of the side hulls, but such an optimization needs to be tuned to a specific operating speed.

B. RECOMMENDATIONS

Recommendations for continuing studies are the following:

1. Analyze the effect of side hull symmetry on wave making resistance of the powered trimarans.

2. Analyze the effect of the angle-of-attack of side hull on wave making resistance of the powered trimarans.

3. Analyze the effect of the side hull displacement on wave making resistance of the powered trimarans.

LIST OF REFERENCES

[1] B.B. Ackers, T. J. Michael, O.W. Tredennick, H.C. Landen, E.R. Miller III, J. P. Sodowsky, J.B. Hadler. "An Investigation of the Resistance Characteristics of Powered Trimaran Side-Hull Configurations," *SNAME Transactions*, v. 105, pp. 349-373. 1997.

[2] W.J. van Griethuysen, R.W.G. Bucknall, J.W. Zhang. "Trimaran Design-Choices and Variants for Surface Warship Applications," paper presented at the International Symposium: Warship 2001: Future Surface Warships, London, UK, 20-21 June 2001.

[3] D.E. Gadd. "A Method of Computing the Flow and the Surface Wave Pattern Around Full Forms," *Transactions of Royal Association of Naval Architects*. v. 113. 1976

[4] C.W. Dawson. "A Practical Computer Method for Solving Ship-Wave Problems," paper presented at The 2nd International Conference on Numerical Ship Hydrodynamics, 1977

[5] S. Purvin. "*Hydrodynamic Design of High Speed Catamaran Vessels*," Master's Thesis. M.I.T. Massachusetts, February 2003.

[6] J.N. Newman, *Marine Hydrodynamics*, 7th Print, the MIT Press, 1992

THIS PAGE INTENTIONALLY LEFT BLANK

INITIAL DISTRIBUTION LIST

1. Defense Technical Information Center
   Ft. Belvoir, Virginia

2. Dudley Knox Library
   Naval Postgraduate School
   Monterey, California

3. Mechanical Engineering Department Chairman, Code ME
   Naval Postgraduate School
   Monterey, California

4. Naval/Mechanical Engineering Curriculum Code 34
   Naval Postgraduate School
   Monterey, California

5. Professor Fotis Papoulias, Code ME
   Department of Mechanical Engineering
   Naval Postgraduate School
   Monterey, California

6. Deniz Kuvvetleri Komutanligi
   Personel Daire Baskanligi
   Bakanliklar, Ankara, Turkey

7. Ltjg. Zafer ELCIN
   Viraca Mah. Ikiz Evler Sitesi
   E-1 Blok M.Kemal Pasa
   16500 Bursa, Turkey